ÉCOLE POLYTECHNIQUE FÉDÉRALE DE LAUSANNE
ELECTRICAL AND ELECTRONIC SECTION
POWER ELECTRONICS LABORATORY

MASTER THESIS

MVDC NETWORKS: STUDY OF DIFFERENT ARCHITECTURES

STUDENT
Patricia Penadés Huesca

SUPERVISOR
Renan Pillon Barcelos

ADVISOR
Prof. Dražen Dujić

LAUSANNE, JULY 13TH 2022.

ABSTRACT

Energy distribution grids are mostly affected by the transition towards more sustainable energy systems. In this way, medium voltage direct current (MVDC) systems have great potential to be considered as an alternative to conventional AC networks, taking advantage on renewable and energy storage systems integration. The key advantage of DC power systems compared to AC counterparts is the higher efficiency of power transmission and distribution under the same voltage levels. Apart from that, frequency synchronization is not required , and there is no need for reactive power compensation.

To promote this technology, this project investigate and analyze various types of architectures in MVDC power distribution networks. These architectures are radial, characterized by having one main path transmitting the energy from sources to consumers; ring, a closed loop that provides multiple paths between the sources and consumers; and mesh, where there are greater interconnections between the nodes.

In order to analyze the three types of configurations, three areas will be considered: an urban area, a rural area and a residential area. Simulations are conducted using steady-state models over the course of one day, these incorporate dynamic energy sources, dynamic consumption points and DC transformers (DCTs). Integrating DCTs in the systems developed throughout this project and having a system with different voltage levels is also an essential part. In each section, there is a description of the different energy sources, consumption, electrical connections between different points, and the location of the DCTs, being as realistic as possible. DCTs operate in open loop, it means that there is not voltage control. In power flow study, once the simulations are implemented, different aspects are analyzed for each case, such as total consumption, the contribution of each energy source, the amount of energy flowing through each DCT, voltage at each node and losses. In this part, simulations are carried out using PLECS software.

Furthermore, an analytical model is used to study impedance response of each node. First, the voltage at the nodes can be calculated with this model without having to run simulations. Following that, the method of analyzing the impedance in a grid node, a consumption point, and in DCT are explained. Finally, the effect of length on impedance is also examined.

Keywords : MVDC; power flows; nodal impedance assessment.

ACKNOWLEDGEMENT

First of all, I would like to thank Mr. Renan Pillon, my supervisor, for all his time invested, his patience with me and for his advices during the project.

My gratitude also goes to Prof. Dražen Dujić for giving me the opportunity to join Power Electronics Laboratory during these months.

Lastly, I would like to express my gratitude to my family for their unconditional support.

LIST OF ABBREVIATIONS

AC	Alternating Current
DC	Direct Current
DCDS	Direct Current Distribution System
DCT	Direct Current Transformer
ESS	Energy Storage System
HVDC	High Voltage Direct Current
LVDC	Low Voltage Direct Current
MVDC	Medium Voltage Direct Current
PDN	Power Distribution Networks
PV	Photovoltaic
RES	Renewable Storage System

CONTENTS

LIST OF FIGURES

LIST OF TABLES

1 | INTRODUCTION

Promotion of sustainable development has become one of the hottest topics in the fight against global warming. Renewable energies play a key role in reducing polluting emissions and guaranteeing a promising future. Moreover, it reduces carbon footprint; they come from unlimited sources and do not depend on the decrease in reserves over time; they stimulate self-consumption and can help to reduce energy dependence. However, they have some disadvantages such as the dependence on atmospheric events; in some cases, such as generation of solar energy, it requires a large space; in addition it is not easy to carry out its storage, so it is necessary to consume at the moment. These characteristics must be taken into account when designing future electrical distribution systems.

A large part of the expansion in transmission system has been in AC due to the use of transformers, which have a wide range of voltages. However, power transmission projects in HVDC and MVDC have opened up new pathways. In spite of the fact that most energy transmission projects currently use alternating current, there are many HVDC projects and this technology has gain several new applications. In contrast, MVDC projects are currently less common due to lack of existing technology. Many studies are conducted and more projects are being developed. This thesis is motivated by the challenges in the development of MVDC systems with Direct Current Transformers (DCT). DCT is used in DC PDN to connect different DC power sources and loads. The DCT acts as an isolated dc-dc power converter in this context, acting as a transformer between two dc lines, and operating in an open-loop, meaning it does not receive voltage or power set points. Yet, as a bidirectional element, the DCT is capable of following the natural power flow.

Some of the application examples of DC technology are: public transportation in trains and subways, ships and airplanes board grids, and data centers. Considering that most new energy applications including renewable, e-mobility, and storage are internally DC based, DC or hybrid AC/DC distribution provides connections via DC-DC converters that are more efficient and architecturally simpler. In spite of the fact that DC distribution grids have yet to be deployed since some key technologies are still in development, a number of advantages have been identified and proved, including [1]:

- Integration and distribution of renewable energy generation.
- Enabling power grids and lines to handle a greater volume of renewable energy, electric vehicles, and other DC-based loads.
- Improving energy and resource efficiency of the system.
- Development of new energy markets (e.g. future energy communities including the self-supply).
- Easily in the incorporation of storage facilities.
- Use of resources in production and operation that are environmentally friendly and sustainable.
- Reduction of operational and investment costs.

In next chapter (Chapter 2) this topic is deepened by making a comparison between AC and DC networks, MVDC PDN applications and explaining the different types of architectures. Next, a diagram is presented indicating the methodology used to carry out the project.

1.1 METHODOLOGY

For a better understanding of this project, Fig. 1.1 shows, through an organization chart, the methodology that has been carried out for the development of the study.

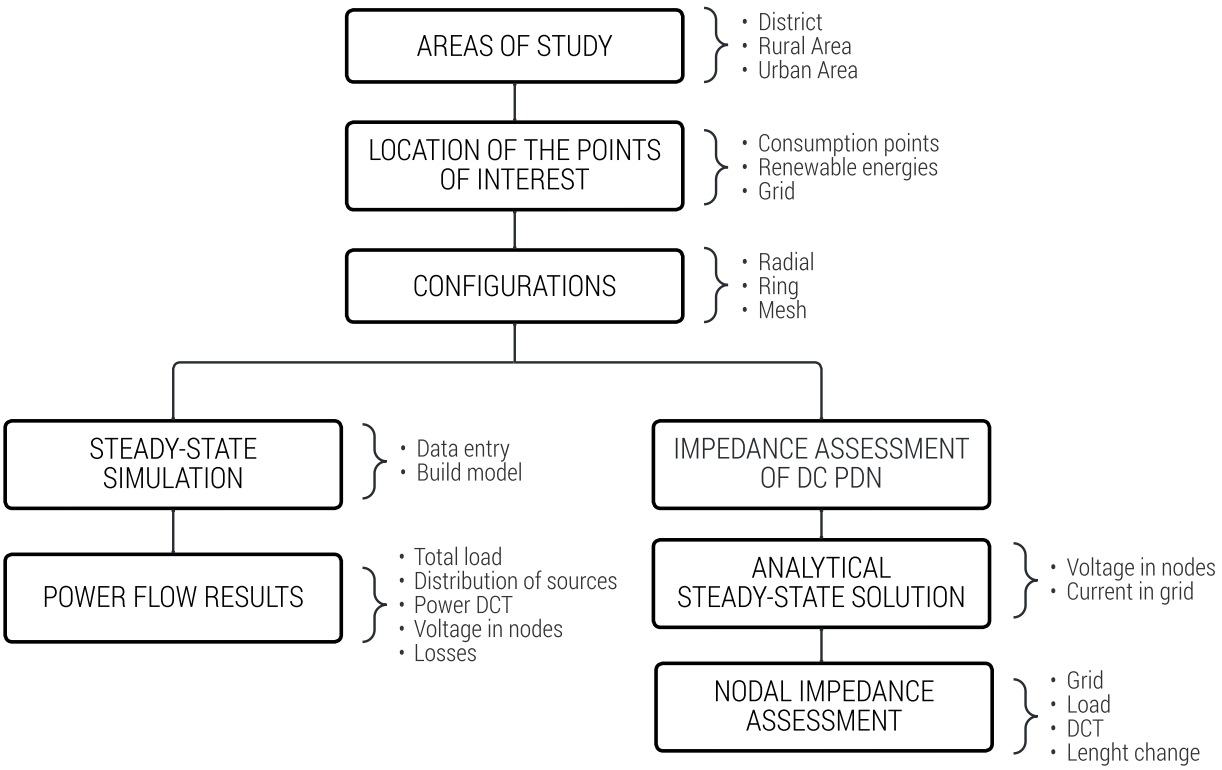

Fig. 1.1 Project methodology

The first step is to analyze the three study areas and collect the available information (total consumption of the area and energy production). The next step is to distribute those consumption and energy sources throughout each area, indicating where it is located. Once the points of interest have been located, the electrical lines are traced for each type of configuration in each different area, then the lengths of these lines are measured. Once the systems have been defined, we proceed to the part of the simulations and calculations. In the steady state simulation, the consumption data, energy sources, DCTs and electrical lines are introduced and model is built. The results are analyzed. Then, we go to the analytical model and build our system with the corresponding equations until we obtain the expected results and compare them with simulations.

2 STATE OF THE ART

Traditionally, power distribution networks have been developed with AC technology. Increasing interest in direct current grids has occurred in recent years due to the possibility of integrating renewable energy sources, such as solar energy or wind energy, and energy storage devices, including batteries, supercapacitors, and recharging points for electric cars. There are also other applications in different domains of MVDC, as explained in Subsection 2.2.1. Figure **2.1** shows the transition to DC distribution networks. As can be seen, in DC, the main path is in DC and, this is connected to the rest of the nodes with different DC converts to adapt the voltage. DC PDN (Power Distribution Networks) have the objective to satisfy the demand and ensure suitable and uninterrupted operation, avoiding violating the physical limits of its components or losing system stability.

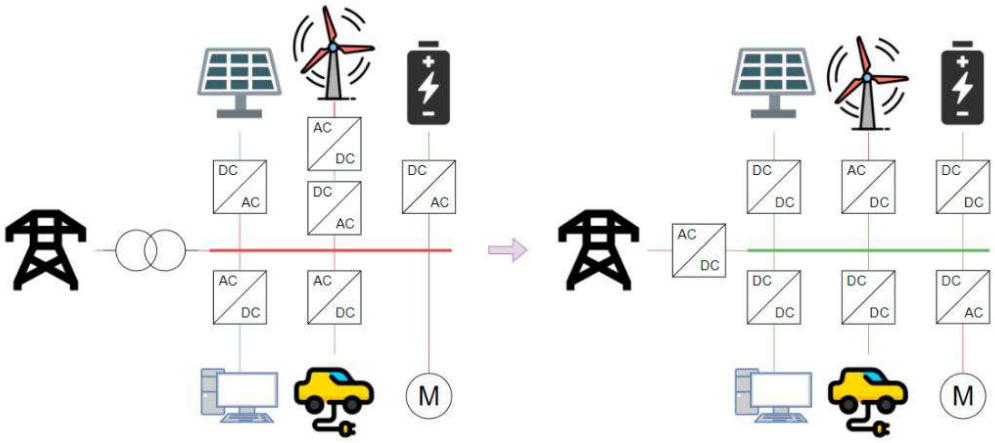

Fig. 2.1 Transition from AC (left) to DC (right) power distribution networks. [2]

2.1 COMPARISON OF AC AND DC IN POWER DISTRIBUTION NETWORKS

Immediately following the invention of the transformer, three-phase AC transmission and distribution grids became and remain the fundamental of a safe and efficient electricity supply system. In modern power system, DC is becoming a more accessible component due to advances in power semiconductor devices and cable technology [3]. In comparison with AC systems, DC power distribution networks offer some distinct advantages:

- **Encourage renewable energies.** Most of the renewable energy sources and the energy storage systems generate the power in DC, so it would be more effectively incorporated in a DC system than in an AC system, not only for the generation but also for the transmission and distribution. The main loads in hour houses are also in DC, so if the transmission is in DC the AC/DC converters are not necessary, these are replaced by the DC/DC converters which are smaller and more efficient [2].
- **Transmission efficiency.** In DC system the skin effect does not take place. As consequence, losses are reduced, and smaller cables are used for the same flow current. Moreover, in DC it is only needed two conductors instead of three conductors for transferring the current. It is possible to use only a single conductor of the DC transmission system if the ground is used as the return path of the system. Furthermore, there is no transmission loss caused by the reactive current in DC systems [4].
- **There is no need of synchronization, and the control is less complex.** In case of using DC PDN, the integration of renewable energy in DC does not require frequency synchronization and neither control the reactive power. Therefore, the control and operation of the network are also affected because it becomes less complicated. DC systems rise the stability, reliability, and quality. In contrast, in AC microgrids the frequency requires to be fixed at 50 or 60 Hz during the operation time [2], [4].
- **Best efficiency and integration of DC in low voltage.** The cost is reduced in the DC grid due to the AC/DC converters are avoided. Electronic devices such as computers, LEDs, and TV are certainly more compatible with DC power supply. In this way, the losses decrease, and energy is saved [2].

On the other hand, some disadvantages of DC PDN are:

- **High protection cost.** The circuit breaker and equipment are under development in DC systems. As there is no natural zero crossing of the current in the DC grid, protection is more difficult to control compared to AC grid protection [2].
- **Absent of specific standards.** Several parameters, such as voltage levels, need to be specified in a system to be implemented correctly. The fact that DC is not as common as AC applications result in a lack of standards when it comes to their part. To facilitate DC entry into the electrical system, this issue must be examined. The new technology is not widely tested under real conditions[2]. AC technology provides the means to develop more efficient and cost-effective equipment because electrical energy production, transmission, and distribution are based on it.
- In terms of **construction cost**, AC networks are less expensive than DC. The reason for this is that DC technology has developed more recently and the innovation in those areas is integrated into the price [2].

The comparison of AC and DC is outlined in Table 2.1.

Table 2.1 Comparison between AC and DC solutions for power distribution networks with renewable integration.

CATEGORY	MVAC	MVDC
Integration of RES, ESS and DC loads	Not effective	Effective
Control	Complicated: Voltage and regulation is needed	Easy: No frequency control, no reactive power
Skin effect	Yes	No
Standards and technology development	Sufficient	Insufficient
Protection	Developed. Cost-effective circuit breaker	Underdeveloped. High-cost circuit breaker
Construction cost	Low	High

2.2 MVDC NETWORKS

There are three levels of voltage in DC: i) High voltage (HV), from 100 kV to 800 kV; ii) Medium voltage (MV), from 1.5 kV to 100 kV; and iii) Low voltage (LV), which is less than 1.5 kV. Nowadays, the LVDC is very developed due to their use in homes, buildings, electric vehicle charging infrastructure and datacenters. The same is true for HVDC, for example, it is used for connecting remote generation and remote loads, and for connecting offshore wind farms [1]. However, MVDC is not fully explored.

The motivation of implementing MVDC distribution grids is also driven by the possible interconnection with existing AC grids to provide additional services. MVDC is beginning to be considered as an alternative for enhancing transfer capacity and providing increased power quality at distribution networks. Also, it can work with renewable energies and energy storage systems [5]. Nevertheless, the main challenge is to build a DCT. Developing high power medium voltage converter technologies that offer galvanic insulation is necessary to support the development of medium voltage direct current grids. With increasing line lengths and power, DC transmission offers more benefits. Thus, the economic viability of MVDC grids is still in question [6].

The DC transformer (DCT) adapts voltage levels and isolates the electrical lines between nodes in MVDC, they are constantly under study and development. To build a medium frequency transformer for DC there are some challenges such as business case, cost, efficiency, reliability, availability and galvanic isolation seen as necessary. The motivation is to have a lower volume for a easier system integration, lower weight, less material with lower investment cost and lower environmental footprint, improved efficiency for each application specific case, and modularity for fractional power processing [7]. It is highly desirable to have open loop operation so the DCT operates as a AC transformer, without imposing any voltage or power set point. This leads to simple model and reduce its impact on the system stability. DCT, as a bidirectional device, recognizes how power is flowing and allows it to flow naturally through its branches in the most convenient direction. Fig. 2.2 shows a bidirectional LCC.

The voltage level for MVDC has not been standardized internationally. In the studied DC PDN the main voltage used are 10 kV, 5 kV and 2.5 kV [9]. In [10] it was used these voltage and the DCT has a power rating of 10 MW. A variety of Pilot Projects using other voltages are shown in [1], such as: Angle DC, where the nominal DC voltage is 27 kV, ABB HVDC Light, With a nominal DC voltage of 15.9 kV and the AC output voltage has a nominal value of 17.9 kV, or Siemens MVDC PLUS, with DC voltages of 20 kV and 50 kV. Other researches uses 6.6 kV and 12 kV such as in [11].

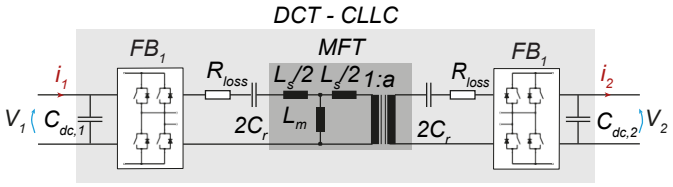

Fig. 2.2 DC transformer topology, FB bidirectional LLC [8]

Next section shows different applications and architectures in MVDC.

2.2.1 APPLICATIONS

In distribution grids, DC technology has not yet been established as the networks are currently based on AC technology. However, there are increasing numbers of projects and research studies examining the use of MVDC PDN as shown in Figure 2.3.

- **Electrical ship.** DC grid systems on board marine vessels are becoming more popular as emerging technologies. Several benefits can be gained from this technique, including:
  - Savings on fuel thanks to the suppressing of the service generators, allowing the propulsion system to be fully utilized [12].
  - Furthermore, AC components like transformers and cables can be minimized, increasing available space and a weight reduction [13].
  - The power network no longer operates at 50/60 Hz. Due to the wider fuel-efficient loading range of variable speed diesel generators in comparison to conventional fixed speed diesel generators, they can operate at a greater fuel efficiency.
  - ESS and future energy sources can be easily integrated into a DC on-board system with minimal changes made to the system [4].
- **Railway Electrification**. A train powered by electricity does not emit greenhouse gases and is more beneficial to the environment than a diesel train. For low speed and urban rail systems, LVDC/MVDC has traditionally been used; for intercity and highspeed rail systems, MVAC is used. AC supply lines have some disadvantages, such as the need for reactive power compensation [14].
- **Power Systems**. Due to its ease of use, AC technology has been utilised because it is possible to increase voltage with transformers. Most of HVDC stations are build with current source inverter (CSI). Nevertheless, advances in voltage source converters (VSCs), which are typically more efficient than CSI designs, have enabled the introduction of more advanced HVDC systems promoting DC systems, such as MVDC PDN [14]. The advantages of this as explained in section 2.1.

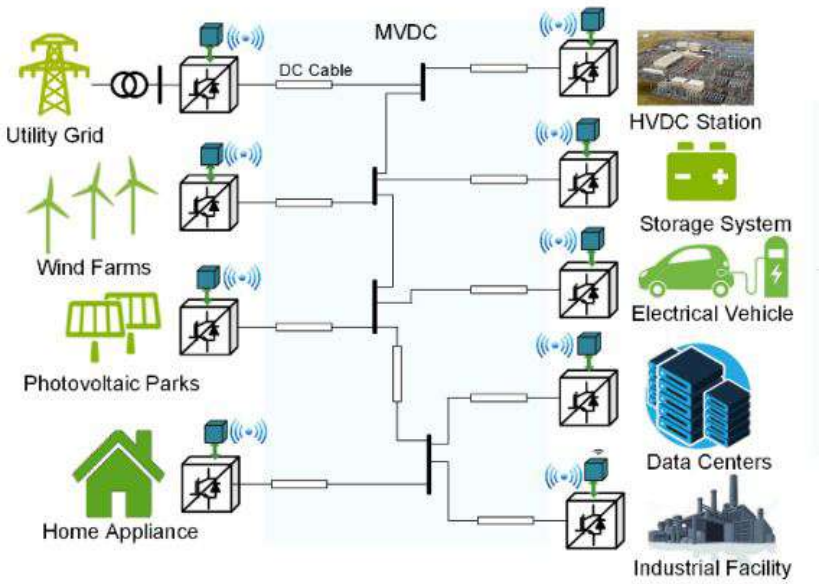

Fig. 2.3 MVDC Applications in future grids [15].

2.2.2 ARCHITECTURES

Power production of renewable energies is changeable and uncertain, it depend on the conditions of the weather. Owing to these, the way that MVDC system is connected is important for the purpose of ensure the reliability of the system, and for supply all the loads in each moment.

There are different types of architectures such as, radial, ring and mesh configuration. Each one of them has their advantages and disadvantages. In this project, different simulations have been carried out analysing and comparing each of these three types of configurations in different cases. In current system of transmission, generation and distribution of electrical energy, these topologies are applied.

- RADIAL CONFIGURATION

For power distribution grids, radial networks are commonly used, especially, it is extensively used for LVDC residential loads [16]. This topology is a tree shape, with no close loops. As can be seen in Fig. 2.4, the energy flows from the main feeder and then create the main DC bus and the main path. The different renewable generation resources and consumption are connected to this path.

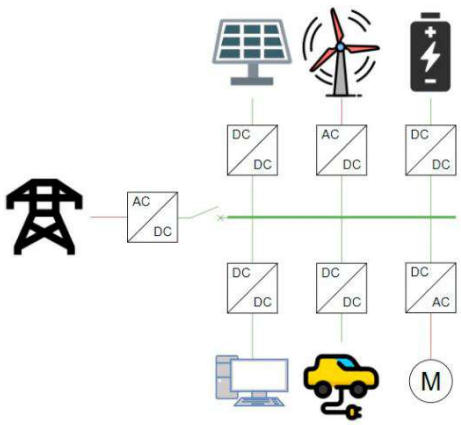

Fig. 2.4 Scheme of radial configuration with renewable energies, batteries and different types of loads [2].

The benefits of this are the following: This is the simplest system and most economical topology due to fewer cables are use it. The coordination and design of circuit protection are relatively simple for a radial network system. The rating requirements for components can be easily determine [2]. Also, the system is easier to analyze and operate when the station is located at the center of the load.

On the contrary, the reliability of the distribution system with this structure is relatively low, if a fault occurs all the lines down-stream will lose power. Radial networks appear to have very little flexibility in their growth when observed from the planning side. This means that if the consumption increase and exceeds the original system, in radial, new feeders need to be created. In most cases, new cables or other components would need to be installed to accommodate the load addition or new generation integration unless the original cables and components were oversized. Thus, this will add to additional expenses [2], [17], [18].

- RING CONFIGURATION

Fig. 2.5 illustrates the ring configuration made up of lines forming geometrical loops, providing two alternative paths for power flow throughout the grid, therefore it is more reliable. As a result, the voltage stability and power losses are more suitable, but a more refined protection system is needed [19].

Ring networks allow the utility to send power to any point on the ring. Due to this, many of the loads on the ring can still be run without interruption of service. Residential areas, with multiple directions of current flow, commonly use this topology [20].

The advantages of this are the following: higher reliability to consumers compared to radial grids. Each bus has the protection switches situated before and after. Consequently, fast-acting DC switches, offer enough flexibility by isolating the faulty bus [2]. This de-energizes the fault zone and all breaker are opened. The supply is guaranteed through the alternative path.

The disadvantages are: Highly depends on AC grid supply. A fault in the AC feeder does not allow the DC microgrid system to get its power from the AC grid [4]. Compared to a radial system, a ring system is only slightly more complex, but its major disadvantage is it supply all the capacity and cost of a ring system [19].

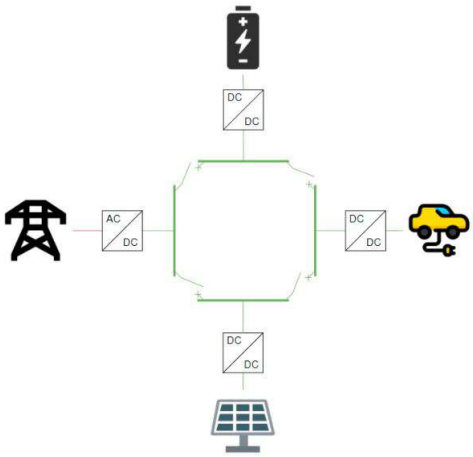

Fig. 2.5 Scheme of ring configuration with renewable energies, batteries and different types of loads [2].

- MESH CONFIGURATION

In mesh configuration, shown in Fig. 2.6, also known as a multi-terminal grid, several connections are offered to every node of the grid, there are more than one feeder to supply power to various parts of the system. Although it offers flexibility, it can also be challenging in terms of operation and protection [19]. There are applications of similar architectures in various HVDC systems, such as off-shore wind farms as well as underground urban distribution networks [4].

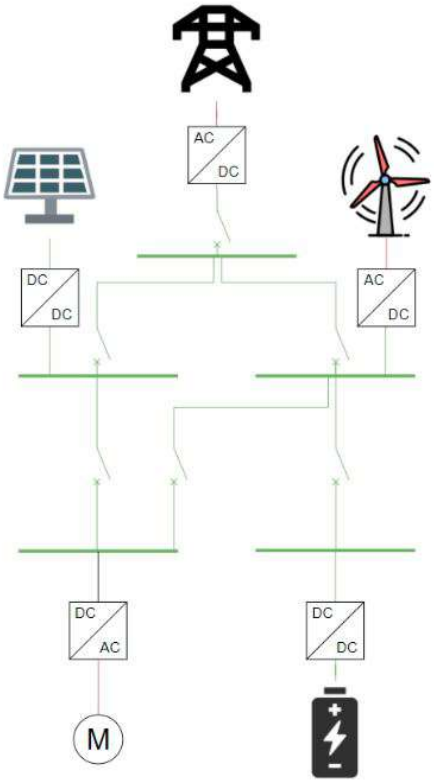

Fig. 2.6 Scheme of mesh configuration with renewable energies, batteries and different types of loads [2].

Among the benefits of this are: It is an efficient method for short-distance transmissions and integrates well with existing networks. Thus, a radial network can become a mesh network. Radial systems are the easiest to protect, whereas mesh networks have a higher short circuit power. Mesh networks have a relatively balanced voltage profile and high reliability due to their redundancy [19].

Negative aspects include: A complex designing. Mesh grid configurations are more complicated than ring and radial grids because they include many different connections between nodes. Because of this, they are quite challenging to operate and protect [19].

To conclude this section, Table 2.2 presents an overview of the three configurations [20], [2].

Table 2.2 Comparison of the main characteristics between radial, ring and mesh configuration.

CHARACTERISTICS	RADIAL	RING	MESH
Sources	Multiple	Multiple	Multiple
Cost	Low	Medium	High
Simplicity	High	Medium	Low
Maintenance	Low	Medium	High
Stability and Reliability	Low	Medium	High
Easy integration RES	Yes	Yes	Yes

Steady-state analysis consists of modeling the entire system and working in steady state, without changes in the system caused by faults or other factors. Nevertheless, these models take long processing times and also its modeling, which may be non-efficient for large scale DC power grids [21]. There are analytical models that allow solving the power flow from a series of equations such as Modified Mode Analysis (MNA), it is easily implementable for systems with multiple nodes [8]. In AC, two methods are commonly used to determine power flow in an electrical system. Gauss-Seidel method, which consists of calculating, through an iterative procedure, the voltage at each node based on the available voltage and power values in the previous iteration. And Newton-Raphson method, which consists of successively obtaining new voltage and power values through first-order approximations of the nonlinear functions involved.

In HVDC networks, similar research has been done about what type of architecture is better as shown in [21]. That paper discussed aspects of steady-state optimal power-flow and transient simulations in a large, combined AC/DC network. The simulations performed for four different DC network topologies (radial, ring shaped, lightly meshed, and densely meshed) and three different ground fault locations. A comparison of all scenarios has been made in terms of overall system losses, transient fault currents, and postfault contingencies. It demonstrated that a ring-shaped topology performs best in terms of transient overcurrents due to the low and equally distributed number of feeders per busbar, but has large overall system losses in the steady-state operation given the long transmission distances and low number of cables. On the other hand, a densely meshed grid provides low system losses, but high transient overcurrents, because of the increased number of feeders per busbar and short transmission distances to strong AC nodes. It concludes that this topology is the best in terms of reliability and flexibility for power exchange, but the investment costs are high due to the large number of cables. DC topologies cannot satisfy all aspects simultaneously and individual calculations must be done for each network and power-flow scenario. This project follows the same route but focusing on MVDC PDN and not going to transient analysis as faults.

Part I

POWER FLOW ANALYSIS

3 | SCENARIOS UNDER STUDY

Three different demonstration scenarios have been considered for the purpose of carrying out the study of networks in MVDC. A **district**, which is a residential area, a **rural area**, and an **urban area** have been chosen in this case. In this investigation, some of the data referred to these three scenarios are taken from a study by Romande Energie [22]. Romande Energie Electric network in local balance Demonstrator (REEL Demo) focuses on investigating how control and management system of the future electricity grid can be improved, focusing on the automation of active distribution networks. For this, three demonstrations sites (district, rural area and urban area) are taken as an example. So, it is analyzed which network control solution is more suitable for different voltage levels. Also, testing and validation solutions for the monitoring and management of the future active power grid, at different scales namely Smart City, Grid, Building or Home is done. The electrical networks presented in this report are in alternating current, thus, the system is adapted to MVDC power distribution network, using the same data.

The study areas have renewable energy integrated. On the basis of REEL Demo, the analysis of this project will be conducted with real data and carried out with the most realistic simulations possible to integrate it with current consumption and networks. Also, this has been done in order to have greater variety in terms of number of consumers, length of lines, different load profiles, the number of transformers used, production of renewable energy, and the difficulty of drawing the lines to generate electricity.

Each case study can be further divided into zones and the consumption varies by zone (for example, to distinguish between the eastern and western sections of a place, each piece is a different zone). In the three cases, only total consumption and the production of the area were known, based on the study of Romande Energie. In other words, it was not known in detail how the consumption was distributed (knowing how many watts or how many buildings there are in each zone). Because of this, to build the final distribution networks, several steps have been developed, and specific aspects have been considered:

- First, the study area has been divided into different zones to establish the location of a group of consumers.
- Then, the **consumption** of the loads corresponding to each case has been estimated based on the total consumption and the number of buildings in each zone. This means that not all consumption is the same and there are certain zones with a greater demand than others. For the location of the PVs, it has been examined using the satellite view of Google Maps, where this type of installation already existed, to make it as realistic as possible. District area has two types of consumers: houses and farms. Rural area has only houses. And in Urban area, new profiles have been included to have a greater variety; this area has houses, restaurants, schools, supermarkets, industry, and a hospital. Fig. **4.1** shows the load profiles of each type of consumer.
- It has been defined through which places the **electric lines** could run to reach the points where it has been defined the consumers. It is easiest and most logical to trace the route of the networks close to roads or paths. Although, in certain circumstances, these lines cannot be drawn due to factors such as the area's geography, the presence of mountains, or for reasons of security or protected areas. Once the layout of the lines has been established, the length of each line has been measured.
- The **voltage** level for the networks was 10 kV, 5 kV, and 2.5 kV, according to comments in 2.2.
- The **DCT** location is determined to change voltage, this usually takes place when you connect the PVs to the network.
- To develop each diagram, first it was designed the radial topology, and then, the two other **configurations**. In ring architecture, the main ring has the highest voltage to minimize losses and the number of DCT. For mesh, new lines were added to the radial for connect nodes that had not been previously connected.
- In order to simplify the comparison of the results of the simulations, to name nodes in schemes, the same number corresponds to the same **node** in each type of configuration.

In following sections, it is described each scenario in detail. First, a brief description of each case is provided. Then, an aerial view is used to show where the lines run, and then the scheme is displayed which the nodes with numbers, and the consumption points with letters and numbers. Loads appear in white, renewable sources in yellow and the main grid in blue. Tables specified the distances of lines, the number of consumers, and energy sources. The nomenclature used to name lines follows the rule of indicating the nodes between which this line is located. For the same study area, the location of the loads and sources is the same. Furthermore, voltage of each line and location of the transformers are also shown in the schemes. Fig. **3.1** displays the models to simulate. Ultimately, this thesis deals with the planning of DC PDN, and the following comparisons are worthy to compare with the actual AC power distribution networks.

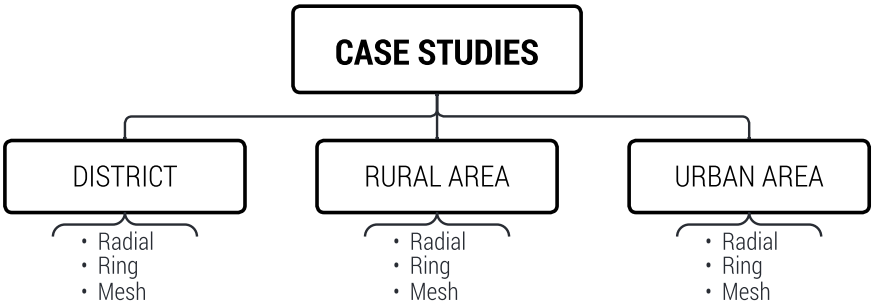

Fig. 3.1 There are three study zones and three configurations are analyzed in each zone, so there are 9 different models.

3.1 DISTRICT

Chapelle-sur-Moudon is a Swiss town located in the canton of Vaud. This district consists of 57 residential blocks and 9 farms with a total of 88 consumers. There are two PV production, one with a peak installed power of PV 72 kW, and other big producer with 192 kW PV [22]. Figure 3.2 shows an areal view of the District case, and Table 3.1 shows the data corresponding to the consumption and the maximum generation of the photovoltaic panels. The distribution of the loads was made from the zones differentiated by the roads. The PVs are located where photovoltaic panels are currently installed. And the grid is location in a position intermediate.

Fig. 3.2 Aerial view of Chapelle-sur-Moudon (District case) with location of the grid (blue), 6 consumers (white) and 2 PVs (yellow).

Table 3.1 Information of Chapelle-sur-Moudon (District case) with the number and type of consumers at each point and maximum PV production of each PV source.

Load	Consumers	Load	Consumers	Source	kW
a1	20 h[1]	b1	6 h	PV1	192
a2	10 h	b2	2 h, 2 f	PV2	72
a3	10 h, 3 f[2]	c	9 h, 4 f		

[1] residential houses, [2] farm.

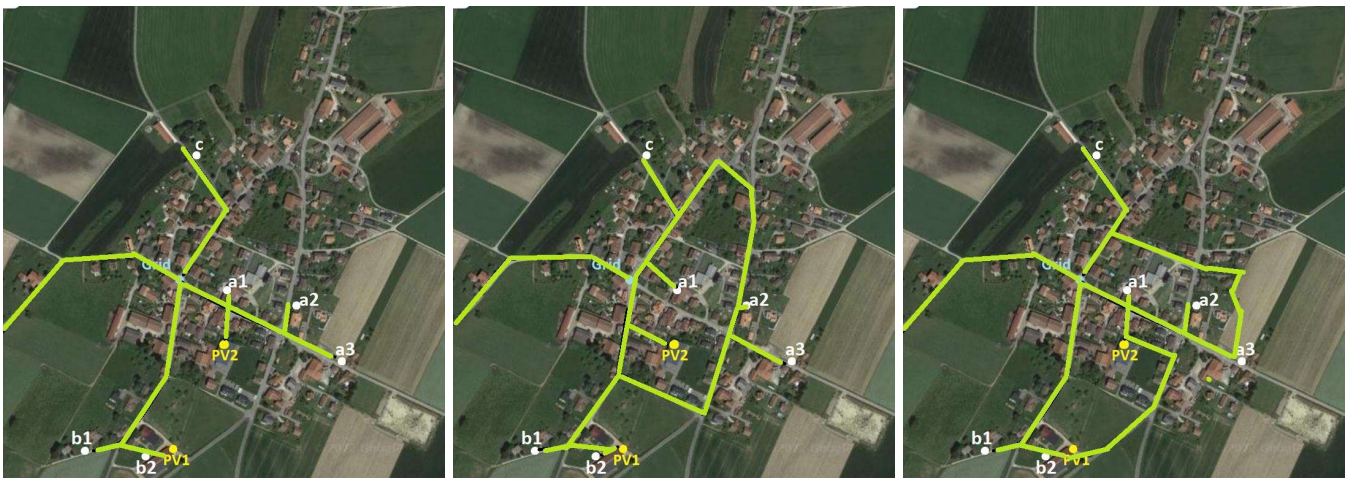

Fig. 3.3 Layout electrical lines for District case: (a) Radial Configuration; (b) Ring Configuration (c) Mesh Configuration.

3.1.1 RADIAL CONFIGURATION

Radial configuration is the most simple and has the fewest lines. Electrical lines follow roads in this configuration. To draw power lines, we started from the node where grid is located (node 1) and from there the lines were drawn following the existing paths until reaching the rest of nodes, doing in a simplest way. Figure **3.4** illustrates the scheme of this configuration with the number of each node, and Table **3.2** describes the length of each line. The main line is in 10 kV (blue color), and there are two DCTs. one for each PV. One of them connects with PV1 and load b2 in node 5, and the other only connects with PV2. The 13 power lines have a total length of **6.32 km**. The longest line is the line that joins nodes 1 (grid) and 8 with 5 km, and the shortest is the line joining nodes 2 and 3 (load b1) with 16 meters. There are 16 nodes, 12 nodes in 10 kV and 4 nodes in 5 kV.

To make the diagram, 10 kV lines are in blue, and orange lines correspond to 5 kV. Nodes are named with numbers and follow an order. Node 1 corresponding to the grid, and then we go to left part of the diagram to continue with node 2, which is the first node that joins the grid with left part of the diagram, and from there we continue the numbering from left to right and then down. In aerial view of Disctrict case there are three different zones: left zone (loads, b1, b2 and PV1), central zone (PV2, loads a1, a2 and a3) and right zone (load c). So, the nomenclature of loads first has a letter, which indicates the zone in which it is located (a, b or c), and if there is more than one load in that zone, a number is added to differentiate loads from the same zone.

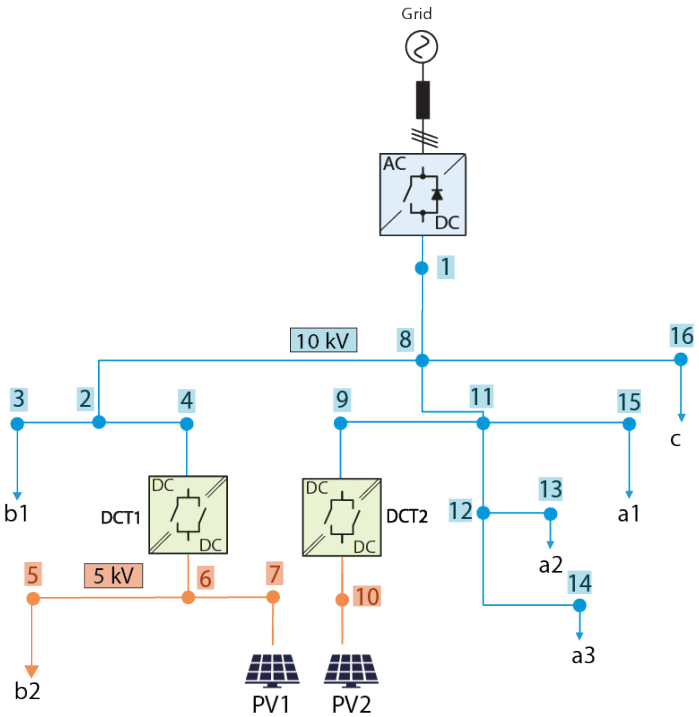

Fig. 3.4 Diagram of the radial configuration for District case with the grid, the 6 consumers, the 2 PVs, the 2 DCTs and the 13 power lines.

Table 3.2 Length of the 13 power lines in radial configuration for District case. Subscripts indicate the starting and ending nodes of the line.

Line	Length (m)	Line	Length (m)	Line	Length (m)	Line	Length (m)
l_{1-8}	5000	l_{6-5}	77	l_{11-12}	91	l_{8-16}	331
l_{8-2}	270	l_{6-7}	97	l_{12-13}	57		
l_{2-3}	16	l_{11-9}	83	l_{12-14}	90		
l_{2-4}	53	l_{8-11}	106	l_{11-15}	51		

3.1.2 RING CONFIGURATION

In this configuration, lines form a closed area following the existing paths. Then join this ring, all nodes. This main ring has been drawn at a voltage of 10 kV to have less losses. Figure **3.5** shows how the scheme for this configuration looks, and Table **3.3** indicates the length of each line. Like in radial configuration, there are two DCTs, one for each PV and they connect the sames nodes like in radial. The 18 power lines have a total length of **6.71 km**, a little bit more than in radial. Line l_{17-12} may seem to be the longest but this is not the case. The longest line connects nodes 1 (grid) and 8 with 5 km, and now, the shortest is the line joining nodes 12 and 13 (load a2) with 21 meters. There are 20 nodes, 16 nodes in 10 kV and 4 nodes in 5 kV.

Nodes have the same nomenclature as in radial case, that is, in radial case load b2 corresponded to node 5, and now in ring load b2 is also node 5, so it may seem that now the nomenclature of the nodes do not follow a logical order. But this has been done to compare more easily the results knowing that nodes represent the same point.

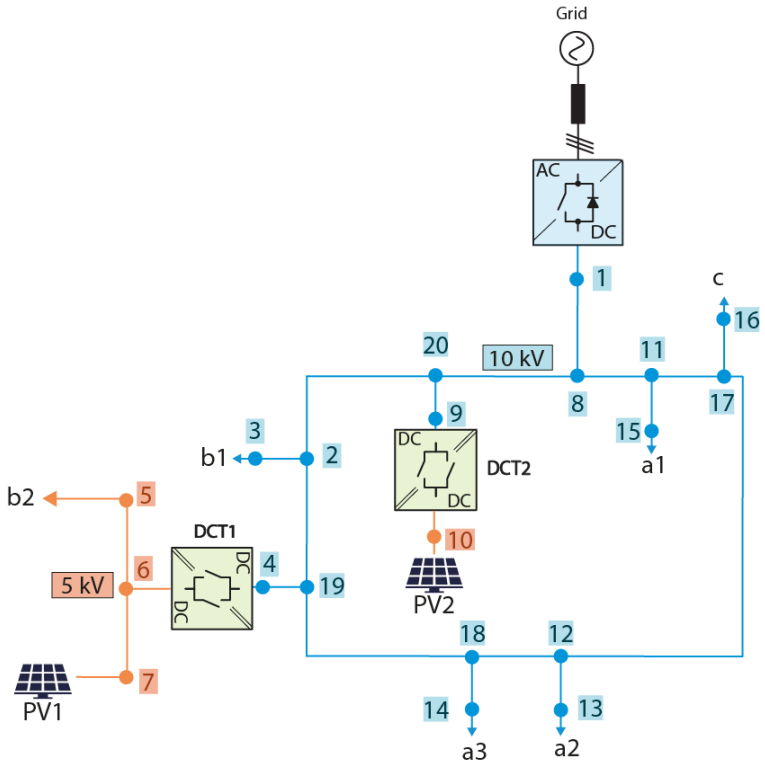

Fig. 3.5 Diagram of the ring configuration for District case with the grid, the 6 consumers, the 2 PVs, the 2 DCTs and the 18 power lines.

Table 3.3 Length of the 18 power lines in ring configuration for District case. Subscripts indicate the starting and ending nodes of the line.

Line	Length (m)	Line	Length (m)	Line	Length (m)	Line	Length (m)
l_{1-8}	5000	l_{17-12}	284	l_{19-4}	106	l_{2-20}	75
l_{8-11}	44	l_{12-13}	21	l_{6-5}	40	l_{20-9}	73
l_{11-15}	76	l_{12-18}	73	l_{6-7}	23	l_{20-8}	97
l_{11-17}	104	l_{18-14}	90	l_{19-2}	68		
l_{17-16}	131	l_{18-19}	263	l_{2-3}	144		

3.1.3 MESH CONFIGURATION

Two lines were added to radial configuration to create a mesh. These join nodes 6 and 10 to each other, so the production of PV2 or PV1 can be transported to other zones; and the line that joins nodes 14 and 17 to join the central zone with the zone on the left (load c). To have a greater variety, one of the new lines has a voltage of 10 kV and the other 5 kV. Now if one of the DCT stops working the other DCT can feed the rest of the loads. Figure **3.6** is an illustration of this configuration with numbers indicating each node, and Table **3.4** provides the line lengths. The 15 power lines have a total length of **7.13 km**. Since there are more lines, the total length is greater. Line connecting nodes 1 (grid) and 8 has the longest length with 5 km, and the shortest is the line joining nodes 2 and 3 (load b1) with 16 meters. There are 17 nodes, 13 nodes in 10 kV and 4 nodes in 5 kV. Because radial scheme is used as a reference, the nomenclature of nodes is the same as in that configuration but adding node 17.

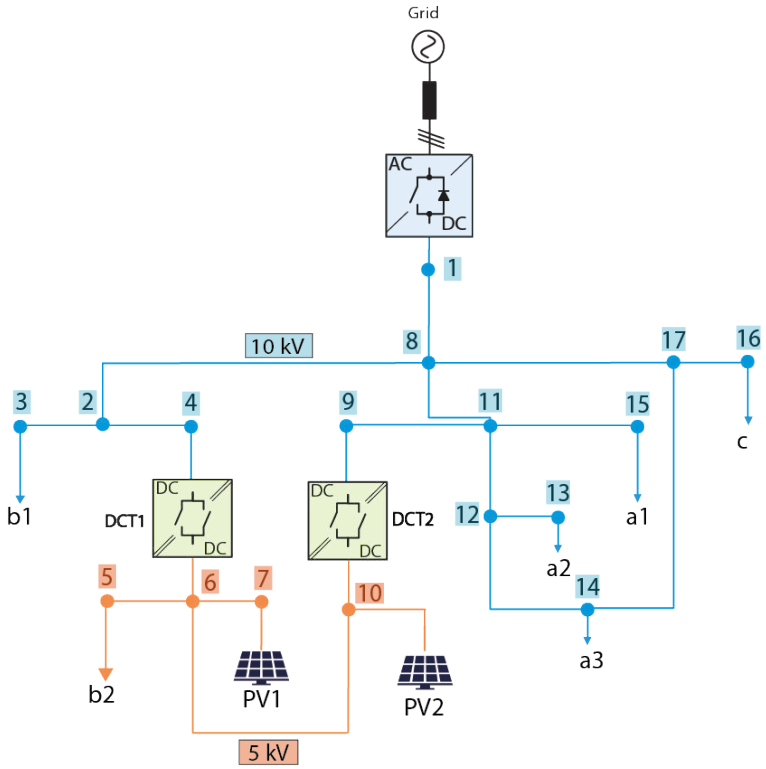

Fig. 3.6 Diagram of the mesh configuration for District case with the grid, the 6 consumers, the 2 PVs, the 2 DCTs and the 15 power lines.

Table 3.4 Length of the 15 power lines in mesh configuration for District case. Subscripts indicate starting and ending nodes of the line.

Line	Length (m)	Line	Length (m)	Line	Length (m)	Line	Length (m)
l_{1-8}	5000	l_{6-5}	77	l_{11-12}	91	l_{8-17}	331
l_{8-2}	270	l_{6-7}	97	l_{12-13}	57	l_{17-14}	386
l_{2-3}	16	l_{11-9}	83	l_{12-14}	90	l_{10-6}	423
l_{2-4}	53	l_{8-11}	106	l_{11-15}	51		

3.2 RURAL AREA

Aigle is a Swiss commune in the canton of Vaud. This case consists of an 815 kW Hydro power plant and a large 1660 kW PV installation. During winter, power consumption can reach 4.3 MW, and during summer, 2.9 MW [22]. Winter case is the selected due to the more power. A view of this case is shown in Figure 3.7, and Table 3.5 displays the maximum generation and consumption data. The main line is in 10 kV, and there are two DCTs. One before load d, in the event that PV installations are made in the future, and other on the right side due to PV and the hydro power plant.

In the case of consumers, the area has been divided into five different zones (Figure 3.7), all of this consumers are residential houses. Due to their size, two of these zones have a higher rate of consumption (d and e). The rest are small rural areas and mountainous areas. In Table 3.5 represents the highest punctual consumption of that zone. The grid is located at a point where there are currently power distribution networks.

Fig. 3.7 Aerial view of Aigle (Rural area) with the location of the grid (blue), the 6 consumers (white) and the 2 renewable energies (yellow).

Table 3.5 Information of Aigle (Rural Area) with the maximum consumption of each consumers at each point and maximum production of each renewable energy source.

Load	kW	Load	kW	Source	kW
a	4.3	d	2601.5	PV	1600
b	172	e	215	Hydro	815
c	17.2	f	1290		

Figure 3.8 displays how the power lines are distributed among the three types of configurations.

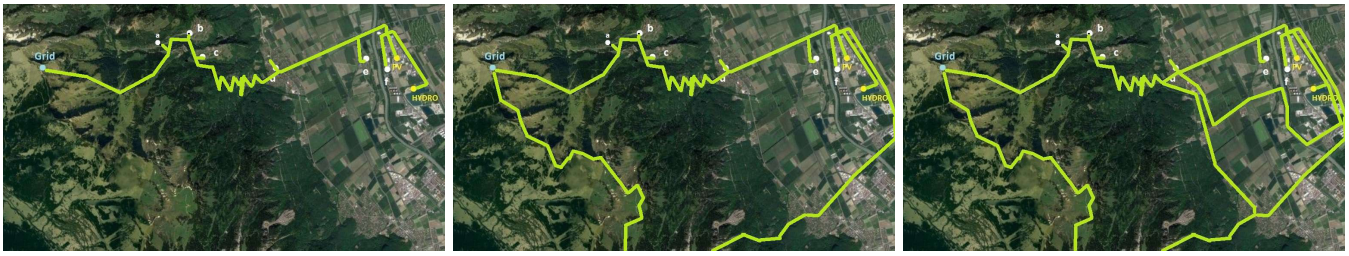

(a) (b) (c)

Fig. 3.8 Layout electrical lines for Rural Area case: (a) Radial Configuration; (b) Ring Configuration (c) Mesh Configuration.

3.2.1 RADIAL CONFIGURATION

Similar to District case, the simplest and shortest configuration is radial. For the layout of the lines, the same route that currently exists has been carried out. Because there are mountainous areas, the route of the power lines must be adapted to this. Finally, each node is joined with the main path. This main road is at 10 kV. The scheme is in Fig. **3.9** and Table **3.6** describes the length of each line. The 13 power lines have a total length of **19.42 km** and the line connecting nodes 4 (load c) and 5 has the longest length with 7 km, and the shortest is the line joining nodes 5 and 6 with 129 meters. There are 16 nodes, 10 nodes in 10 kV and 6 nodes in 5 kV. Since we are in a rural area, the loads are further away from each other and the distances are greater than in the District case.

To make the diagram, 10 kV lines are in blue, and orange lines correspond to 5 kV. Node 1 is the grid, and then, if we continue along the main path (blue line) nodes are named from left to right, and when there is a path parallel to the main line, the nodes of this path are named first and then continue along the main path. There are 5 clearly differentiated zones and that is why the loads are named with different letters (a, b, c, d, e and f).

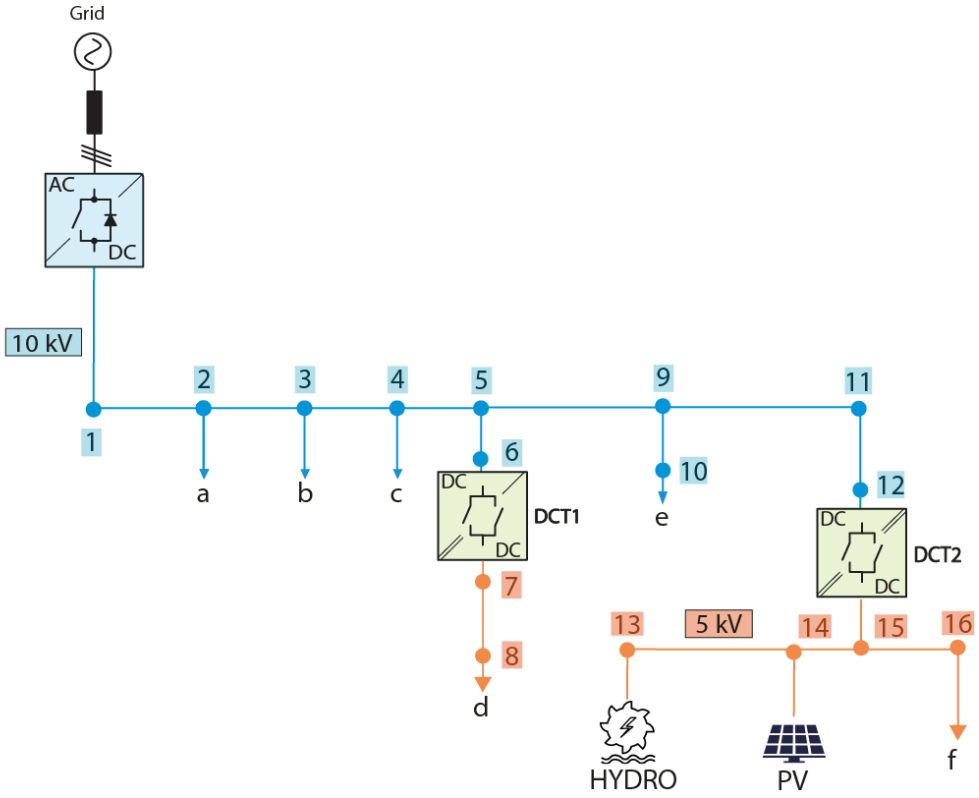

Fig. 3.9 Diagram of the radial configuration for Rural Area case with the grid, the 6 consumers, the 2 renewable energy sources, the 2 DCTs and the 13 power lines.

Table 3.6 Length of the 13 power lines in radial configuration for Rural Area case. Subscripts indicate the starting and ending nodes of the line.

Line	Length (km)	Line	Length (km)	Line	Length (km)	Line	Length (km)
l_{1-2}	3.85	l_{5-6}	0.129	l_{9-11}	0.676	l_{15-16}	0.192
l_{2-3}	1.42	l_{7-8}	0.186	l_{11-12}	0.292		
l_{3-4}	1.32	l_{5-9}	2.14	l_{15-14}	0.144		
l_{4-5}	7	l_{9-10}	0.563	l_{14-13}	1.51		

3.2.2 RING CONFIGURATION

In ring configuration, **52.22 km** is the total length of the 14 power lines. The scheme is represented in Fig. **3.10** and Table **3.7** describes the length of each line. Currently, there is an electric line already built that goes from the point called Grid to the bottom (Fig. **3.8** b). So, this line has been taken in advantage to build ring and mesh. To do this, a new line has been added that crosses the mountains to reach the consumers on the right side, it is the line which join node 1 with 11. The main ring is in 10 kV. Now, node 1 (grid) and node 11 are connected by the longest line, it has 32.80 km, and the shortest is the line joining nodes 5 and 6 with 129 meters. There are 16 nodes, 10 nodes in 10 kV and 6 nodes in 5 kV and they have the same nomenclature as in radial case.

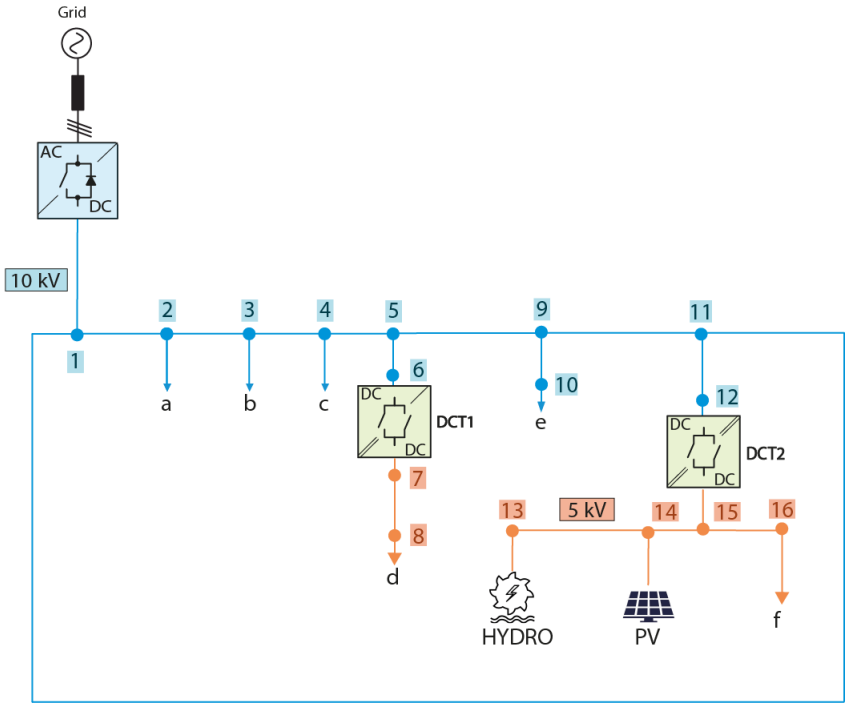

Fig. 3.10 Diagram of the ring configuration for Rural Area case with the grid, the 6 consumers, the 2 renewable energy sources, the 2 DCTs and the 14 power lines.

Table 3.7 Length of the 14 power lines in ring configuration for Rural Area case. Subscripts indicate the starting and ending nodes of the line.

Line	Length (km)	Line	Length (km)	Line	Length (km)	Line	Length (km)
l_{1-2}	3.85	l_{5-6}	0.129	l_{9-11}	0.676	l_{15-16}	0.192
l_{2-3}	1.42	l_{7-8}	0.186	l_{11-12}	0.292	l_{1-11}	32.80
l_{3-4}	1.32	l_{5-9}	2.14	l_{15-14}	0.144		
l_{4-5}	7	l_{9-10}	0.563	l_{14-13}	1.51		

3.2.3 MESH CONFIGURATION

To create a mesh, two lines were added to the ring configuration. These join nodes 17 and 18 to each other; and node 8 with 19 so the production of renewable energy sources can be transported to other zones. In order to have a greater variety, one of the new lines has a voltage of 10 kV and the other 5 kV. Fig. **3.11** represents the scheme, and Table **3.8** describes the length of each line. The total length of the 18 power lines is **64.15 km**. The longest line connecting nodes 1 (grid) and 18, it has 26.39 km, and the shortest is the line joining nodes 5 and with 129 meters. There are 19 nodes, 12 nodes in 10 kV and 7 nodes in 5 kV. Because radial scheme is used as a reference, the nomenclature of nodes is the same as in that configuration but adding node 17, 18 and 19.

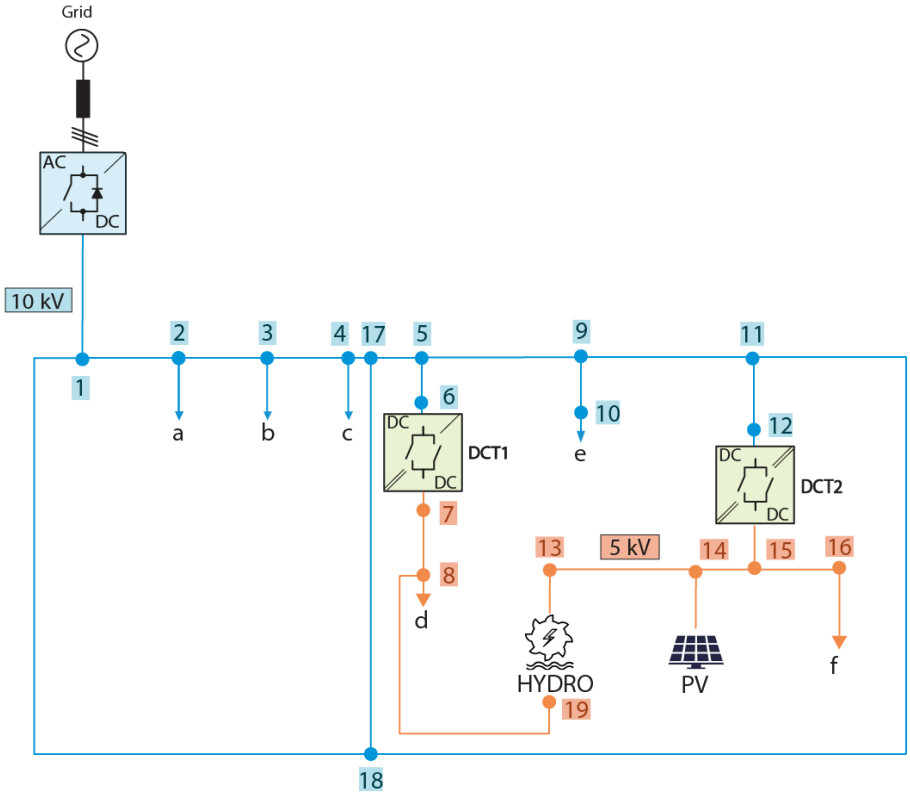

Fig. 3.11 Diagram of the mesh configuration for Rural Area case with the grid, the 6 consumers, the 2 renewable energy sources, the 2 DCTs and the 18 power lines.

Table 3.8 Length of the 18 power lines in mesh configuration for Rural Area case. Subscripts indicate the starting and ending nodes of the line.

Line	Length (km)	Line	Length (km)	Line	Length (km)	Line	Length (km)	Line	Length (km)
l_{1-2}	3.85	l_{17-5}	2.14	l_{9-10}	0.563	l_{14-13}	1.51	l_{18-1}	26.39
l_{2-3}	1.42	l_{5-6}	0.129	l_{9-11}	0.676	l_{15-16}	0.192	l_{8-19}	7.22
l_{3-4}	1.32	l_{7-8}	0.186	l_{11-12}	0.292	l_{11-18}	6.44		
l_{4-17}	4.86	l_{5-9}	2.14	l_{15-14}	0.144	l_{18-17}	4.71		

3.3 URBAN AREA

The last case corresponds to the urban environment. Rolle is a Swiss commune in the canton of Vaud, located in the district of Nyon. This area combines commercial and residential customers. PV units produce a total of 430 kW.[22]. This case is illustrated in Figure **3.12**, and the maximum amount of production and consumption is displayed in Table **3.9**. The main line is in 10 kV, and there are eight DCTs. In this case, in order to have a greater range of data, the analysis area includes 2.5 kV areas as well. The electric line that connects grid 1 with grid 2 is the one that is currently found, for this reason the layout is made from this.

Besides the 1727 houses, new types of load profiles have been added. It had been included 3 supermarkets, 4 schools, 8 restaurants, a hospital and industry. For safety reasons, the hospital will have two DCTs and two power lines. In addition, there are two grids points because it is located in an area with better connections to the electricity grid. Figure **3.13** displays how power lines are distributed across the three configurations.

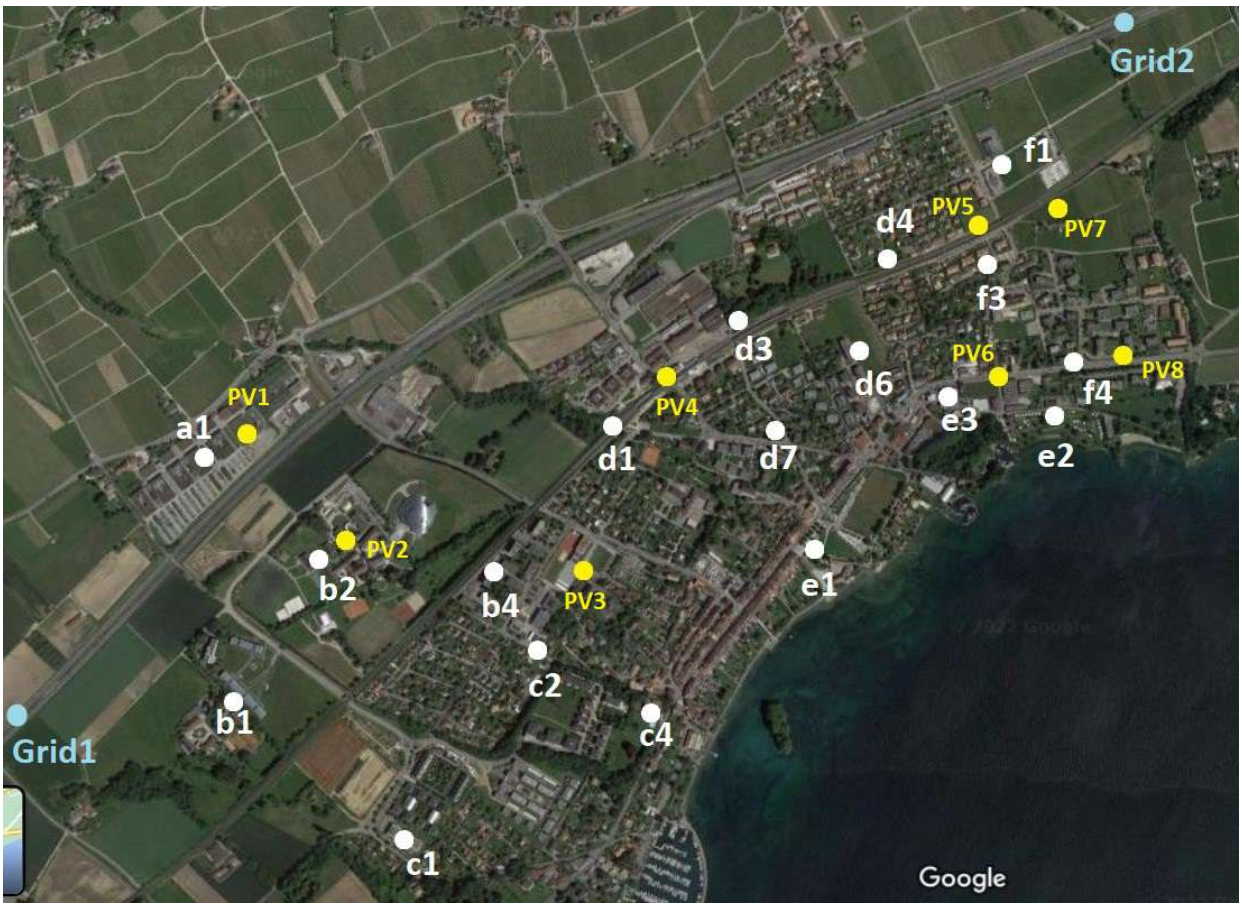

Fig. 3.12 Aerial view of Rolle (Urban area) with the location of the 2 grids (blue), the 18 consumers (white) and the 8 PVs (yellow).

Table 3.9 Information of Rolle (Urban Area) with the number and type of consumers at each point and maximum PV production of each PV source.

Load	Consumers	Load	Consumers	Load	Consumers	Source	kW	Source	kW
a1	Industry	c4	75 h, 3 r[3]	e1	340 h, 1 su, 1s	PV1	170	PV5	100
b1	30 h[1]	d1	30 h, 1 r	e2	82 h	PV2	20	PV6	20
b2	10 h, 1 s[2]	d3	48 h	e3	20 h	PV3	30	PV7	40
b4	70 h, 1 s	d4	170 h	f1	45 h	PV4	30	PV8	10
c1	120 h	d6	62 h	f3	1 hospital				
c2	220 h	d7	84 h, 2 su[4], 1s	f4	321 h, 4 r				

[1] residential houses, [2] school, [3] restaurant, [4] supermarket.

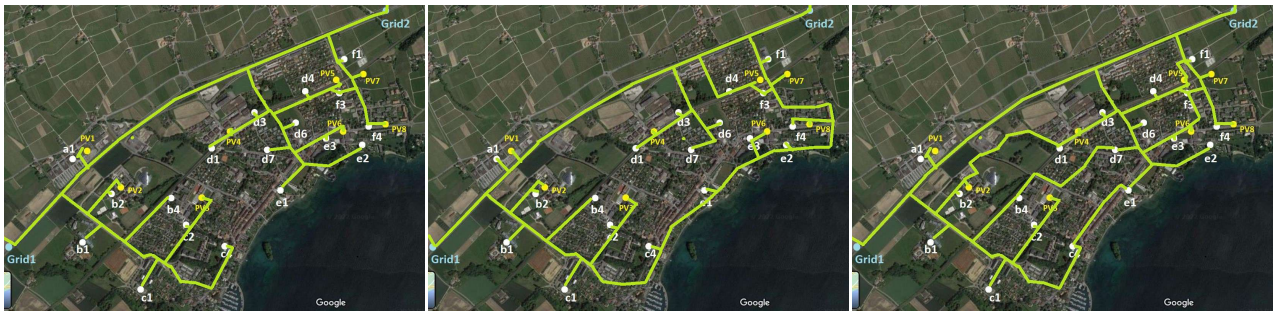

(a) (b) (c)

Fig. 3.13 Layout electrical lines for Urban Area case: (a) Radial Configuration; (b) Ring Configuration (c) Mesh Configuration.

3.3.1 RADIAL CONFIGURATION

In this case, we start from the existing network between Grid 1 and Grid 2 and starting from this main 10 kV line, four paths have been traced, starting from nodes 3, 17, 21 and 39, to reach the rest of nodes. The path that leaves node 17 is used to feed the industry and has its own transformer. Then, lines coming from nodes 3, 21 and 39 are traced along the existing paths connecting with loads and PVs remaining. As mentioned, the hospital, node 45, is powered by two lines, if any line stops working, the other line can continue to feed the hospital, since its operation is important at all times. The scheme is represented in Fig. **3.14** and Table **3.10** describes the length of each line. In total there are 8 DCTs distributed throughout the area. The 40 power lines have a total length of **22.78 km**. Longest line connects nodes 49 (grid 2) and 48, it has 7 km, and shortest is the line joining nodes 46 (load f4) and 47 (PV8) with 20 meters. There are 49 nodes, 11 nodes in 10 kV, 26 nodes in 5 kV and 12 nodes in 2.5 kV.

To develop the diagram, 10 kV lines are in blue, orange lines correspond to 5 kV, and pink lines are in 2.5 kV. The main path is in 10 kV, and different lines join it to reach the points of consumption and PVs. For the nomenclature of nodes, we start with node 1, and we continue numbering in order to left until we reach node 3, where there is a fork. Thus, we continue numbering along that line (node 4). At the end of the line (node 16) is reached, we return to the main path in blue and follow the same method. There are 6 different zones separated by the DCTs, and that is why the 18 loads are named with different letters and numbers (a, b, c, d, e and f).

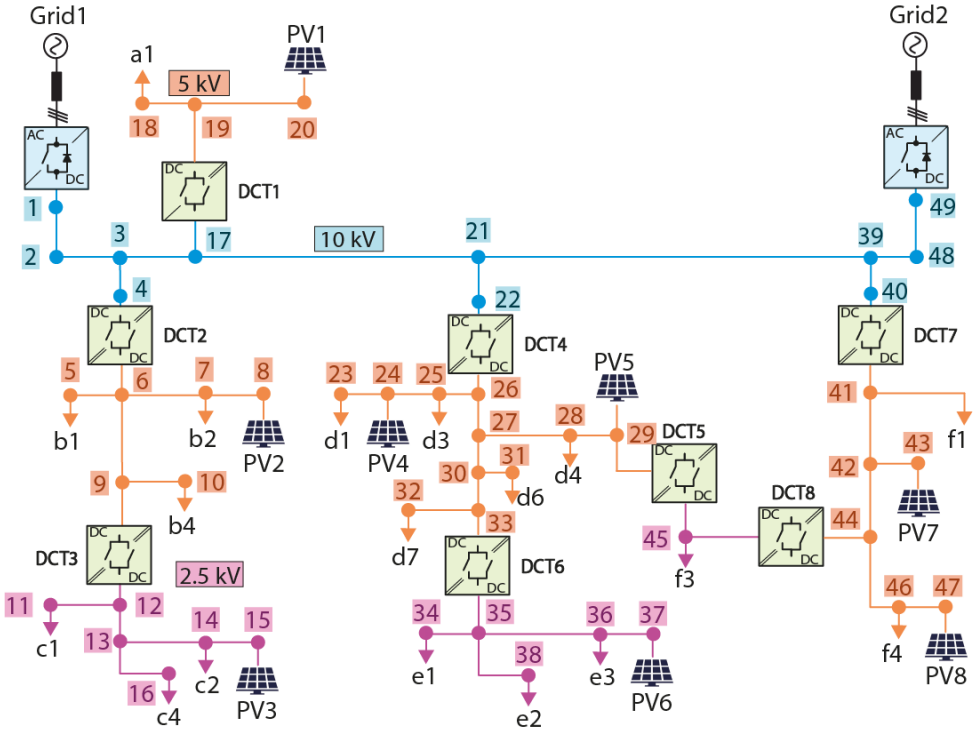

Fig. 3.14 Diagram of radial configuration for Urban Area case with the 2 grids, 18 consumers, 8 PVs, 8 DCTs and 40 power lines.

Table 3.10 Length of the 40 power lines in radial configuration for Urban Area. Subscripts indicate starting and ending nodes of the line.

Line	Length (m)	Line	Length (m)	Line	Length (m)	Line	Length (m)	Line	Length (m)
l_{1-2}	5000	l_{11-12}	82	l_{19-20}	75	l_{28-29}	171	l_{21-39}	523
l_{2-3}	1570	l_{12-13}	140	l_{17-21}	1150	l_{27-30}	70	l_{39-40}	246
l_{3-4}	209	l_{13-14}	125	l_{21-22}	243	l_{30-31}	34	l_{41-42}	240
l_{5-6}	100	l_{14-15}	130	l_{23-24}	253	l_{30-33}	83	l_{42-43}	30
l_{6-7}	439	l_{13-16}	600	l_{24-25}	50	l_{32-33}	270	l_{44-46}	340
l_{7-8}	40	l_{3-17}	393	l_{25-26}	365	l_{34-35}	500	l_{46-47}	20
l_{6-9}	339	l_{17-19}	74	l_{26-27}	147	l_{35-36}	174	l_{29-45}	224
l_{9-10}	544	l_{18-19}	340	l_{27-28}	194	l_{35-38}	248	l_{48-49}	7000

3.3.2 RING CONFIGURATION

To trace a closed ring path, the charges at the bottom are connected to each other, creating nodes 16, 17, 18 and 19. In this case, the nomenclature of the nodes is not the same as in the radial case. In other words, in the radial case, load b1 was node number 5, but now that load is number 7. This has been done in order to follow an order when establishing the number of each node. This only happens in this case, for the cases of District and Rural area it does not happen. Now there are two more DCTs. The main ring has been made at 5 kV and not at 10 kV to have a lower number of DCTs. There are 41 power lines with a total length of **24.05 km**. The longest line connects nodes 28 (grid 2) and 29, it has 7 km, and the shortest is the line joining nodes 8 and 11 with 20 meters. There are 48 nodes, 3 nodes in 10 kV, 36 nodes in 5 kV and 9 nodes in 2.5 kV. Table **3.11** specifies the length of each line, while Fig. **3.15** shows the scheme.

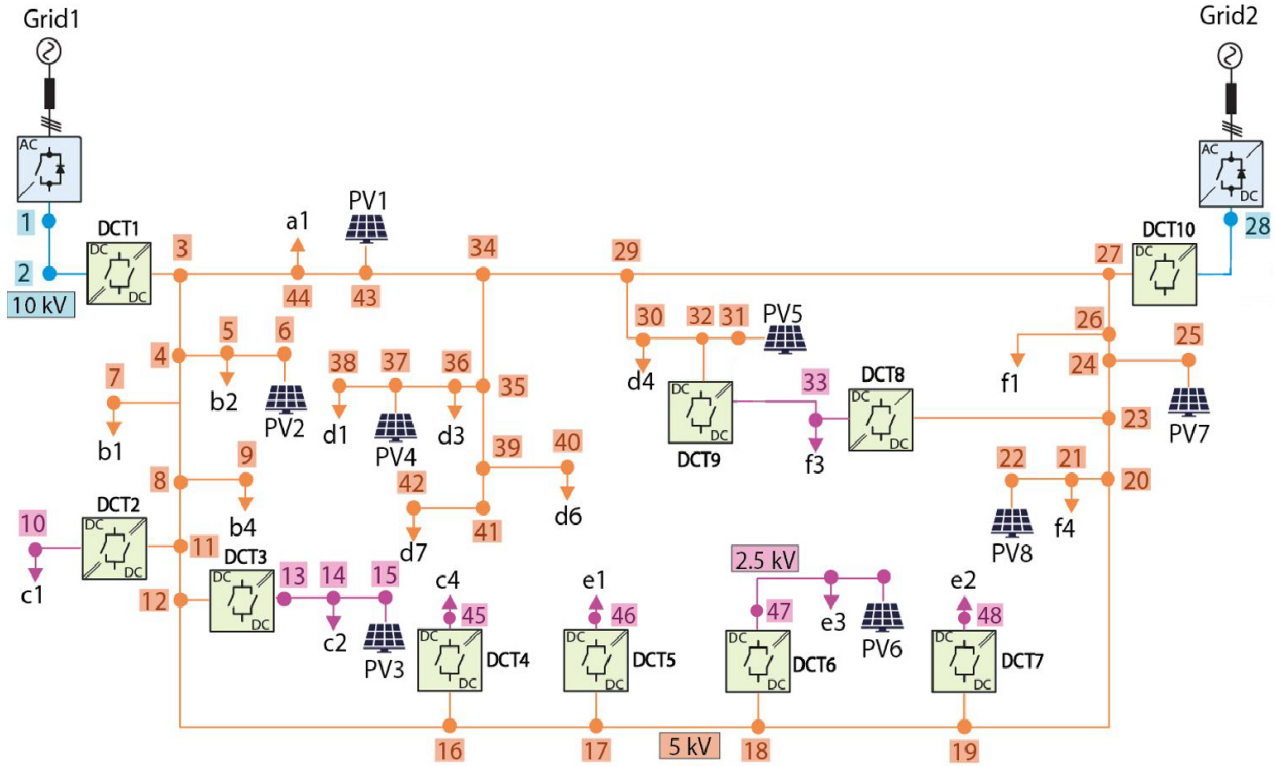

Fig. 3.15 Diagram of the ring configuration for Urban Area case with the 2 grids, the 18 consumers, the 8 PVs, the 10 DCTs and the 41 power lines.

Table 3.11 Length of the 41 power lines in ring configuration for Urban Area case. Subscripts indicate the starting and ending nodes of the line.

Line	Length (m)	Line	Length (m)	Line	Length (m)	Line	Length (m)	Line	Length (m)
l_{1-2}	5000	l_{10-11}	82	l_{21-22}	20	l_{30-32}	50	l_{39-41}	83
l_{2-3}	1570	l_{11-12}	140	l_{20-23}	450	l_{32-33}	174	l_{41-42}	270
l_{3-4}	209	l_{13-14}	125	l_{24-25}	36	l_{29-34}	378	l_{34-43}	1224
l_{4-5}	439	l_{14-15}	130	l_{24-26}	240	l_{34-35}	242	l_{43-44}	280
l_{5-6}	40	l_{12-16}	600	l_{26-27}	246	l_{35-36}	365	l_{44-3}	393
l_{4-7}	100	l_{16-17}	443	l_{27-28}	7000	l_{36-37}	50		
l_{4-8}	339	l_{17-18}	446	l_{27-29}	391	l_{37-38}	253		
l_{8-9}	544	l_{18-19}	534	l_{29-30}	483	l_{35-39}	217		
l_{8-11}	10	l_{19-20}	244	l_{30-31}	171	l_{39-40}	34		

3.3.3 MESH CONFIGURATION

To build this model, we start from the design made for the radial situation and add 5 lines to interconnect different nodes. The added lines join nodes 8 with 23, 10 with 32, 16 with 34, 29 with 41, and 37 with 45. New DCTs are not added. The total length of the lines is **24.44 km**. There are 45 power lines. The line connecting nodes 48 and 49 (grid 2) has the longest length with 7 km, and the shortest is the line joining nodes 46 (load f4) and 47 (PV8) with 20 meters. The longest line connects nodes 28 (grid 2) and 29, it has 7 km, There are 49 nodes, 11 nodes in 10 kV, 26 nodes in 5 kV and 12 nodes in 2.5 kV. Like in the other cases, Fig. **3.16** illustrate the system andTable **3.12** indicates the length of each line.

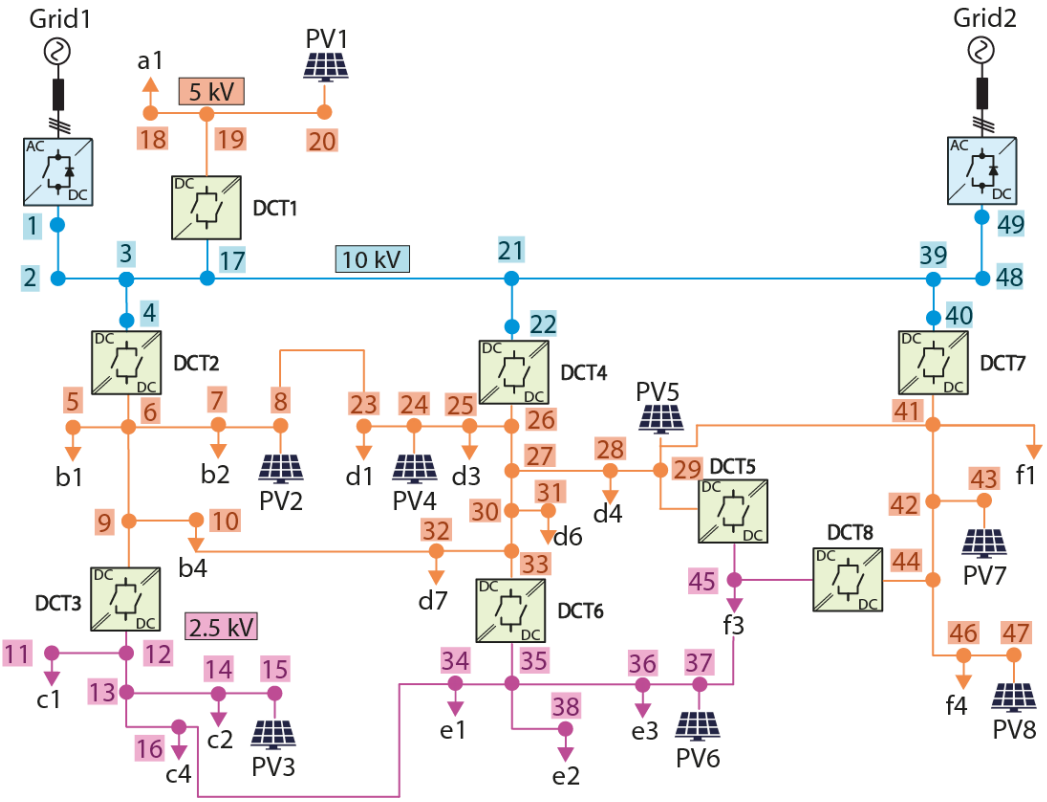

Fig. 3.16 Diagram of the mesh configuration for Urban Area case with the 2 grids, the 18 consumers, the 8 PVs, the 8 DCTs and the 45 power lines.

Table 3.12 Length of the 45 power lines in mesh configuration for Urban Area case. Subscripts indicate the starting and ending nodes of the line.

Line	Length (m)	Line	Length (m)	Line	Length (m)	Line	Length (m)	Line	Length (m)
l_{1-2}	5000	l_{11-12}	82	l_{19-20}	75	l_{28-29}	171	l_{21-39}	523
l_{2-3}	1570	l_{12-13}	140	l_{17-21}	1150	l_{27-30}	70	l_{39-40}	246
l_{3-4}	209	l_{13-14}	125	l_{21-22}	243	l_{30-31}	34	l_{41-42}	240
l_{5-6}	100	l_{14-15}	130	l_{23-24}	253	l_{30-33}	83	l_{42-43}	30
l_{6-7}	439	l_{13-16}	600	l_{24-25}	50	l_{32-33}	270	l_{44-46}	340
l_{7-8}	40	l_{3-17}	393	l_{25-26}	365	l_{34-35}	500	l_{46-47}	20
l_{6-9}	339	l_{17-19}	74	l_{26-27}	147	l_{35-36}	174	l_{29-45}	224
l_{9-10}	544	l_{18-19}	340	l_{27-28}	194	l_{35-38}	248	l_{48-49}	7000
l_{8-23}	500	l_{10-32}	139	l_{16-34}	389	l_{29-41}	346	l_{37-45}	338

4 POWER FLOW ANALYSIS

In this part of the project, simulations of the different scenarios described in chapter 3 will be performed. PLECS software was used for this purpose. These simulations are carried out in order to study how power flow behaves. DC systems are bidirectional and power flows depend only on voltage, and DC current follows the voltage and path of least resistance. This is differently of what happens in AC system, where power flows are determined by the voltage and phase [23]. In order to carry out the study of power flow, it is first necessary to build and model the system.

4.1 MODEL CONSTRUCTION

The simulations have been carried out with the model steady-state. 'Steady state' refers to the condition of an electronic circuit or network when the effects of transients no longer have any effect. After a transient (initial, oscillating or turbulent) state passes away, a steady state is reached. This topic is important because many design specifications of electronic systems are given as steady state characteristics. The different elements that form the model are explained below, as well as how they have been implemented in PLECS. There are transmission lines, loads, energy sources and DCT. Moreover, to carry out the calculations, the method per unit has been employed. Simulation time is 0.023 seconds, this is extrapolated and each simulation is equivalent to a day.

- **Loads and energy sources:** Various bibliographic sources were consulted in order to determine load profiles for each type of consumption. Later on, the bibliographic reference is listed next to each consumption (Fig. **4.1**): farm [24], school [25], restaurant [26], supermarket [27], industry [28], hospital [29] and house [26]. Also, the renewable energies production are obtained in the same way for the hydro power plant [30] and for the PV [31]. On the other hand, to implement the loads in PLECS they have been introduced as current sources. The PV and hydro power plant are also modeled as current sources, while the grid is modeled as a voltage source. Fig. **4.2** shows these models.

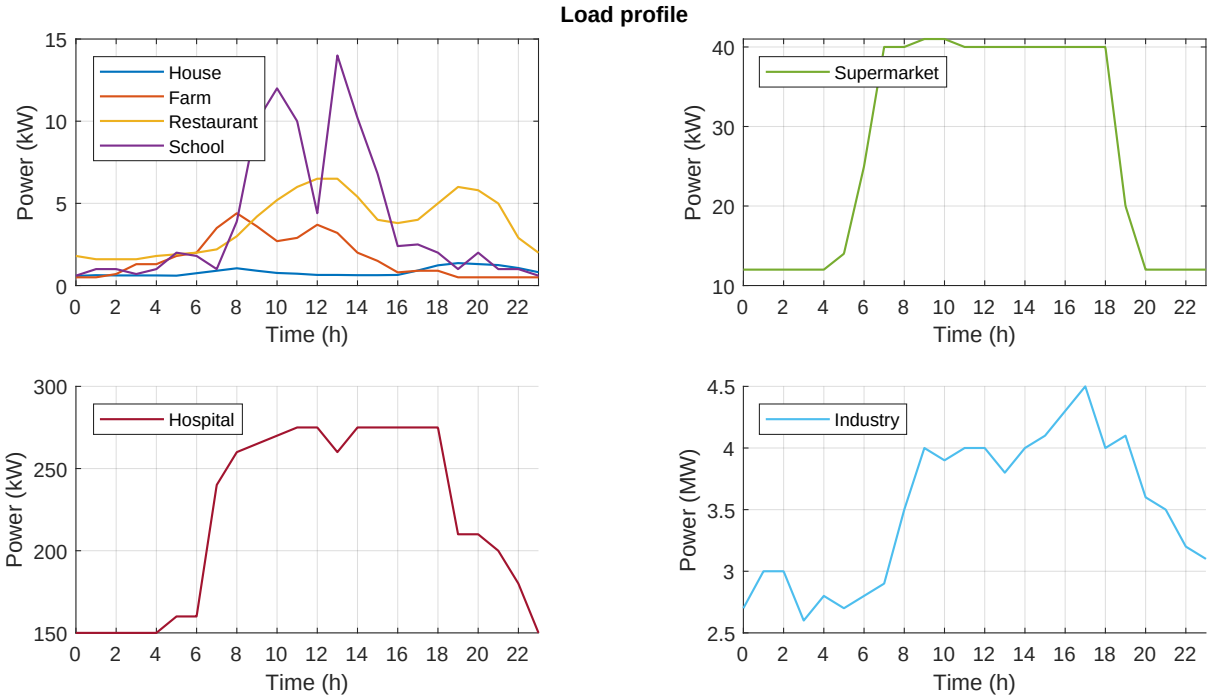

Fig. 4.1 Load profiles of the different types of consumers.They are shown on separate charts due to the different power ranges.

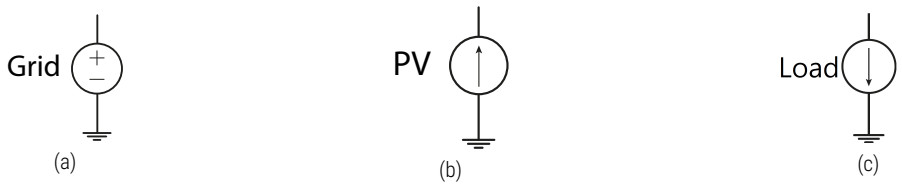

Fig. 4.2 Illustration of how the different elements are modeled: (a) Grid model; (b) PV model; (c) Load model.

- **Transmission lines:** The DC grid is only modeled by resistive lines. The value used for the resistor is shown in Table **4.1**. But these data must be adapted to our system since there are lines that are at 10 kV, 5 kV and 2.5 kV. Information about the electric lines (r_{line}) used in the model can be found in Table **4.3**.

Table 4.1 Medium Voltage Data Cable [32].

	Value	Unit
Voltage	11	kV
Resistance	17.6	mΩ/km

- **DCT:** Since the DCT operates in an open loop, it does not receive voltage or power set points. As a bidirectional device, the DCT recognizes the direction of power flow and lets the current flow naturally through its branches in the most convenient direction. In the steady state model, the method used to determine the DCT is described in detail in [8] and in [10]. In Table **4.2** the values of the parameters used for the calculation of the resistence of the DCT are shown. Fig. **4.3** (a) shows the model. Then, in Table **4.3** is shown the final value used in the simulation (r_{dct})

Table 4.2 Parameters used for model the DCT

	Value	Unit		Value	Unit
R_{total}	50.7	mΩ	f_s	5	kH
r_{c1}	10^{-3}	Ω	L_s	6.45	μH
r'_{c2}	10^{-6}	Ω	C_r	157.08	μF

Table 4.3 Data information for the resistance of the electrical lines depending on their voltage, and the resistance for model the DCT.

	Value	Unit		Value	Unit
$r_{line_{10\,kV}}$	0.0018	pu/km	$r_{dct_{10\,kV}}$	0.0065	pu
$r_{line_{5\,kV}}$	0.0070	pu/km	$r_{dct_{5\,kV}}$	0.0259	pu
$r_{line_{2.5\,kV}}$	0.0282	pu/km	$r_{dct_{2.5\,kV}}$	0.1037	pu

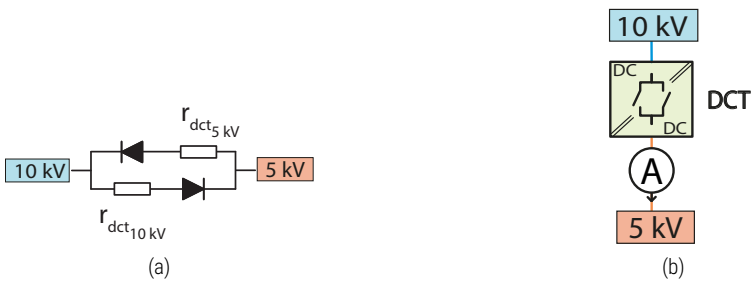

Fig. 4.3 Illustration of the models: (a) DCT model; (b) Position and direction of the ammeter to measure power in DCT.

4.2 RESULTS OF POWER FLOW ANALYSIS

Now, the results of the simulations are displayed. The three study areas are divided into sections, and within each section the results for each configuration are also presented. First, electricity demand is shown to see the consumption of each load separately, which it not depend on the type of configuration. The total consumption and breakdown of each energy source is then displayed. Also, the power exchanged in DCTs and voltages in each node and in DCTs are shown. Finally, losses are shown in a table. The first case for which the results are shown is the District case, then the rural area case, and finally, the urban area case. The following lists describe the results found once simulations have been conducted, in the same order that they appear for each scenario:

- Electricity demand: shows the consumption of each of the different consumption points individually throughout a day. Consequently, it can be seen where the biggest consumption happens and where the least consumption takes, as well as what happens at any particular time.

- Energy Sources and Total Load: On the one hand, these graphs show energy sources, which displays where the electricity is coming from, and total consumption (the sum of the consumption points shown in the electricity demand graphs above). Power sources are displayed individually. When the power value of general electrical network is negative, it means that at that moment, there is more production than consumption of renewable energy, so the excess power is put on the electricity grid. On the other hand, the production of PV is shown, it occurs in the central hours of the day, it starts to produce a little at 6 am and stops at 20 pm. The total consumption curve is used to compare maximum consumption and know when it happens. Additionally, depending on the type of configuration, the grid curve varies, which is most evident in the urban area case.

- Power DCT: these graphs allow knowing the power that passes through the DCT at any moment and thus verify that the capacity limits (1pu=10 MW) are not exceeded. When the values change from negative to positive, or vice versa, it means that the direction of the power flow changes. Consequently, with these plots, we can know the direction of the power flow in the system. It is important to note that the measurements shown in the graphs are on the lower voltage side, i.e., if it is a DCT from 10 kV to 5 kV, the measure is on the 5 kV side. As well as, the ammeter's direction is from the larger to the smaller side, Fig. 4.3 (b) shows the model. Furthermore, depending on the type of configuration, the power exchanged is different.

- Voltage in nodes: For each node of the network, the voltage has been measured for the moment the maximum consumption occurs. This is done to see that the values are typical and there are no voltage excesses or shortages in some nodes.

- Voltage in DCT: There is voltage measured on both sides of the DCT. These graphs show the maximum voltage values. In addition to this, you can see when power flow direction changes.

- Losses: finally, the line losses in the entire system and the losses in each of the lines have been calculated. Total losses are calculated by taking into account the total energy sources minus the total consumption throughout the day. For each configuration, a table illustrates the maximum loss that occurs on the day, the average throughout the day, and the percentage of losses calculated on the total generated. Line losses are used to identify which lines have higher losses.

- Also note that in the graphs time is represented on the x-axis and this is equivalent to a whole day. The simulation is done in milliseconds. As a result, 0.002 seconds equals 02:00 am. Further, power is shown as per unit, so it must be accounted for that $S_{base} = 10\ MW$.

4.2.1 DISTRICT CASE

District case has one grid, 6 consumption points and 2 PVs. Results show loads profiles and the contribution of each energy source, energy exchanged by the two DCTs, voltage in pu at nodes and losses.

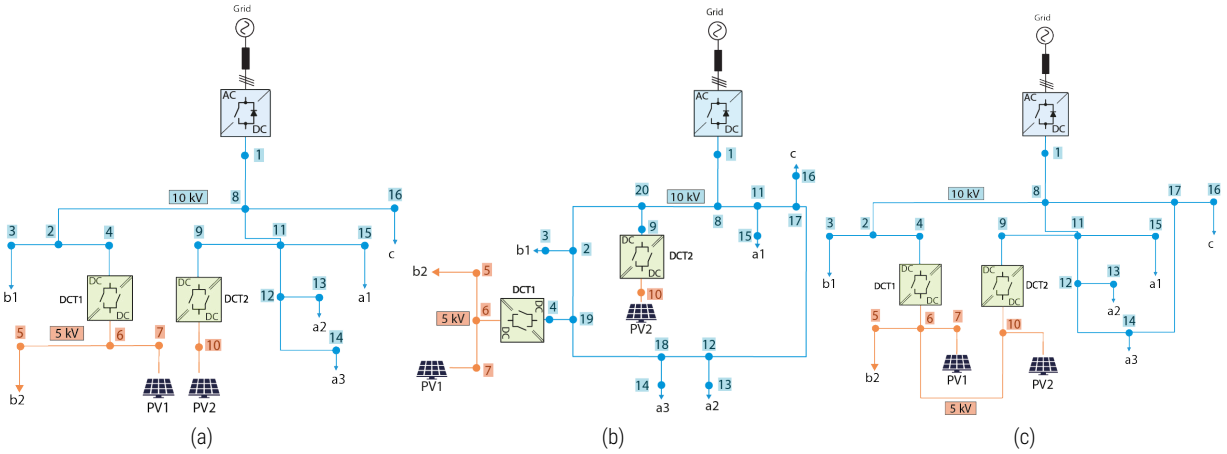

Fig. 4.4 Schemes for the District case: (a) Radial configuration; (b) Ring configuration; (c) Mesh configuration.

- ELECTRICITY DEMAND

Following the entry of data from Table 3.1, the following figure (Figure 4.5) shows how the demand is distributed over time. There are in total 6 consumption points. As a result of the greater number of consumers, loads a1 (20 houses), a3 (10 houses, 3 farms) and c (9 houses, 4 farms) present the highest consumption. Although a1 has a greater number of houses than c, during the central hours of the day c is greater than a1. The farms have higher consumption than the houses during the day. Therefore, between the main hours of the day, the consumption point c, which has 4 farms, is greater than the consumption point a1, and especially in the evening, it can be seen that a1 is much larger. The early morning hours and the end of the day are times when consumption is the highest. This is mainly due to the fact that in those periods of time people are at home, and from the evening there are more people at home and therefore the activities at home are greater than during the day.

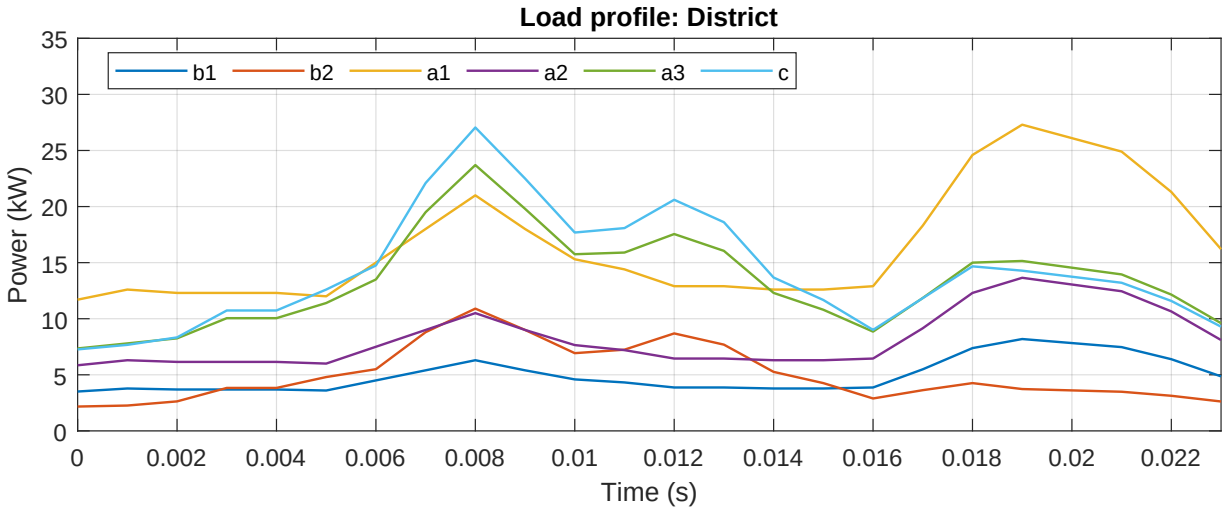

Fig. 4.5 Electric demand of the 6 consumption nodes throughout a day. Load c has the highest consumption point (District case)

- ENERGY SOURCES AND TOTAL LOAD

According to Table 3.1, PV1 produces 192 kW and PV2 produces 72 kW, as seen in Figure 4.6). The average total consumption throughout the day is 63.25 kW. Moreover, 08:00 is the time of greatest demand, with a value of 99.45 kW, which is a 53.23 % more than the average.

The total installed PV capacity (264 kW) is greater than the maximum consumption. So, solar energy exceeds the consumption in the middle of the day, and the grid is under consumption, at that time as the surpluses are poured into it. Finally, due to the fact that there are not many consumption and production points, the differences between radial, ring, and mesh configurations in this analysis are minimal. For this reason, the three configurations are not represented in the figure and only the radial case is represented.

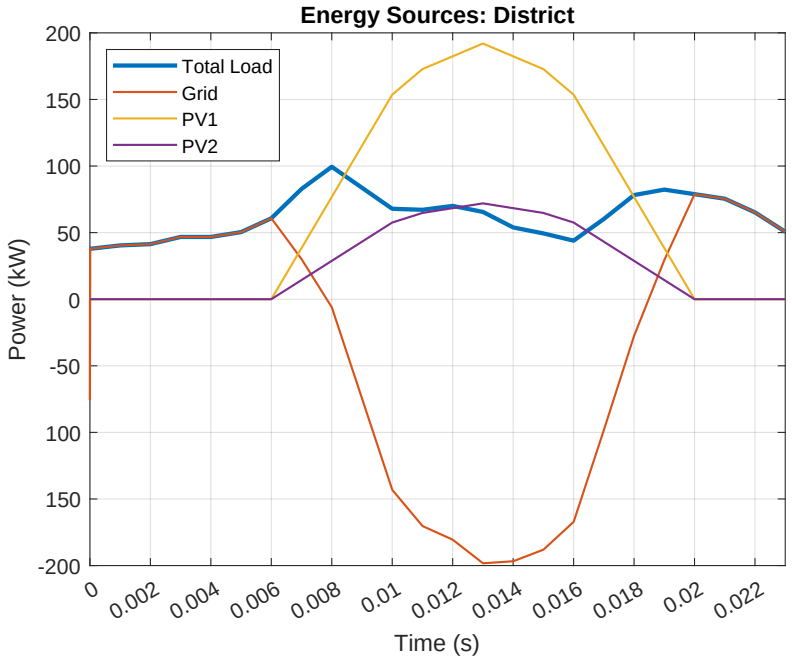

Fig. 4.6 Total system demand of the 6 consumers and breakdown of energy input from the grid and the 2 PVs for the three configurations (District case)

- POWER DCT

Figure **4.7** shows how power flows through DCTs to change voltage. DCT1 is connected to a load and PV1, while DCT2 is connected to PV2. Thus, when photovoltaic starts producing power, power flow is negative, that is, it moves from the 5 kV side to the 10 kV side. The energy capability of the DCT is not exceeded, as 1 pu (10 MW) is not reached in power. To see the differences between configurations, solid lines represent DCT1 and dotted lines represent DCT2.

Blue color is used to radial configurations, green for ring and orange for mesh. Both in DCT1 and DCT2 the results in radial and ring are the same, that is why radial line is thicker than ring and mesh lines to know that it is equal to ring. This may be due to the small number of consumers. And in orange, those of the mesh case. Due to the connection between nodes 6 and 10, the power that passes through these two DCTs is very similar, so there is very little difference between them; in the radial case happens the contrary. By doing so, the two DCTs work in a similar way, preventing one from being more charged than the other.

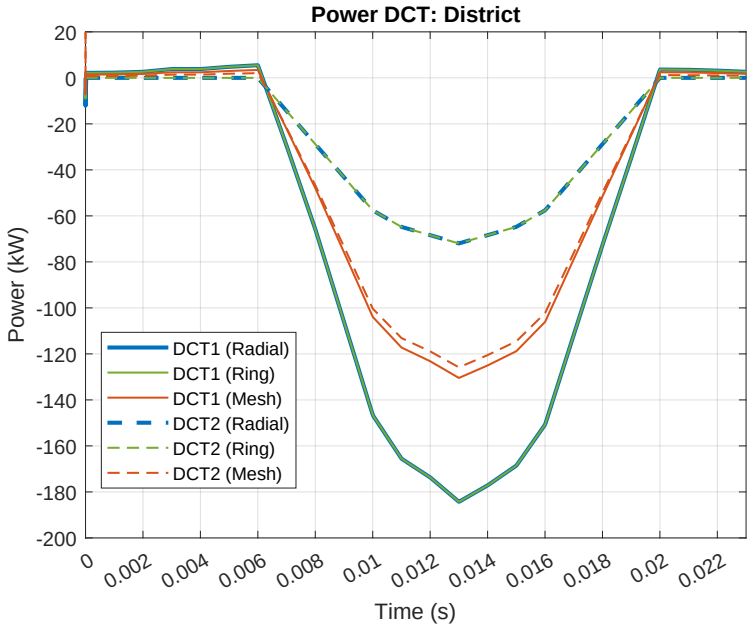

Fig. 4.7 Power exchanged by the 2 DCTs in the three configurations (District case)

- VOLTAGE IN NODES

Figure 4.8 illustrates the voltage in each node for the time of greatest consumption, at 08 am. At this moment, PV production exceeded consumption. Due to this, nodes 5, 6, 7 and 10, which are located at the PV production points and after the DCT, have a higher pu voltage. The radial and ring have very similar voltages, but for the mesh case in nodes 5, 6 and 7 the voltage is lower because the power is more distributed through the lines.

The voltage at node 4, in all three types of configurations, is less than the voltage at node 6. This means that the direction of power flow is from node 6 to node 4, because PV1 produces more than it does. which require the load b2. The same happens with PV2, the voltage at 10 is higher than at 9 because PV2 is producing and the energy produced goes to DCT2. For the mesh case, the direction of the power in the line that joins nodes 6 and 10, noting that the voltage is greater in 6 than in 10, is from node 6 to 10 since PV1 has a higher production than PV2. The grid has a voltage of 1 pu because it is a voltage source, so source is well controlled. Due to this, the small difference between voltages is mostly small voltage drops on the lines.

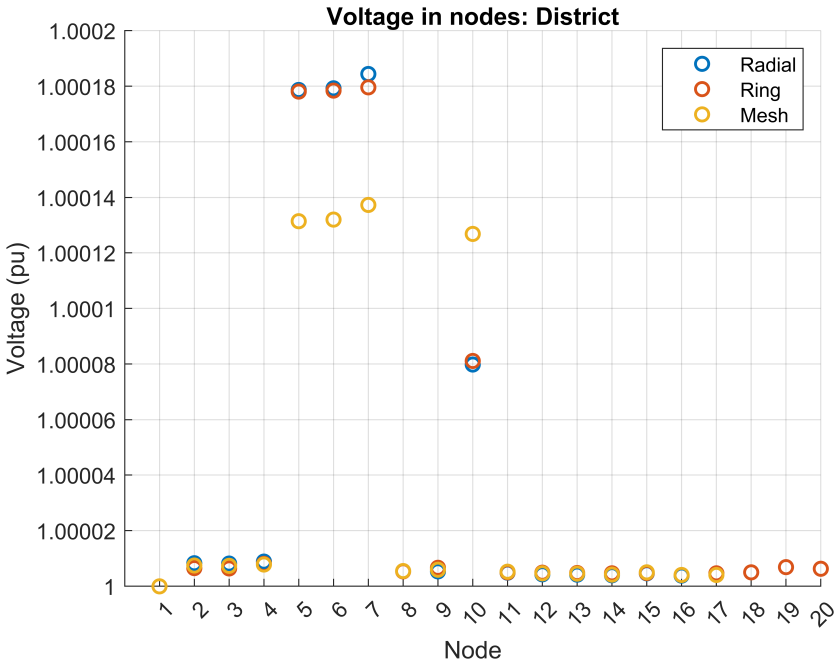

Fig. 4.8 Voltage in nodes at 08 am in the three configurations (District case)

- VOLTAGE IN DCT

Figure **4.9** illustrates the voltage in both sides of the two DCTs. The maximum voltage match with the moment of maximum PV production. Furthermore, it can be seen that at the moments when the orange line (voltage measurement in the 5 kV part) exceeds the blue line (10 kV) the direction of the power flow changes. When PVs starts to produce energy, starting at 6 am in the two DCTs, power flow goes from 5 kV side to 10 kV side. And when it stops producing, at 8 pm the flow direction reverses.

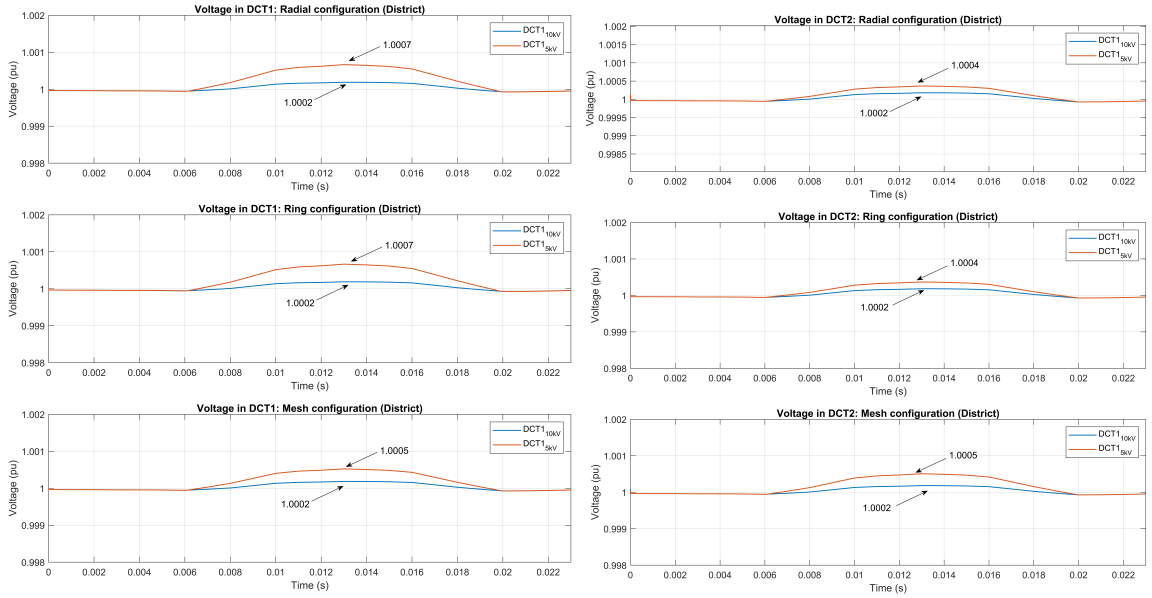

(a) (b)

Fig. 4.9 Voltage on the DCTs throughout the day. It is indicated for the moment of maximum production, at 01 pm, the voltage on both sides of the transformer on the 10 kV side (blue) and on the 5 kV side (orange) (Distric case): (a) DCT1; (b) DCT2.

- LOSSES

Finally, Table **4.4** shows that mesh has lower total losses. To calculate losses, first, the sum of all loads was made, and the sum of the different energy sources. Once these operations have been carried out, total load is subtracted from total source and with this total losses are calculated. Average losses indicate the average of losses in the entire system over the course of a day. To calculate them, all system losses are added up throughout the day and then that value obtained is divided by the total number of values obtained throughout a day. This is done because there are times throughout the day when the losses are greater, when there is more energy transported, and times when they are less. After calculating losses in each of the lines, it is obtained that the line with highest losses in the three configurations is the line corresponding to DCT1, it is $line_{2-6}$ for the radial and mesh case and $line_{19-6}$ for the ring case. This is because PV1 produces a large amount of energy and this part of energy is carried on that line. From lowest to highest percentage of losses in that line is mesh, radial and ring.

Table 4.4 Maximum losses, average losses and total losses in the three configurations (District case).

Losses	Radial	Ring	Mesh	Unit
Maximum losses	257.3	254.2	213.7	W
Average losses	64.3	63.4	54.7	W
Total Losses	0.10	0.10	0.09	%

4.2.2 RURAL AREA CASE

There are 6 consumption points, 2 renewable energy sources and one grid in rural area case. Load profiles, the contributions from each energy source, power exchanged by two DCTs, voltage at nodes, as well as losses are shown.

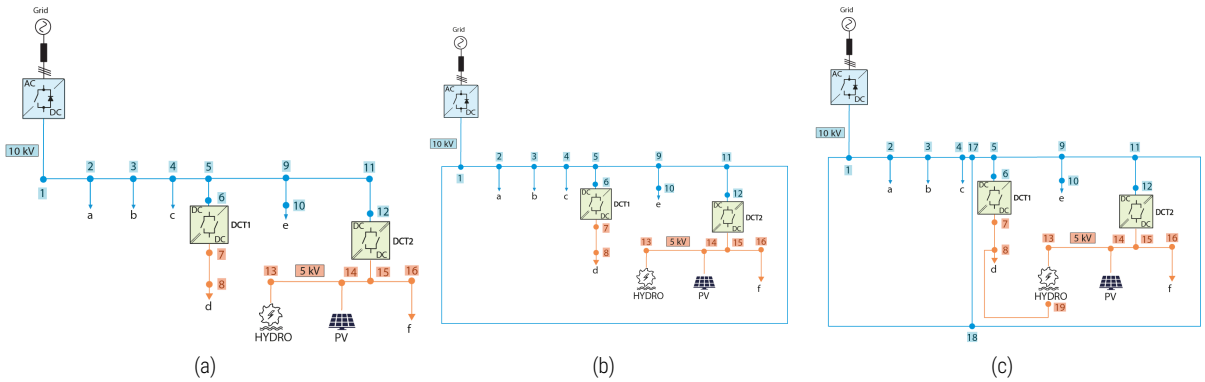

Fig. 4.10 Schemes for the Rural Area case: (a) Radial configuration; (b) Ring configuration; (c) Mesh configuration.

- ELECTRICITY DEMAND

Fig. 4.11 shows the development of the electricity demand over the time after entry the data from Table 3.5. There are in total 6 consumption points. Loads d and f are the loads that consume the most due to the greater number of consumers. Meanwhile, loads a and c have such a small consumption compared to the rest, because of this, they are negligible in the figure. Due to the fact that all loads are houses, the morning and evening are the busiest hours of consumption. At this time, people are at home and they produce activities that consume electricity.

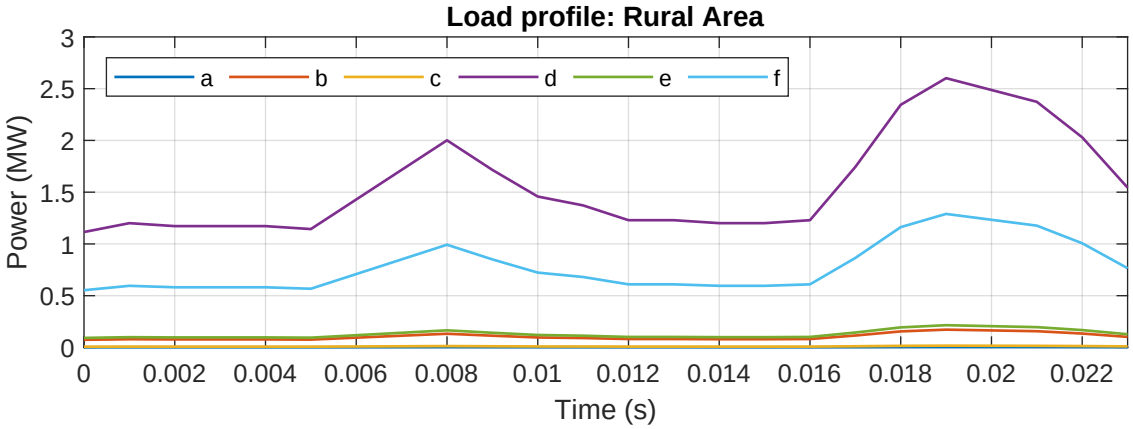

Fig. 4.11 Electric demand of the 6 consumption nodes throughout a day. Load d has the highest consumption point (Rural Area)

- ENERGY SOURCES AND TOTAL LOAD

Based on Table 3.5, PV maximum production is 1600 kW, and the hydro power plat maximum generation is 815 kW. Throughout the day, the average total consumption is 2626.63 kW. Furthermore, 07 pm is the time of greatest demand, with a value of 4300.15 kW, which is a 63.72 % more than the average.

Here, the grid does not have negative power. In the right-hand part of the figure, a zoom was made to see the differences in the grid depending on the topology. Despite the minimal changes, it is apparent that the radial topology consumes more energy. The cause of this is that since fewer lines connect the loads with the producers, more energy must be taken from the grid to transport it to more distant points of consumption such as d, e, and f, and there are associated losses in the transport of energy. Fig. 4.12 correspond to these description. At the time of maximum PV production, there is also hydro power production and therefore, the contribution from the grid is almost zero. It can be said that in those moments, the consumption is supplied with renewable energies.

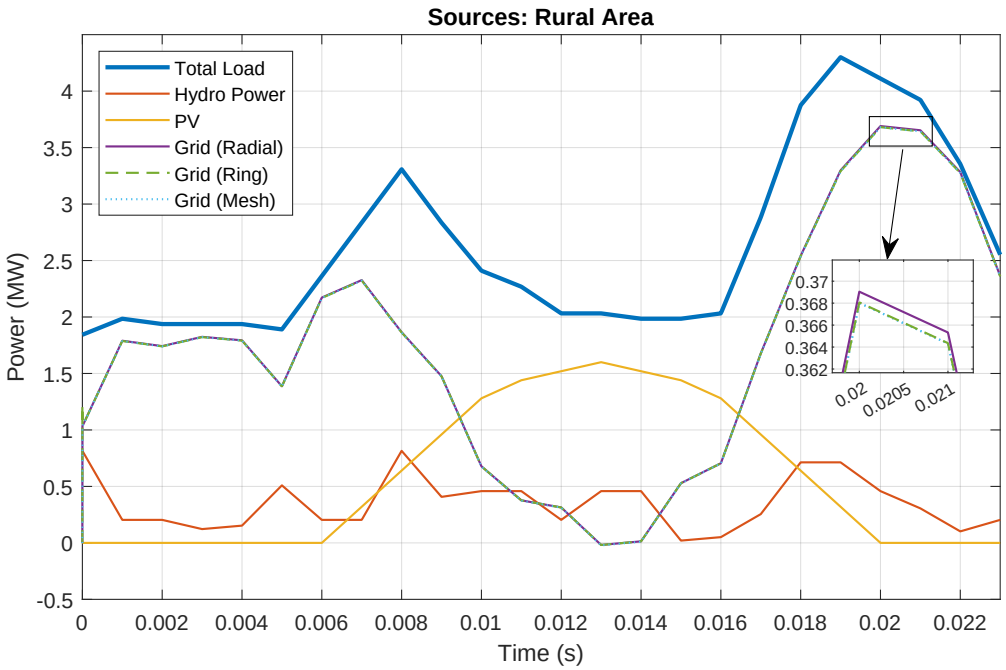

Fig. 4.12 Total system demand of the 6 consumers and breakdown of energy input from the grid and the hydro power plant, and the PV for the three configurations (Rural Area)

- POWER DCT

Figure 4.13 , shows how power flows through DCTs to change voltage. Radial configurations use blue, rings use green, and mesh uses orange. The results in DCT1 and DCT2 are very similar for radial and ring results, which is why radial lines are thicker than ring lines and mesh lines indicate it is equal to ring. There may not be enough consumers, which may explain this like in District case. There are also mesh cases in orange. DCT1 will always be positive since it feeds a load and there is no output on the other side. However, DCT2 has negative power at times, so we always know the direction of the power flow. As a result, during the hours of solar energy production, and since there is also hydropower production, some of the energy is taken to the main 10 kV line that connects with the rest of the consumers. Since the line DCT2 mesh (orange dashed line) is smaller than DCT2 radial (blue dashed line), it means that part of the power in mesh case goes from node 19 to node 8.

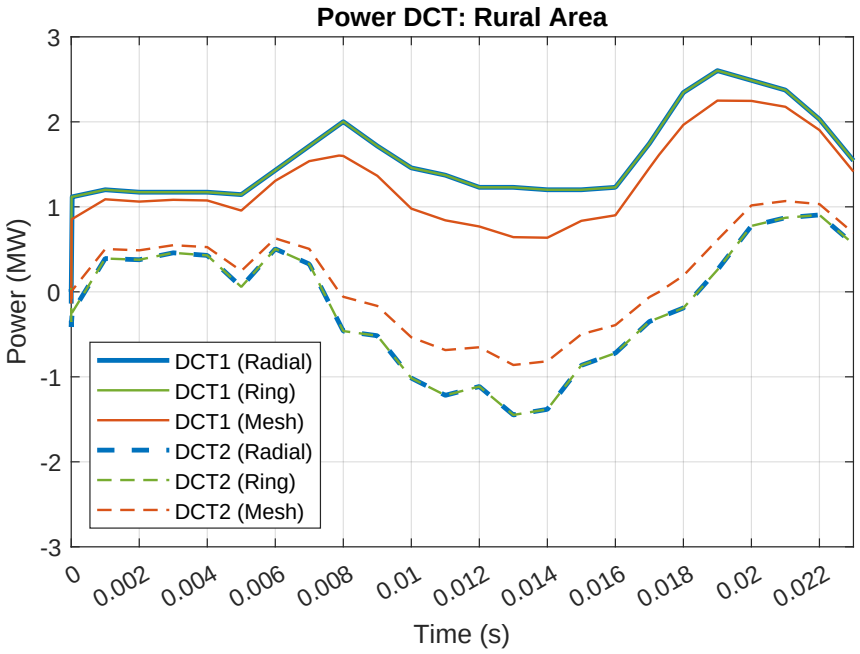

Fig. 4.13 Power exchanged by the 2 DCTs in the three configurations (Rural Area)

- VOLTAGE IN NODES

Figure **4.14** illustrates the voltage at each node for the time of greatest consumption, at 07 am. The node with the highest voltage is the grid (node 1), which means that no energy is injected into the network because the direction that the energy follows starts from node 1. In radial case, the voltages in the nodes are less than in the rest of the configurations, this is because by having only one path, all the energy is transported by the main path and there are greater differences between nodes. Furthermore, in the mesh case, it can be seen how the voltage at node 19 is higher than at node 8, which means that energy from the hydro power flows to supply other loads.

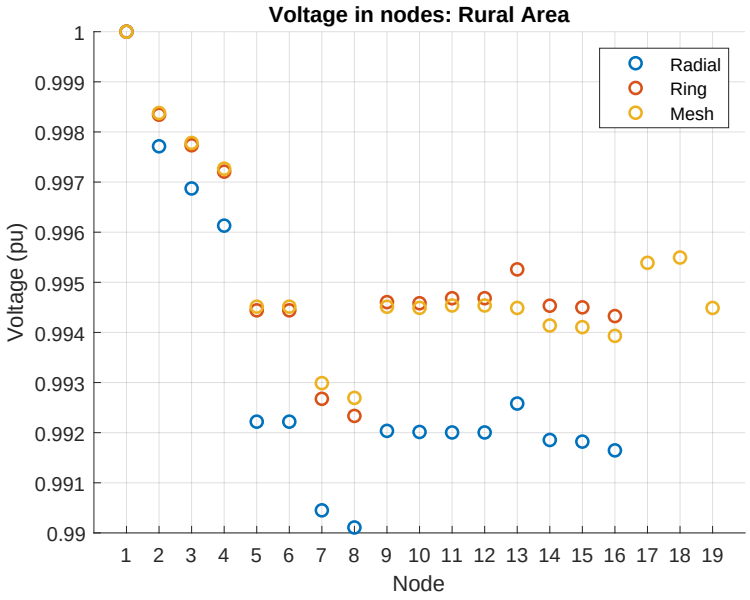

Fig. 4.14 Voltage in nodes at the time of greatest consumption, 07 pm, in the three configurations (Rural Area)

- VOLTAGE IN DCT

Figure **4.15** express the voltage in both part of the two DCT. Like in the other case, the maximum voltage match with moment of maximum PV production. It can also be seen that at the moments when the orange line (voltage measurement in the 5 kV part) exceeds the blue line (10 kV), it indicates a change in the direction of power flow. This only happens for DCT2, for DCT1 it does not happen because it feeds a load and it will always go in the direction of the node that is at 10 kV (node 6) to the node that is at 5 kV (node 7). In DCT2, for radial an ring configuration power flow changes a little bit after 7 am, and for mesh at 8 am because also feeds load d. And at 7 pm the flow direction reverses for radial and ring, for mesh this happens before, at 6 pm. It must be remembered that there is also production of hydro power.

- LOSSES

Lastly, Table **4.5** display the losses. As in the District case, the mesh configuration is the one with the lowest losses. After calculating the losses in each of the lines, it is obtained that the line with the highest losses in radial and ring configuration is $line_{4-5}$, because this is one of the longest lines and carries a large amount of energy to power the loads. And for the mesh case is $line_{8-19}$ because the energy produced by the hydro power plant is transported. From lowest to highest percentage of losses in the line with more losses would be ring, radial and mesh.

Table 4.5 Maximum losses, average losses and total losses in the three configurations (Rural Area case).

Losses	Radial	Ring	Mesh	Unit
Maximum losses	37.74	27.97	27.08	kW
Average losses	13.17	10.42	9.24	kW
Total Losses	0.50	0.40	0.35	%

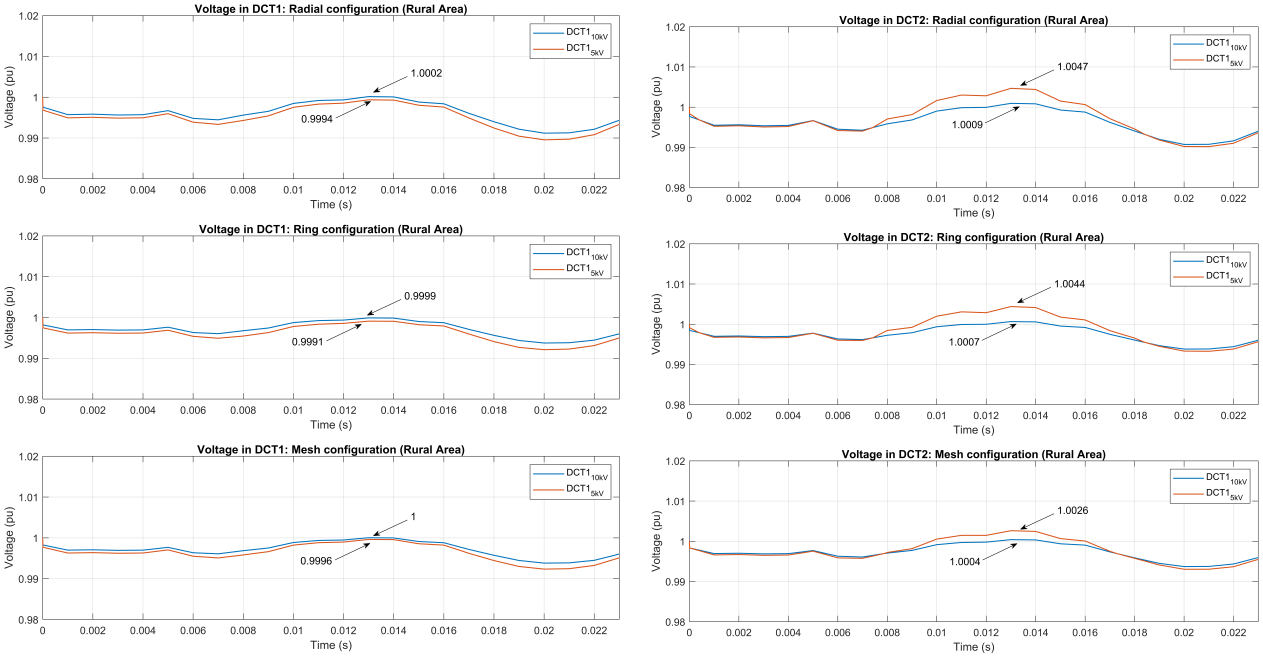

(a) (b)

Fig. 4.15 Voltage on the DCTs throughout the day. It is indicated for the moment of maximum production, at 01 pm, the voltage on both sides of the transformer on the 10 kV side (blue) and on the 5 kV side (orange) (Rural Area): (a) DCT1; (b) DCT2.

4.2.3 URBAN AREA CASE

Urban Area has two grids, 18 consumers, 8 PVs and 8 DCTs for radial and mesh and 10 DCTs for ring. Results show loads profiles and the contribution of each energy source, energy exchanged by the two DCTs, voltage in pu at nodes and losses.

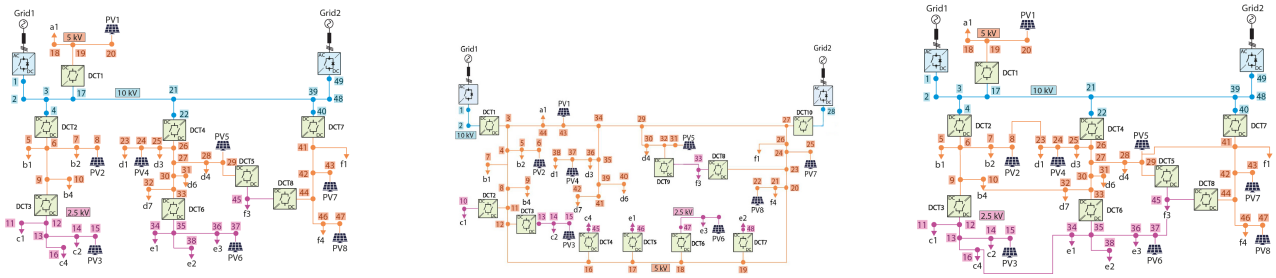

(a) (b) (c)

Fig. 4.16 Schemes for the District case: (a) Radial configuration; (b) Ring configuration; (c) Mesh configuration.

- ELECTRICITY DEMAND

The electricity demand in this case is shown in two different images. The reason is that load a1 represents the typical consumption of an industry (Figure **4.17**), and its consumption is much higher than in the other zones (Figure **4.18**). Scales used on the y-axis of each figure reflect this. The total number of consumption points is 18. The consumption is highest in load a1 (industry) and in load e1 (340 houses, 1 supermarket and 1 school). Here it also happens that the consumption is higher in the early morning and in the evening since most of the consumers are homes.

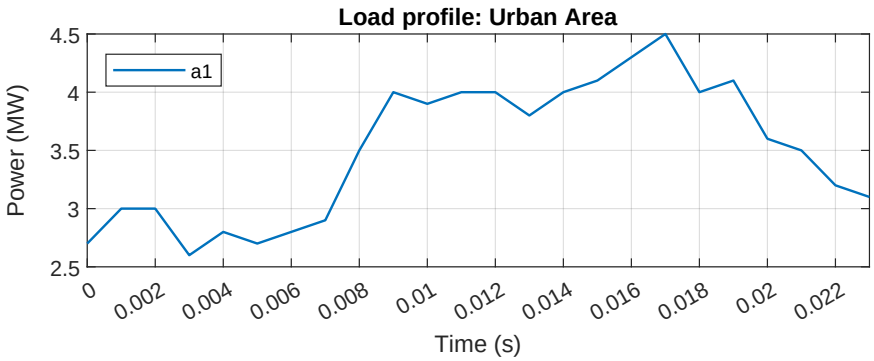

Fig. 4.17 Electricity demand for the industry throughout a day (Urban Area). This load profile is the one with the highest consumption in the entire urban area.

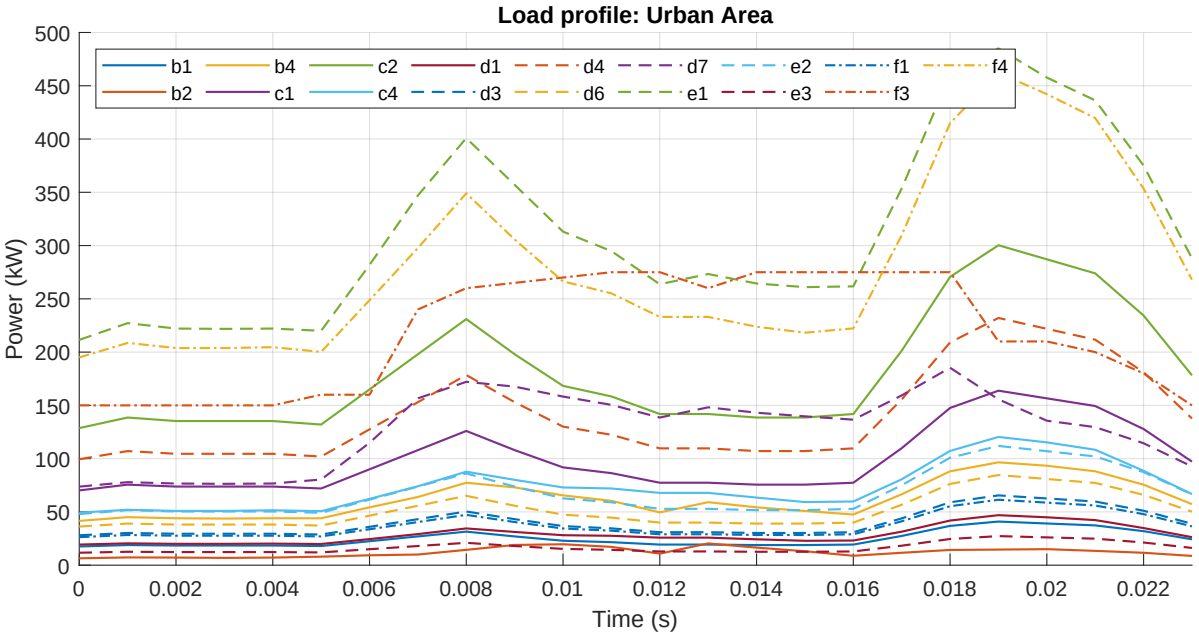

Fig. 4.18 Electric demand of the 17 consumption nodes throughout a day. Load e1 has the highest consumption point (Urban Area)

- ENERGY SOURCES AND TOTAL LOAD

Following the analysis of the results, in Figure **4.19** (b) it can be seen the PV production values. Because there are a total of 8 photovoltaic plants , and each plant's production is less than the total consumption, in this case it has been decided to represent the data in plot graphs with different y-axis values. The average total consumption throughout the day is 5.321 MW. Moreover, 07 pm is the time of greatest demand with a value of 6.779 MW, this is a 27.4 % more than the average.

Comparing it with the District and Rural Area cases, there are now major differences respect to the ring configuration. This is due to the greater number of consumption points, the greater number of lines, the greater number of PVs and because now the amounts of energy transported are much greater. Radial and mesh configurations are similar. The power provided by grid 1 is greater than grid 2 because it is closer to the study area.

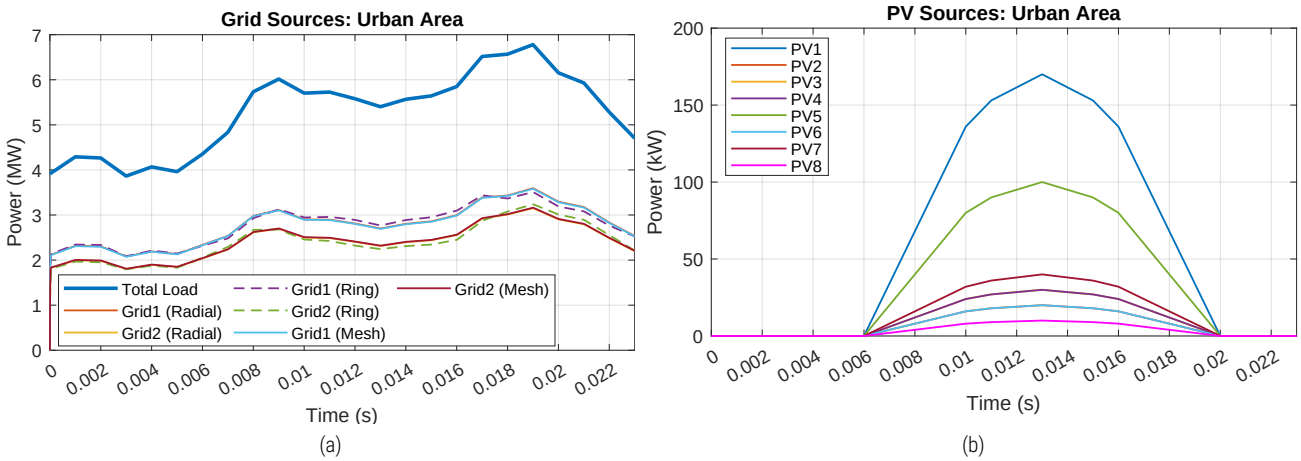

Fig. 4.19 Energy Sources and Total Load (Urban Area): (a) Total system demand of the 18 consumers and breakdown of energy input from the 2 grids for the three configurations, Grid 1 greater than Grid 2; (b) Production of the 8 PVs.

- POWER DCT

Here, it is necessary to represent results in several images. As a result of the greater number of consumers, PVs, and the number of power lines, there are differences between the three configurations. We should pay attention to DCT1 (Fig. 4.20 (a)), it is the one that connects to industry and this consumer requires a lot of energy. However, capacity is not exceeded. It must be taken into account that if new industries were to be created in the future, the DCT1 would become important. Because it would be necessary to incorporate new DCTs in order not to exceed the operating capacity of DCT1. The other DCTs to be monitored are those feeding the hospital, which in the radial and mesh case are DCT 5 and DCT 8 (4.20 (b)). If one stops working, the other would still have enough margin to continue working independently and avoid overcapacity in the event of one not working. As is logical, there is a better balance between the power exchanged between DCTs in the mesh case. Meanwhile, in ring configuration (4.21), DCT1 and DCT10 exchange the most energy because they are connected to the main network.

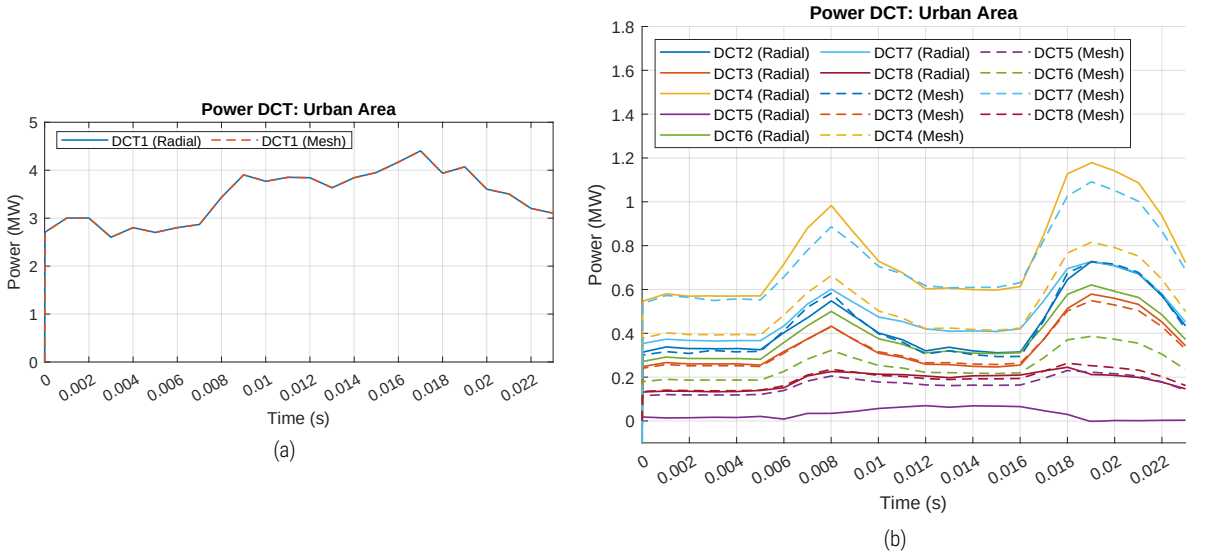

Fig. 4.20 Power exchanged by the 8 DCTs in Radial (solid line) and Mesh (dashed line) configuration (Urban Area): (a) DCT1 ; (b) from DCT2 to DCT8.

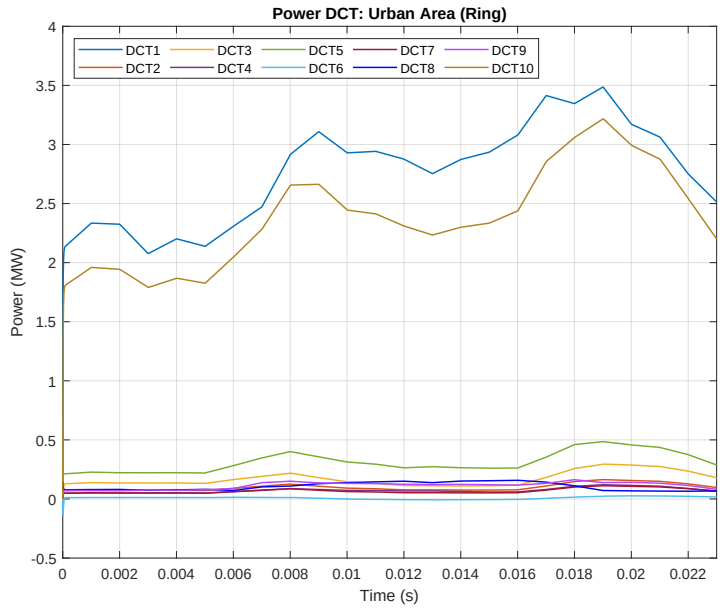

Fig. 4.21 Power exchanged by the 10 DCTs in Ring configuration (Urban Area). DCT1 (blue line) and DCT10 (brown line) are connected to grid and exchange the most energy.

- VOLTAGE IN NODES

In Fig. **4.22** it can be see the voltage in each node at 07 pm. Nodes in this case do not have the same nomenclature as in the radial case. In other words, in the radial case, load b1 was node number 5, but in radial it is node number 7. It was done in order to establish the number of each node in an orderly manner. Note that this did not happen in the district and rural area cases.

The network nodes have the highest voltage, which means that no energy is injected into the network. Seeing the voltages, the different zones in which the urban area is divided can be easily differentiated. Comparing the radial and mesh cases, we see that in some cases the voltages are similar (nodes 5 to 10), in other cases the mesh voltage is higher than the radial (nodes 11 to 16, and nodes 23 to 33), and moments in which the radial voltage is greater than the mesh (nodes 41 to 47). These differences are due to the fact that, as in the mesh case, there are greater connections between nodes, the lines transport less energy because there is greater distribution and greater balance, and with this, the voltage differences between the different zones are smaller.

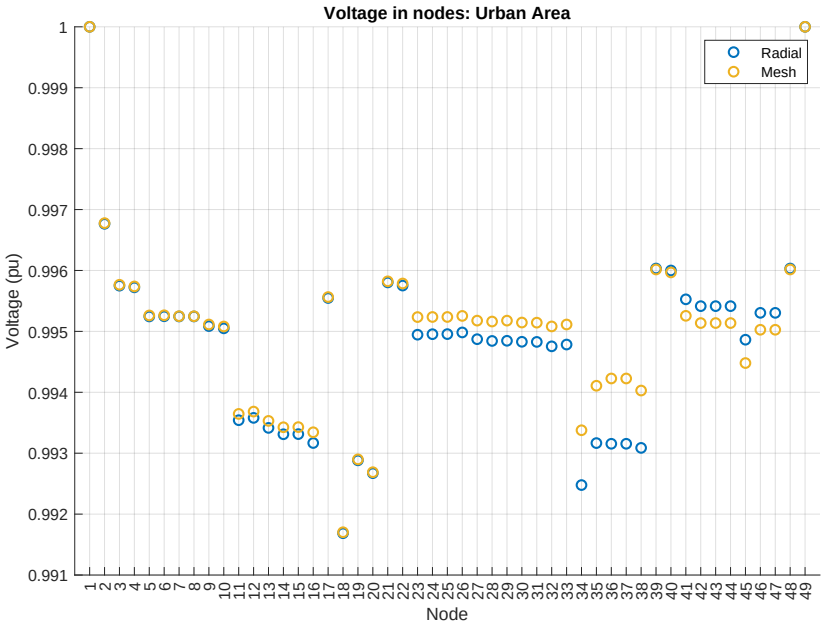

Fig. 4.22 Voltage in nodes at 07 pm in the three configurations (Urban Area)

.

- VOLTAGE IN DCT

Figure **4.23** illustrates voltage in both part of all the DCT fora radial and mesh configurations and Figure **4.24** for ring configurations. In mesh (M) and radial (R) case there are 8 DCTs in total. DCT1, DCT2, DCT4 and DCT7 work between lines that are at 10 kV (higher side) and 5 kV (lower side). The DCT3, DCT5, DCT6 and DCT8 operate between lines between 5 kV and 2.5 kV (higher and lower sides, respectively). At some moments blue or orange lines are not seen, this is because results for radial and ring are the same.

For radial case, the blue curve (higher voltage side) is always above the orange curve (lower voltage side), so the direction of power flow through the DCTs is always the same. This is because there are now more PVs spread throughout the area and the production of each individual PV is smaller compared to the loads around it. For example, PV2 produces a maximum of 20 kW and the loads that are in the same zone (b1, b2 and b4) together have a consumption of 98 kW for the moment of maximum production, at 1pm. For mesh case the same thing happens, yellow line (higher voltage side) is always above purple line (lower voltage side), the reason is the same.

In ring case, there are 10 DCTSs. In this case, DCT1 and DCT10 work between lines that are at 10 kV (higher side) and 5 kV (lower side), the rest, operate between 5 kV and 2.5 kV (higher and lower sides, respectively). The same thing happens here as in previous configurations, DCTs always have the same power flow direction, except for DCT6. DCT6 connects with load e3 and PV6 and now when PVs produce energy, at 9 am power flow goes from 2.5 kV side to 5 kV side. At 5 pm the flow direction reverses.

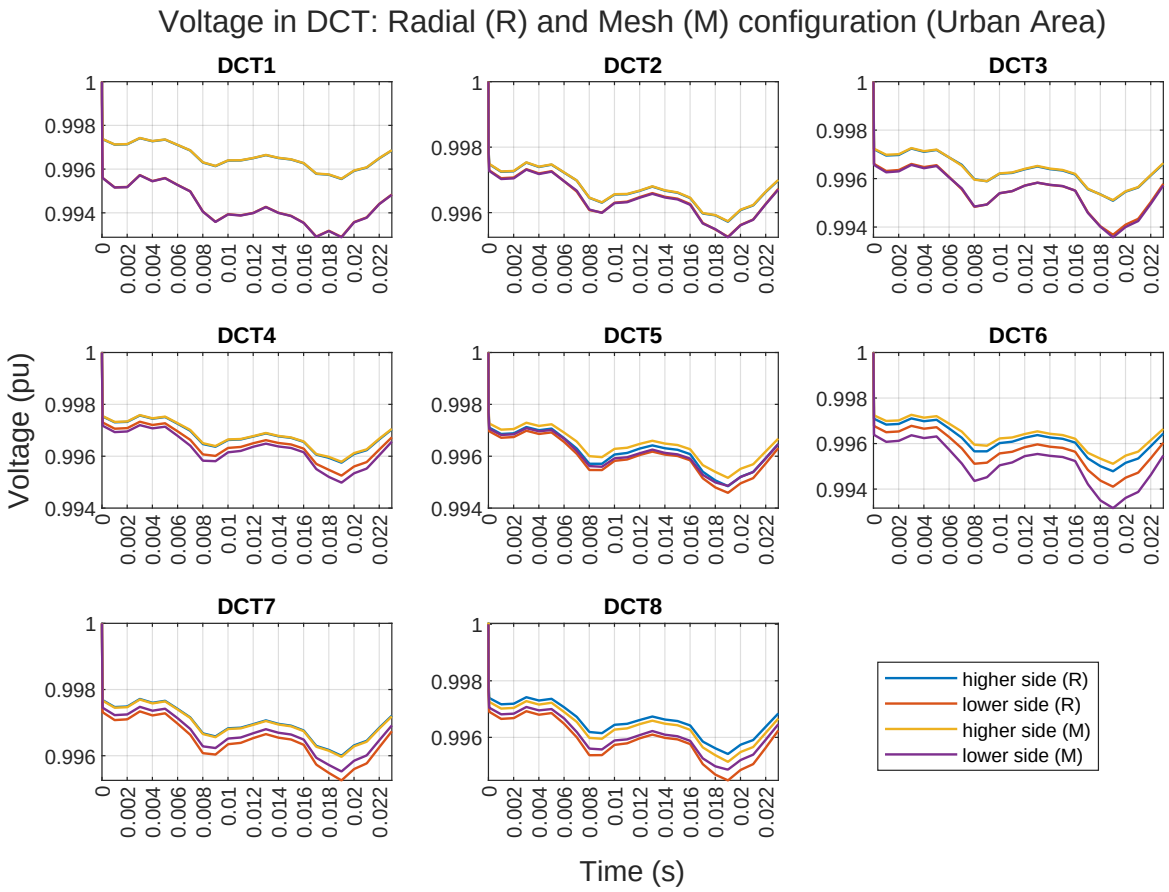

Fig. 4.23 Voltage on the 8 DCTs throughout the day for radial (R) and mesh (M) configurations (Urban Area)

.

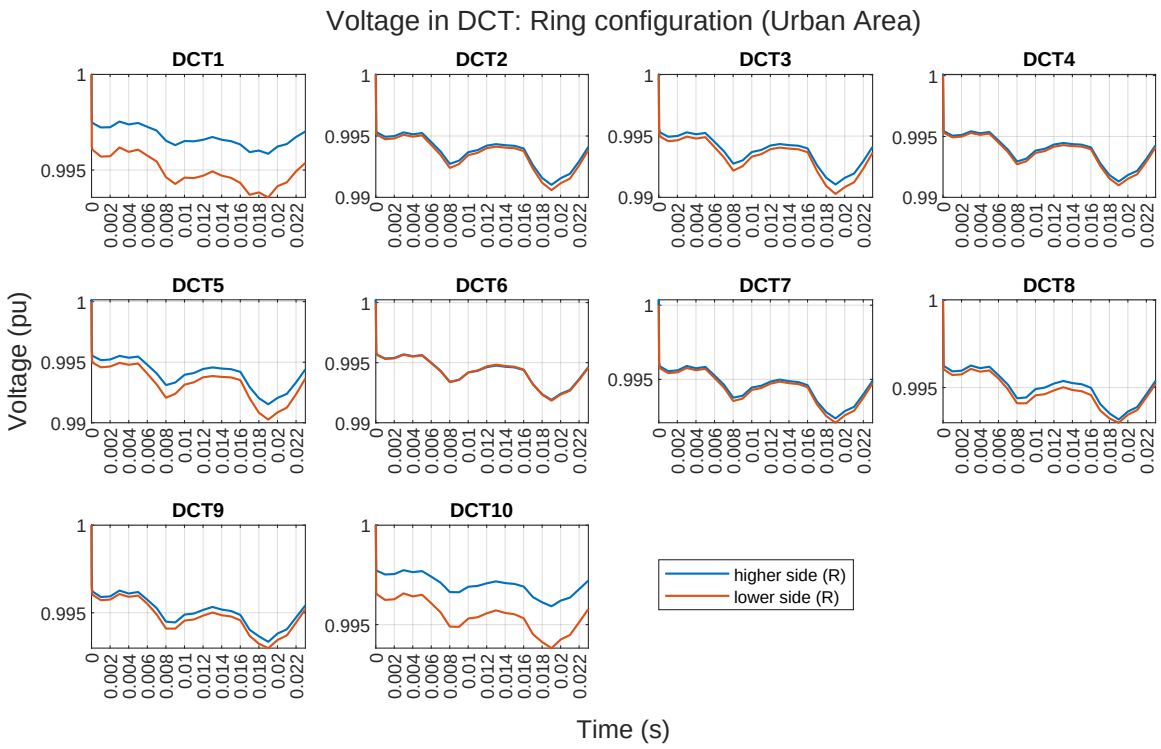

Fig. 4.24 Voltage on the 10 DCTs throughout the day in ring configuration (Urban Area)

.

- LOSSES

Finally, Table 4.6 display the losses. Mesh and radial losses are less than in ring configuration. As there is a greater amount of energy transported throughout the system, the losses are greater than in the District and rural area cases. Maximum losses and average losses also happen in ring case.

Table 4.6 Maximum losses, average losses and total losses in the three configurations (Urban Area case).

Losses	Radial	Ring	Mesh	Unit
Maximum losses	52.73	152.30	52.01	kW
Average losses	31.50	93.37	31.24	kW
Total Losses	0.59	1.78	0.59	%

4.3 CONCLUSIONS OF POWER FLOWS RESULTS

As the systems are larger, and there are a greater number of loads, sources and lines, differences between the three types of configurations are greater. This can be seen in the graphs that show each energy source contribution (Energy sources). In District there is hardly any difference between the settings in grid profile. In Rural Area differences can already be seen, radial configuration in this graph is the one that contributes with most energy, this is due to the fact that network has greater losses and has to transport large amounts of energy to reach all the points of consumption. In loss table, it can be seen how radial configuration has more losses for this reason and the mesh configuration has lower losses because it has a greater number of lines and possible paths through which the energy can be directed. In Urban Area, radial and mesh have the same losses and the contribution of the network is similar, and with ring there is more difference.

Regarding DCTs, it has been observed that in mesh configuration there is a smaller difference between the energy that passes through each DCT, this happens for the three areas of study. That is, there is more balance than in the other two configurations. And finally, knowing the voltage at the nodes has allowed knowing the direction of the power and verifying that the DCTs can work bidirectionally.

Part II

IMPEDANCE ASSESSMENT OF DC PDN

5 | ANALYTICAL SOLUTION

This part focuses on calculating voltage node analytically and computing impedance characteristics of each node. This is important for understanding stability and expansion capabilities, although these questions are not addressed in this thesis. Furthermore, the method used is scaleable, it is used to analyze the different types of configurations. Consequently, this analysis allows us to understand how each configuration behaves.

5.1 STEADY-STATE

In previous chapter, the voltage at each node was obtained. As detailed in [8], an analytical method allows to calculate the voltages at the nodes, and the current injected into the system through a series of equations. The novelty applied in this method is that the loads are now dynamic and vary over time. In this method, since it is a steady-state solution, there are only resistive elements in the lines. First, the steps to follow are presented, and then an example will be shown in the appendix for a greater understanding. Moreover, in the Appendix all the final results are shown for the three types of configurations in the case of District, Rural area and Urban Area. Using this method, it can be performed the impedance analysis in the next part. These are the steps:

1. Calculate the Nodal Admittance (Y_{nodal}):

$$Y_{nodal} = a^T y_p a \tag{5.1}$$

   Where a is the incidence matrix, in this matrix, the columns correspond to the number of nodes and the rows to the element (electrical line) number. To build incidence matrix we look at the element, each element is between two nodes. So we put a 1 in the node with the lowest numerical value and a -1 in the node with the highest numerical value. y_p is a diagonal matrix raised to -1 that represents the resistance in each line (element), so it has the size of the number of elements. This is the principles of the graph theory. In this case, we work in per unit values, so the values for the electric lines are represented in Table 4.3

2. Calculate the rest of the matrix to complete the Modified Nodal Analysis (C, B, D):
   - Matrix C has as number of rows, the number of existing grids, and the number of columns, corresponds to the number of nodes. It is a matrix of zeros except in the node in which there is a grid connection, it has a value of 1.
   - Matrix B is calculated as follows:

$$B = (-C)^T \tag{5.2}$$

   - And, matrix D, is a square zero matrix with the size of the number of grids.

3. Sources and Loads matrix (J, F):
   - J contains the corresponding values of consumption and PV or hydro power production during the 24 hours, since these are modeled in PLECS as current sources. Renewable sources inject energy, which is why they have positive values. On the contrary, the consumptions have negative values. The size of matrix J is as follows, the number of columns will always be 24 due to 24 hours a day, and the number of rows corresponds to the number of nodes.
   - On the other hand, matrix F refers to the grid, which is why its number of columns is 24, and the number of rows will correspond to the grid number. This is a matrix of ones.

4. Describe the Modified Nodal Analysis equation:

$$\underbrace{\begin{bmatrix} Y_{nodal} & B \\ C & D \end{bmatrix}}_{\text{A}} \times \underbrace{\begin{bmatrix} V \\ I \end{bmatrix}}_{\text{x}} = \underbrace{\begin{bmatrix} J \\ F \end{bmatrix}}_{\text{b}} \tag{5.3}$$

5. Solve linear system of (5.3):

$$x = A \backslash b \tag{5.4}$$

   Where, x gives the solution of the voltage in the nodes and the current injected by the grid.

After being calculated in MATLAB (Analytical), voltages and currents in the three cases and for the three types of configurations these were compared with the results in PLECS (Simulation). Once comparisons of the 9 systems have been made, it is concluded that the results are correct. Table **5.1** shows the comparison between the two methods for radial configuration in District. Appendix details how is calculated analytical part for this case.

As can be seen, results are very similar. The voltage at each node can be used to determine direction of power flow. In a line between two nodes, the direction flows from the higher voltage node to the lower voltage node. These results show that incidence matrix is right, this matters to us because for nodal impedance assessment we start from this matrix. It is also shown that the Modified Nodal Analysis is useful for dynamic consumption and for systems with a large number of nodes.

Table 5.1 Comparison between analytical and simulation results radial configuration at 07 am (District).

Voltage	Analytical	Simulation	Unit	Voltage	Analytical	Simulation	Unit
Node 3	0.999974	0.999974	pu	Node 12	0.999972	0.999972	pu
Node 4	0.999974	0.999974	pu	Node 13	0.999972	0.999972	pu
Node 5	1.000051	1.000050	pu	Node 14	0.999972	0.999971	pu
Node 6	1.000051	1.000050	pu	Node 15	0.999972	0.999972	pu
Node 7	1.000054	1.000050	pu	Node 16	0.999972	0.999972	pu
Node 8	0.999973	0.999973	pu	Current	Analytical	Simulation	Unit
Node 9	0.999973	0.999972	pu	Grid	0.003000	0.003013	pu

5.2 NODAL IMPEDANCE

From the previous analytical method now extend the model and the lines are modeled with the model in π. In this way, the admittance at each node can be estimated from the frequency. This is important in order to know in what frequency range resonances can exist. The frequency in this case reaches up to 1000 Hz. Long-line effects can be severe depending on the frequency and length ranges, [8] study this phenomenon. Two cable lengths of 20 km and 50 km are simulated. In case of 20 km cable length, one section π-equivalent model can accurately represent it until 1 kHz. The same can be said for short cables. On the other hand, if one section π-equivalent model is considered for the line of 50 km length, it does not adequately capture the frequency response above 500 Hz. It concludes, to accurately capture the frequency response for long cables, more π-sections or a frequency-dependent model is required.

This part explains the different steps of the method, and then, it presents the results obtained. It compares and analyzes how the impedance varies in the three cases for the three types of configurations. Three nodes are taken to analyze, the network, a load, and the DCT. Additionally, it is studied how the change in length affects the impedance. Equation 5.5 defines the impedance, resistance (R) is the real part of impedance, and reactance (X) is the imaginary part. π model is characterized by having a series resistance with an inductance between two parallel admittances that reflect the capacitance of the line, in Figure **5.1** this can be seen.

$$Z = R + Xj \tag{5.5}$$

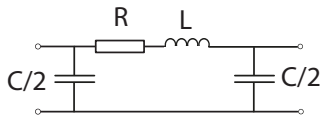

Fig. 5.1 π model

This part is calculated in real values, this are the following steps:

1. Values:
   For the values of resistance, inductance, and capacity, the values corresponding to [32] and [8] are taken. In Table **5.2** the values referred to 5kV are shown.
   To move to the other base we will have to apply the transformer ratio ($at = 2$), and then calculate $rtl' = (1/n^2) \cdot rtl$, $ltl' = (1/n^2) \cdot ltl$, and $ctl' = n^2 \cdot ctl$

Table 5.2 System values [32], [8]

	Symbol	Value	Unit		Symbol	Value	Unit
TL resistance	*rtl*	17.6	mΩ/km	DCT resistance	*rdct*	14	mΩ
TL inductance	*ltl*	0.268	mH/km	DCT inductance	*ldct*	39.97	mH
TL capacitance	*ctl*	0.904	μF/km	DCT capacitance	*cdct*	8	mF

2. Add the inductive part:
   To primitive admititance matrix *yp* calculated in Section 5.1 the inductive part is added. It should be added that the inductance is multiplied by the variable (5.6). Then the impedance is calculated (5.7).

$$s(f) = 2\pi fj \tag{5.6}$$

$$Y_{R+L} = a^T y_p a \tag{5.7}$$

3. Capacitance admittance:
   Next, the capacitance (cap) admittance is calculated (5.8). First, the capacity of each element is calculated $cap_{elements} = s(f) \cdot (ctl \cdot length)/2$ and then the capacity at each node $cap_{nodes} = \sum cap_{elements}$.

$$Y_C = diag(cap_{nodes}) \tag{5.8}$$

4. Grid:
   The grid, represented as a voltage source, is an ac/dc converter. To analyze the impedance, a voltage controller is added, so that the admittance of the network can be calculated as follows:

$$Y_s = \frac{sK_p + K_i}{s} \, x \, K_{Gvi} \tag{5.9}$$

   Where K_p is the proportional gain and K_i is the integration gain. K_{Gvi} is the inner control loop compensation gain, calculated as follows: $K_{Gvi} = 3V_d/2V_{dc}$. Finally, matrix $Y_{sources}$ is calculated, where this is a diagonal matrix with the size of the number of nodes. In the node where the grid is found Y_s will be added, otherwise zero is written. According to [8], $K_p = 0.1251/$, $K_i = 0.051/$,$V_d = 3.3\,kV$, and $V_{dc} = 10kV$,

$$Y_{sources} = diag(Y_s) \tag{5.10}$$

5. Total impedance:
   Finally total impedance matrix (Z) is calculated, each element of this matrix represents a transfer function. And each transfer function gives the response of the voltage for an excitation in current. $Z(f)$ is a square matrix with the size of number of nodes, full of transfer functions that includes the system passive elements and grid control.

$$Z(f) = \frac{1}{Y_{R+L} + Y_C + Y_{sources}} \tag{5.11}$$

5.3 RESULTS FOR NODAL IMPEDANCE ASSESSMENT

A graphical representation of impedance is made after the corresponding calculations are done in MATLAB. Results are presented in Bode plot for easier understanding and interpretation. It allows for characterizing the frequency response of the system. It consists of two separate graphs, one for magnitude and the other for phase. In the phase plot, when the angle is below 0, the behavior is capacitive, and when it is above, it is inductive.

To carry out impedance study, three nodes are studied. One of the nodes corresponds to a grid, the other is a node connected to a load and the last node is for a DCT. Three plots are shown for each node, one for each study area and in turn within each graph the results for the radial (yellow lines), ring (orange lines) and mesh (blue lines) configurations are represented. In addition, it is analyzed for grid node how the impedance behaves if the length of a line varies. The results shown are those obtained by Eq. (5.11). In order to understand the whole system behavior in frequency domain, nodal impedance must be identified.

5.3.1 GRID IMPEDANCE

First, the node corresponding to grid is investigated, which in the three types of study areas (District, Urban Area and Rural Area) corresponds to node 1. In all the three cases, impedance decrease its value when frequency increases. Radial configuration is yellow line, ring is orange, and mesh is blue

Next, it is specified what happens for each zone:

District case (Fig. **5.2** (a)): resonances appear between 200 and 400 Hz. For mesh case, these appear before, then those of ring configuration appear, and finally radial resonance. When resonances happen, for mesh case the angle becomes inductive, and in radial and ring cases this does not happen. It has been analyzed that in other papers such as [33], the behavior of network is similar. In mesh case an initial resonance appears at 5 Hz that does not appear in the other configurations

Rural Area (Fig. **5.2** (b)): mesh case is the one that presents a greater number of resonances, and also these resonances reach higher values of impedance compared to the other configurations. In mesh, these resonances are in 32 Hz and in 500 Hz. For ring and radial there are hardly any resonances, in 500 Hz. In the three configurations initial impedance is the same and the initial angle is closer to 0°.

Urban Area (Fig. **5.2** (c)): it presents more significant oscillations, this may be due to the greater number of connections and loads, there are 49 nodes in this system. Ring case is the one with the least oscillations. In the three configurations initial impedance is the same and the initial angle is closer to 0°.

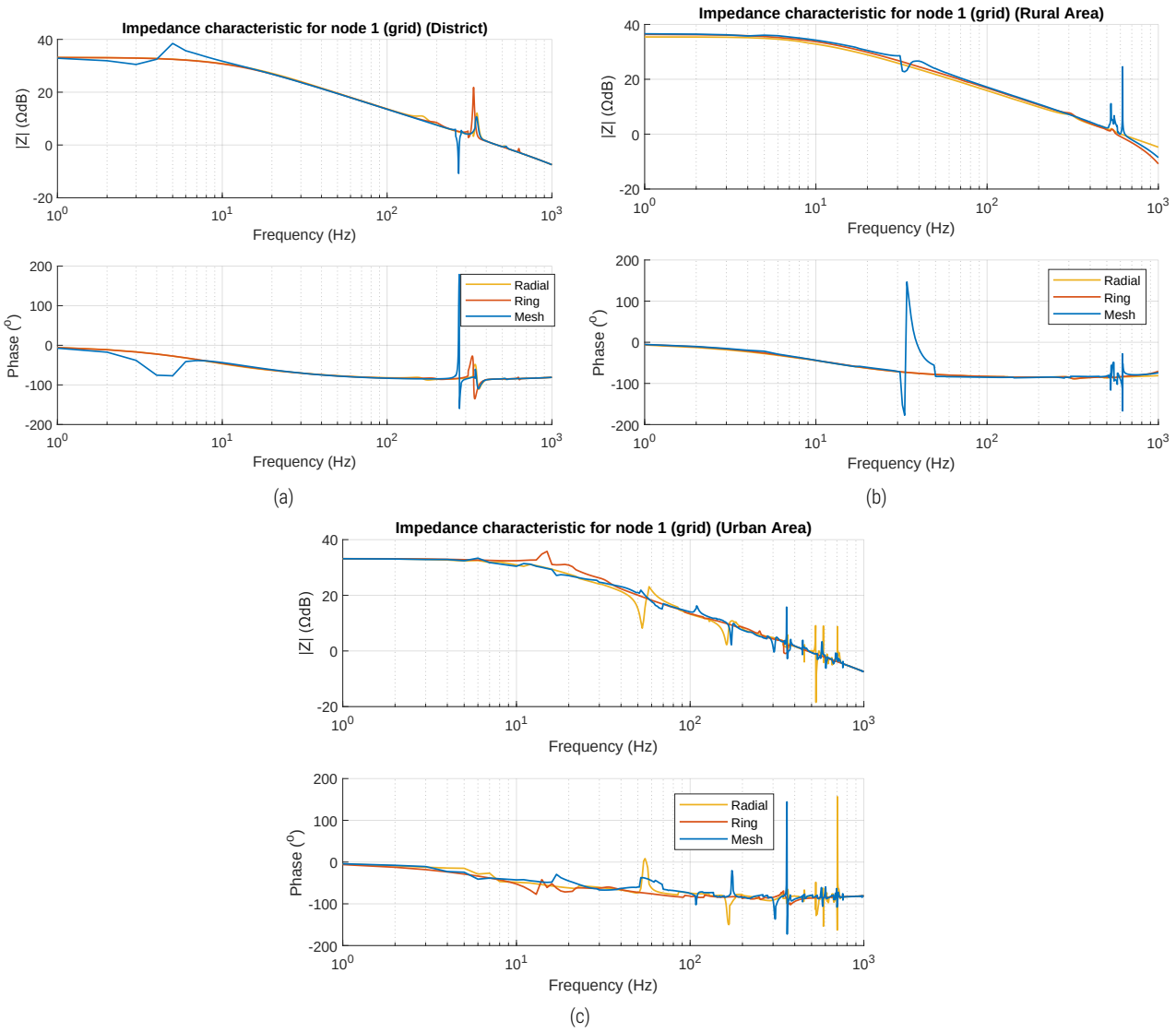

Fig. 5.2 Impedance characteristic of node 1 (grid) using Eq. (5.11) for radial, ring and mesh configurations: (a) District case; (b) Rural Area case; (c) Urban Area case.

5.3.2 LOAD IMPEDANCE

Afterwards, impedance behavior in a node where there is consumption in the three types of study area is presented.

District case (Fig. **5.3** (a)): in this case load c in node 16, has been selected. There is hardly any resonance and depending on the type of configuration, the impedance value is different. Mesh has the maximum impedance with a initial value of 125, then ring and finally radial with a initial value of 51. Behavior is capacitive.

Rural Area (Fig. **5.3** (b)): in this case load e in node 10 has been chosen. Now, resonances appear, especially between 60 and 100 Hz. Ring case is the one with the lowest resonances and mesh case the one with the highest resonances. There is not so much difference with impedance value between the different configurations.

Urban Area (Fig. **5.3** (c)): in this case the impedance node is load b1, in node 5 for radial and mesh configuration, and in node 7 in ring configuration. Ring configuration has lower impedance value than radial and mesh which have the same. Radial and mesh have little resonances but ring has a resonance in 350 Hz. Impedance start with an angle closer to 0°.

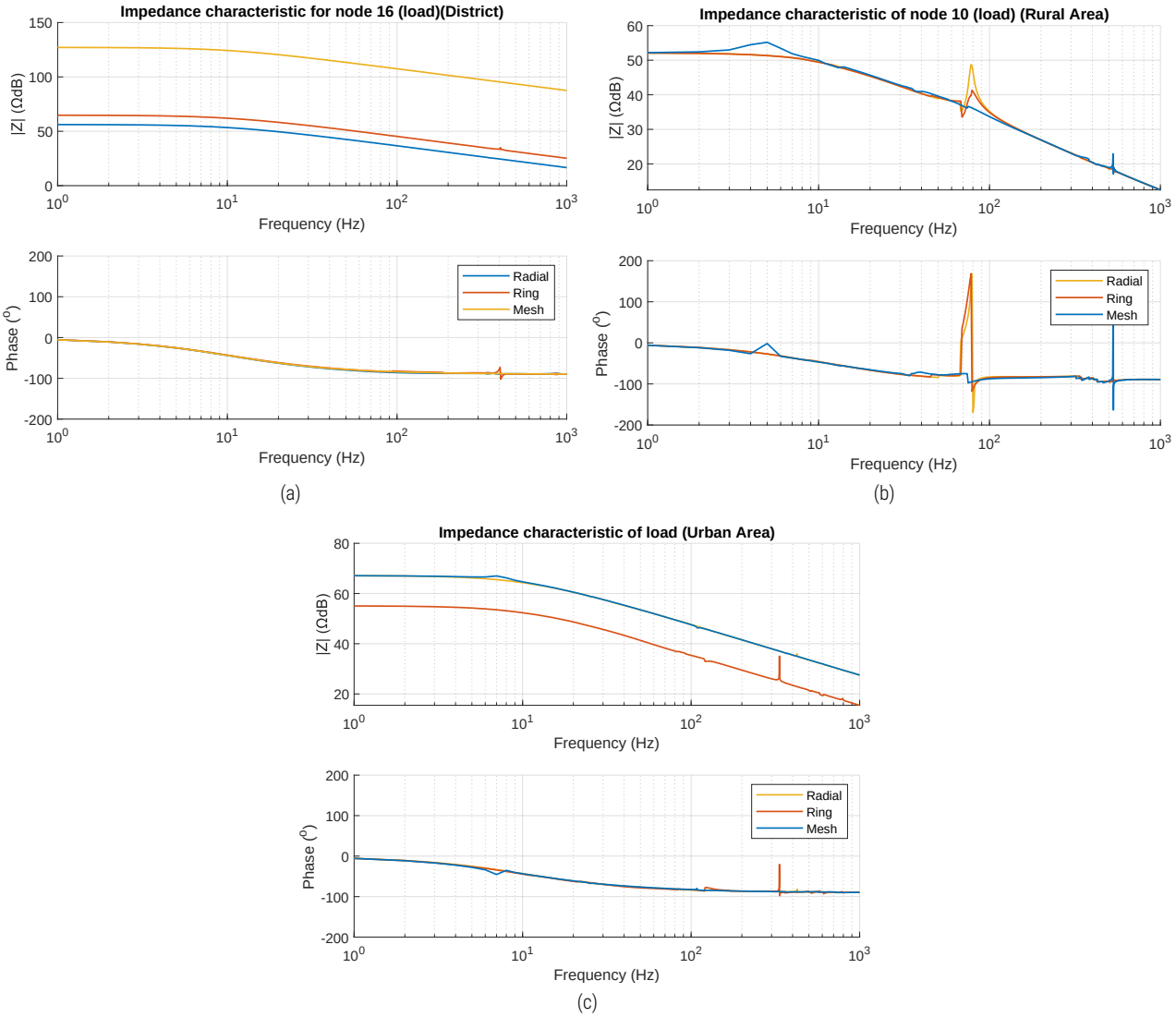

Fig. 5.3 Impedance characteristic of load using Eq. (5.11) for radial, ring and mesh configurations: (a) District case (load c); (b) Rural Area case (load e); (c) Urban Area case (load b1).

5.3.3 DCT IMPEDANCE

Impedance behavior in a DCT in three types of study areas is then discussed

District case (Fig. **5.4** (a)): in this case DCT2 in node 9 has been selected. The impedance value is similar in all three configurations. Resonances occur at almost the same frequencies, between 500 Hz and 1000 Hz. When resonances occur, the behavior becomes inductive. In some frequency ranges the mesh case has some resonances.

Rural Area (Fig. **5.4** (b)): in this case DCT2 in node 12 has been selected. The behavior of the impedance in the three types of configurations is almost the same. At first the impedance barely varies and remains constant up to 20 Hz, from then it begins to decrease until a resonance occurs between 400 Hz and 600 Hz.

Urban Area (Fig. **5.4** (c)): in this case DCT4 is presented, in radial and mesh configuration it corresponds to node 22, and in ring it is node 16. Since the same node is analyzed in radial and mesh cases, as in the previous study areas, there is very little difference between these two configurations. In the case of ring, impedance is lower because it is a different node that feeds different loads. Now there are more resonances than before, especially between 10 Hz and 40 Hz, and between 400 Hz and 800 Hz.

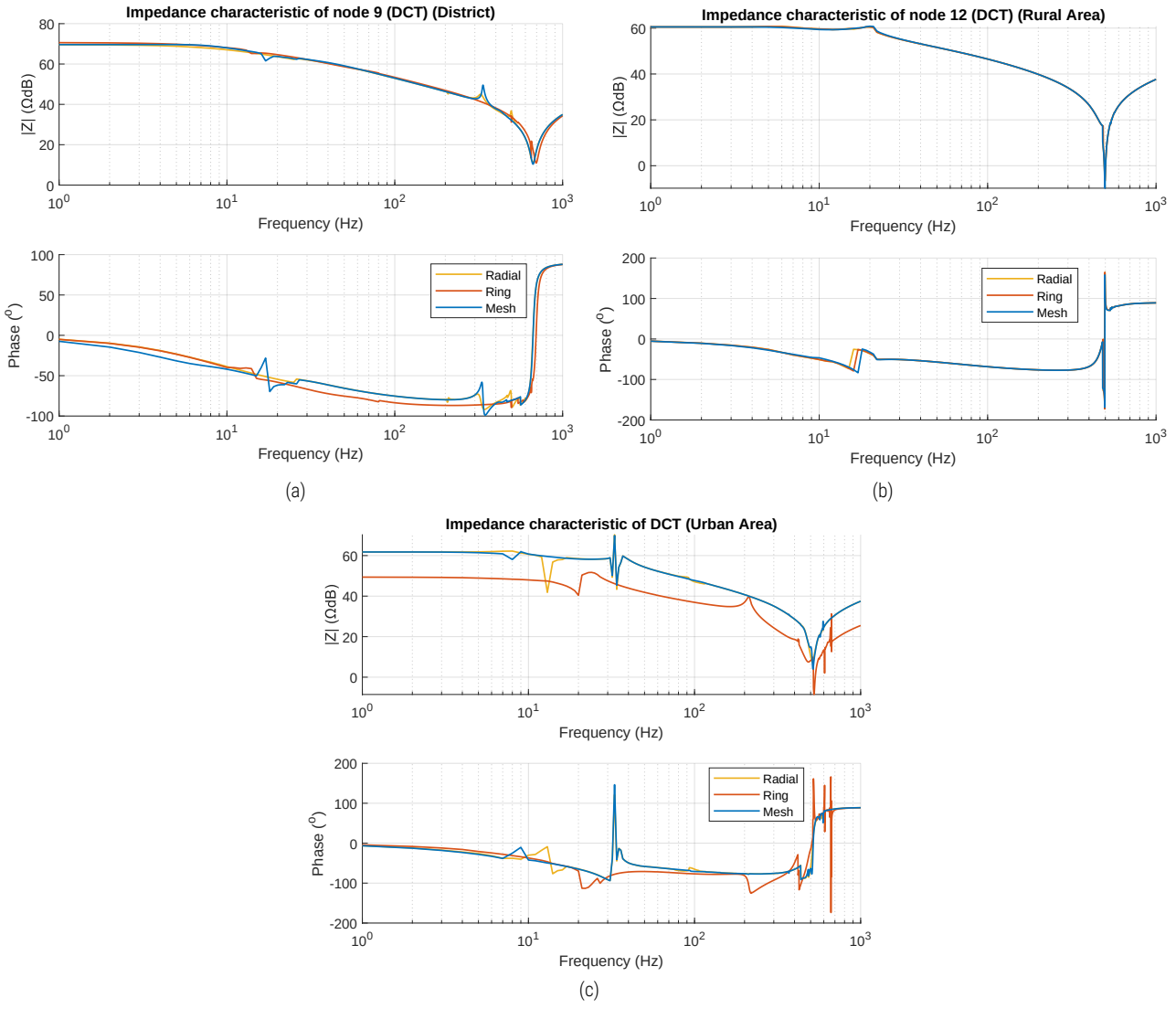

Fig. 5.4 Impedance characteristic of DCT using Eq. (5.11) for radial, ring and mesh configurations: (a) District case (DCT2); (b) Rural Area case (DCT2); (c) Urban Area case (DCT4).

5.3.4 SIMPLE EXAMPLE OF TRANSMISSION LINE IMPACT

The following case analyzes how the impedance varies by changing the length of a line in the three configurations. For this case, node 1 (grid) has been taken for District zone. The initial length is 5 km, this length is modified and it is analyzed what happens in a range from 1 km to 23 km with intervals of 2 km. As can be seen in Fig. **5.5**, the resonant frequency varies and so does the impedance value. If the distance decreases, the resonance appears at lower frequencies, and if the distance increases, the resonance appears at higher frequencies, and after a certain distance they begin to appear earlier and behavior tends to be inductive. This happens in all three configurations equally. It is also observed that as the distance increases, impedance value decreases.

5.4 CONCLUSIONS OF NODAL IMPEDANCE RESULTS

Once results of each of the three nodes (Grid node, load, Node and DCT node) have been presented in the three study areas and for the three types of configurations, various aspects can be concluded. The initial impedance between 0 Hz and 10 Hz in all cases remains practically constant, and when frequency increases, its value decreases. Load node is the node with the highest damping of all, the mesh case being the one with the lowest resonances. The grid node behaves with higher resonances, but now the ring case has damped resonances. And the DCT node also has resonances but it is characterized in that when the resonances appear the value of the impedance decreases drastically. Further, the slope of impedance, when it starts to decrease its value, is much higher than in the load node and grid node.

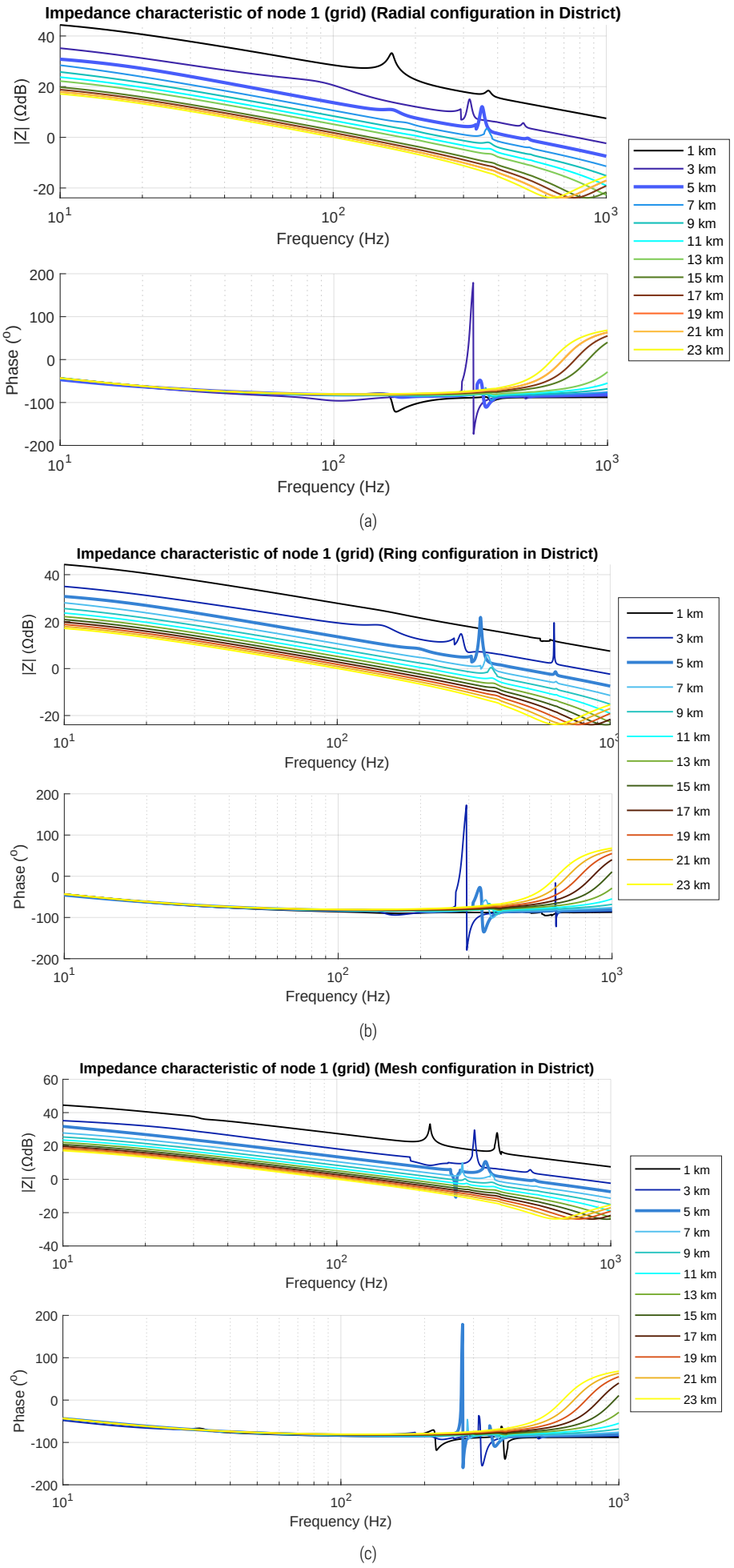

Fig. 5.5 Impedance characteristic of node 1 (grid) depending on lenght in District case: (a) Radial configuration; (b) Ring configuration; (c) Mesh configuration.

6 | CONCLUSION

With the methodology employed, it was possible to study how radial, ring, and mesh configurations behave in DC power distribution networks incorporating DCTs. To achieve this goal, power flow has been studied using steady-state models, and the behavior of impedance in the frequency range of interest has been analyzed using an analytical model.

To begin with, the study systems had to be defined. To perform this, three different areas have been examined to get a better sense of the behavior of each system. The chosen areas have been a residential area (District), a rural area, and an urban area. After that, a study was conducted in each area in a realistic way. This study investigated aspects such as the type of consumers, their distribution and locations, the current energy situation, the location of DCTs, location of the grid, and current electrical layout. Once the different points of interest were located, the layout of future electrical distribution network in DC was drawn up for each study area and for each type of configuration. Power lines were then measured for length.

Once the study was completed, parameters were calculated to build steady-state model. Resistance of the power lines was parameterized, DCT was modeled, and consumption profiles and production of renewable energy sources were also included. Load profiles have been obtained from real data carried out in different studies and projects. In total, nine different models were built.

Having characterized the study area and built a model for each system, different simulations were conducted. Power flow study provides information about the system operating point. As a result of these simulations, total load, contribution of each energy source, energy flowed through the DCTs, losses of the system, and voltage in nodes were presented.

Next, an analytical model was presented to calculate nodal impedance. Initially, equations to calculate operating point of a DC system without the need for simulations were implemented. And voltage at the nodes and the energy injection from the voltage source (grid) were calculated. Using this method, nodal impedance was calculated by constructing electrical lines in π-model. The frequency analysis will provide information about the characteristics of the system. The impedance characteristics of a grid node, load node, DCT node and the behavior of the impedance before changes of length in the lines were shown.

This study has served as a basis to investigate how future DC PDNs could be, thus contributing to implementing sustainable measures. It has been possible to verify how DCT is an isolated dc-dc power converter acting as a power transformer between two DC lines, operating in an open-loop. Additionally, as a bidirectional element, DCT can follow the natural power flow. Also, mesh configuration performs best results in terms of losses as well as distribution and capability in DCTs. In second part, it has been demonstrated that the analytical model can be applied to systems with more nodes and dynamic loads. In addition, the impedance decreases when frequency increases. In general, mesh configuration has more resonances.

DC PDN architectures need further technological development and a stronger business case to replace MVAC networks on a large scale. The use of DC power system comes with additional challenges, including the provision of energy storage systems, protection, coordination, system reconfiguration, development of DCTs at different voltage levels, development of efficient and highly DC circuit breakers and establishment of specific standards and regulations. The impact of changes in the general configuration can be investigated and how those changes affect the power flow. As well as studying the behavior of the system in the event of system failures in a transient state.

The next steps to expand the study of this project would be model the systems but in AC to calculate their behavior and compare the losses with our systems in DC. Calculate investment and operation costs of each type of configuration and compare them with each other to know the difference. Regarding impedance, apply Nyquist stability criterion and calculate eigenvalues and eigenvectors to know the stability of the system.

REFERENCES

[1] W. Group and F. Report, 'DC Networks on the distribution level – New trend or Vision ? Final Report DC Networks on the distribution level – New trend or Vision ?', no. July, pp. 1–113, 2021.

[2] M. Fotopoulou, D. Rakopoulos, D. Trigkas, F. Stergiopoulos, O. Blanas and S. Voutetakis, 'State of the art of low and medium voltage direct current (Dc) microgrids', *Energies*, vol. 14, no. 18, 2021.

[3] F. Mura and R. W. D. Doncker, 'Preparation of a Medium-Voltage DC Grid Demonstration Project', *E.ON Energy Research Center Series*, vol. 4, no. 1, pp. 1–32, 2012.

[4] D. Kumar, F. Zare and A. Ghosh, 'DC Microgrid Technology: System Architectures, AC Grid Interfaces, Grounding Schemes, Power Quality, Communication Networks, Applications, and Standardizations Aspects', *IEEE Access*, vol. 5, no. August, pp. 12 230–12 256, 2017.

[5] M. M. Eissa., *Medium-voltage direct current grids : resilient operation, control and protection*, ser. London: Academic Press. Academic Press, 2019.

[6] M. Mogorovic, 'Modeling and design optimization of medium frequency transformers for medium-voltage high-power converters', p. 148, 2019.

[7] D. Dujic and M. Mogorovic, 'High power medium frequency transformer design optimization', 2017.

[8] R. P. Barcelos and D. Dujic, 'Nodal Impedance Assessment in DC Power Distribution Networks', pp. 1–8, 2021.

[9] ——, 'Direct Current Transformer Impact on the DC Power Distribution Networks', *IEEE Transactions on Smart Grid*, pp. 1–1, 2022.

[10] J. Kucka and D. Dujic, 'Smooth Power Direction Transition of a Bidirectional LLC Resonant Converter for DC Transformer Applications', *IEEE Transactions on Power Electronics*, vol. 36, no. 6, pp. 6265–6275, Jun. 2021.

[11] I. Alhurayyis, A. Elkhateb and J. Morrow, *Isolated and Non-Isolated DC-to-DC Converters for Medium Voltage DC Networks: A Review Ibrahim Alhurayyis, Student Member, IEEE, Ahmad Elkhateb, Senior Member, IEEE and D John Morrow*, Dec. 2021.

[12] M. Carpita, D. Dujic, A. Christe *et al.*, 'Direct current technologies for Switzerland ' s electricity transmission and distribution', pp. 1–32, 2019.

[13] J. Priebe and M. Sieberichs, 'FINAL PROJECT REPORT Center for FEN MVDC Landscape Seed Fund Project MV 12 Final Project Report MVDC Landscape',

[14] S. Coffey, V. Timmers, R. Li and A. Wu G.and Egea-Àlvarez, 'Review of MVDC Applications, Technologies, and Future Prospects', 2021.

[15] S. Peyghami, P. Davari, H. Mokhtari and F. Blaabjerg, 'Decentralized Droop Control in DC Microgrids Based on a Frequency Injection Approach', *IEEE Transactions on Smart Grid*, vol. 10, no. 6, pp. 6782–6791, 2019.

[16] A. Chandra, G. K. Singh and V. Pant, 'Protection techniques for DC microgrid- A review', *Electric Power Systems Research*, vol. 187, Oct. 2020.

[17] G. Bathurst, G. Hwang and L. Tejwani, 'MVDC – The New Technology for Distribution Networks', Tech. Rep.

[18] W. Li, Y. Li, S. Yu *et al.*, 'State of the Art of Researches and Applications of MVDC Distribution Systems in Power Grid', *IECON Proceedings (Industrial Electronics Conference)*, vol. 2019-Octob, pp. 5680–5685, Oct. 2019.

[19] S. B. Siad, 'DC MicroGrids Control for renewable energy integration',

[20] K. Prakash, A. Lallu, F. R. Islam and K. A. Mamun, 'Review of Power System Distribution Network Architecture', *Proceedings - Asia-Pacific World Congress on Computer Science and Engineering 2016 and Asia-Pacific World Congress on Engineering 2016, APWC on CSE/APWCE 2016*, no. December, pp. 124–130, 2017.

[21] M. K. Bucher, R. Wiget, G. Andersson and C. M. Franck, 'Multiterminal HVDC Networks - What is the preferred topology', *IEEE Transactions on Power Delivery*, vol. 29, no. 1, pp. 406–413, 2014.

[22] R. E. ELectric, 'SCCER-FURIES Romande Energie ELectric network in local balance Demonstrator (REEL Demo)', no. May, 2019.

[23] i. W. hc Rik De Doncker, 'Energy System Transition and DC Hybrid Power Systems The Energy System Transition and DC Hybrid Power Systems Introduction • RWTH CAMPUS Cluster Sustainable Energy • Distributed Generation Sector coupling • Research CAMPUS Flexible Electrical Networks M', 2018.

[24] R. Dufo-López, J. Bernal-Agustín, L. Correas-Usón and I. Aso-Aguarta, '"demand side management in hybrid systems with hydrogen storage in several demand scenarios in aragon', Jan. 2008.

[25] Regenera. 'Energy audit of alhama's municipal buildings'. (2016), [Online]. Available: `https://datos.alhamademurcia.es/descargas/6347n-auditoria-energ.-cinco-edificios.pdf`.

[26] ree (red electrica españa). 'Atlas de la demanda eléctrica española. proyecto indel (atlas of spanish electricity demand. indel project)'. (1998), [Online]. Available: `https://www.ree.es/sites/default/files/downloadable/atlas_indel_ree.pdf`.

[27] G. Pressmair, C. Amann and K. Leutgöb, 'Business models for demand response: Exploring the economic limits for small- and medium-sized prosumers', *Energies*, vol. 14, no. 21, 2021.

[28] M. Mirzaei and B. Vahidi, 'Feasibility analysis and optimal planning of renewable energy systems for industrial loads of a dairy factory in tehran, iran', *Journal of Renewable and Sustainable Energy*, vol. 7, p. 063 114, Nov. 2015.

[29] P.-R. Mincu and T. Boboc, 'Load profiles in smart cities', *2017 International Conference on ENERGY and ENVIRONMENT (CIEM)*, pp. 480–484, 2017.

[30] A. Liebman and G. Walker, 'Impacts of vehicle-to-grid (v2g) technologies on electricity market operations', Jan. 2007.

[31] J. Boland, 'Characterising seasonality of solar radiation and solar farm output', *Energies*, vol. 13, p. 471, Jan. 2020.

[32] Nexans, '6-36kV Medium Voltage Underground Power Cables', 2009.

[33] J. Sun, 'Impedance-based stability criterion for grid-connected inverters', *IEEE Transactions on Power Electronics*, vol. 26, no. 11, pp. 3075–3078, 2011.

APPENDIX

A ANALYTICAL STEADY-STATE SOLUTION

A.1 EXAMPLE

Then, the corresponding values to solve the explained method in Section **5.1** are shown with numerical values for radial configuration in District case. In Fig. **A.1** the number of the elements (yellow circles) used for calculating the matrices has been included in each line. Values are in per unit.

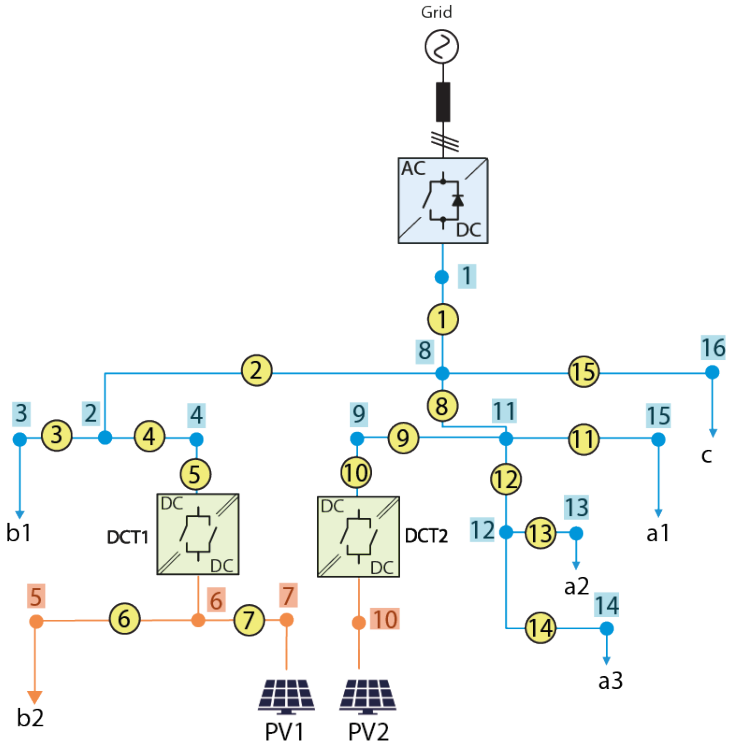

Fig. A.1 Diagram of the radial configuration for District case with the grid, the 6 consumers, the 2 PVs, the 2 DCTs and the 13 power lines. It includes the element number of each line to build the incidence matrix (*a*). There are 16 nodes and 15 elements (yellow circles).

First, incidence matrix (*a*) is constructed. It has 16 columns because there are 16 nodes, and 15 rows because there are 15 elements. As an example, we take element number 1. This element is between nodes 1 and 8. Therefore, in row number 1 and column number 1 we write 1; and in row number 1 and column number 8 write −1. The rest of rows are built in the same way.

$$a_{15\times16} = \begin{bmatrix} 1 & 0 & 0 & 0 & 0 & 0 & 0 & -1 & 0 & 0 & 0 & 0 & 0 & 0 & 0 & 0 \\ 0 & 1 & 0 & 0 & 0 & 0 & 0 & -1 & 0 & 0 & 0 & 0 & 0 & 0 & 0 & 0 \\ 0 & 1 & -1 & 0 & 0 & 0 & 0 & 0 & 0 & 0 & 0 & 0 & 0 & 0 & 0 & 0 \\ 0 & 1 & 0 & -1 & 0 & 0 & 0 & 0 & 0 & 0 & 0 & 0 & 0 & 0 & 0 & 0 \\ 0 & 0 & 0 & 1 & 0 & -1 & 0 & 0 & 0 & 0 & 0 & 0 & 0 & 0 & 0 & 0 \\ 0 & 0 & 0 & 0 & 1 & -1 & 0 & 0 & 0 & 0 & 0 & 0 & 0 & 0 & 0 & 0 \\ 0 & 0 & 0 & 0 & 0 & 1 & -1 & 0 & 0 & 0 & 0 & 0 & 0 & 0 & 0 & 0 \\ 0 & 0 & 0 & 0 & 0 & 0 & 0 & 1 & 0 & 0 & -1 & 0 & 0 & 0 & 0 & 0 \\ 0 & 0 & 0 & 0 & 0 & 0 & 0 & 0 & 1 & 0 & -1 & 0 & 0 & 0 & 0 & 0 \\ 0 & 0 & 0 & 0 & 0 & 0 & 0 & 0 & 1 & -1 & 0 & 0 & 0 & 0 & 0 & 0 \\ 0 & 0 & 0 & 0 & 0 & 0 & 0 & 0 & 0 & 0 & 1 & 0 & 0 & 0 & -1 & 0 \\ 0 & 0 & 0 & 0 & 0 & 0 & 0 & 0 & 0 & 0 & 1 & -1 & 0 & 0 & 0 & 0 \\ 0 & 0 & 0 & 0 & 0 & 0 & 0 & 0 & 0 & 0 & 0 & 1 & -1 & 0 & 0 & 0 \\ 0 & 0 & 0 & 0 & 0 & 0 & 0 & 0 & 0 & 0 & 0 & 1 & 0 & -1 & 0 & 0 \\ 0 & 0 & 0 & 0 & 0 & 0 & 0 & 1 & 0 & 0 & 0 & 0 & 0 & 0 & 0 & -1 \end{bmatrix} \tag{A.1}$$

y_p is a diagonal matrix with the size of the 15 elements. First, vector *rlines* is constructed. In the first element, *rline* is the resistance of element 1 and 5 is the length of element 1.

$$rlines = [rline10 \cdot 5 \quad rline10 \cdot 0.270 \quad rline10 \cdot 0.016 \quad rline10 \cdot 0.053 \quad rwt5 \quad rline5 \cdot 0.077 \quad rline5 \cdot 0.097 \quad rline10 \cdot 0.106$$
$$rline10 \cdot 0.083 \quad rwt5 \quad rline10 \cdot 0.051 \quad rline10 \cdot 0.091 \quad rline10 \cdot 0.057 \quad rline10 \cdot 0.090 \quad rline10 \cdot 0.351]$$

$$y_{p15\times15} = diag(rlines)^{-1} = \begin{bmatrix} 111 & 0 & 0 & 0 & 0 & 0 & 0 & 0 & 0 & 0 & 0 & 0 & 0 & 0 & 0 \\ 0 & 2058 & 0 & 0 & 0 & 0 & 0 & 0 & 0 & 0 & 0 & 0 & 0 & 0 & 0 \\ 0 & 0 & 34722 & 0 & 0 & 0 & 0 & 0 & 0 & 0 & 0 & 0 & 0 & 0 & 0 \\ 0 & 0 & 0 & 10482 & 0 & 0 & 0 & 0 & 0 & 0 & 0 & 0 & 0 & 0 & 0 \\ 0 & 0 & 0 & 0 & 39 & 0 & 0 & 0 & 0 & 0 & 0 & 0 & 0 & 0 & 0 \\ 0 & 0 & 0 & 0 & 0 & 1855 & 0 & 0 & 0 & 0 & 0 & 0 & 0 & 0 & 0 \\ 0 & 0 & 0 & 0 & 0 & 0 & 1473 & 0 & 0 & 0 & 0 & 0 & 0 & 0 & 0 \\ 0 & 0 & 0 & 0 & 0 & 0 & 0 & 5241 & 0 & 0 & 0 & 0 & 0 & 0 & 0 \\ 0 & 0 & 0 & 0 & 0 & 0 & 0 & 0 & 6693 & 0 & 0 & 0 & 0 & 0 & 0 \\ 0 & 0 & 0 & 0 & 0 & 0 & 0 & 0 & 0 & 39 & 0 & 0 & 0 & 0 & 0 \\ 0 & 0 & 0 & 0 & 0 & 0 & 0 & 0 & 0 & 0 & 10893 & 0 & 0 & 0 & 0 \\ 0 & 0 & 0 & 0 & 0 & 0 & 0 & 0 & 0 & 0 & 0 & 6105 & 0 & 0 & 0 \\ 0 & 0 & 0 & 0 & 0 & 0 & 0 & 0 & 0 & 0 & 0 & 0 & 9747 & 0 & 0 \\ 0 & 0 & 0 & 0 & 0 & 0 & 0 & 0 & 0 & 0 & 0 & 0 & 0 & 6173 & 0 \\ 0 & 0 & 0 & 0 & 0 & 0 & 0 & 0 & 0 & 0 & 0 & 0 & 0 & 0 & 1583 \end{bmatrix} \quad (A.2)$$

$$Y_{nodal16\times16} = a^T y_p a =$$

$$\begin{bmatrix} 0.11 & 0 & 0 & 0 & 0 & 0 & 0 & -0.11 & 0 & 0 & 0 & 0 & 0 & 0 & 0 & 0 \\ 0 & 47.26 & -34.72 & -10.48 & 0 & 0 & 0 & -2.06 & 0 & 0 & 0 & 0 & 0 & 0 & 0 & 0 \\ 0 & -34.72 & 34.72 & 0 & 0 & 0 & 0 & 0 & 0 & 0 & 0 & 0 & 0 & 0 & 0 & 0 \\ 0 & -10.48 & 0 & 10.52 & 0 & -0.04 & 0.00 & 0 & 0 & 0 & 0 & 0 & 0 & 0 & 0 & 0 \\ 0 & 0 & 0 & 0 & 1.86 & -1.86 & 0.00 & 0 & 0 & 0 & 0 & 0 & 0 & 0 & 0 & 0 \\ 0 & 0 & 0 & -0.04 & -1.86 & 3.37 & -1.47 & 0 & 0 & 0 & 0 & 0 & 0 & 0 & 0 & 0 \\ 0 & 0 & 0 & 0 & 0 & -1.47 & 1.47 & 0 & 0 & 0 & 0 & 0 & 0 & 0 & 0 & 0 \\ -0.11 & -2.06 & 0 & 0 & 0 & 0 & 0 & 8.99 & 0 & 0 & -5.24 & 0 & 0 & 0 & 0 & -1.58 \\ 0 & 0 & 0 & 0 & 0 & 0 & 0 & 0 & 6.73 & -0.04 & -6.69 & 0 & 0 & 0 & 0 & 0.00 \\ 0 & 0 & 0 & 0 & 0 & 0 & 0 & 0 & -0.04 & 0.04 & 0 & 0 & 0 & 0 & 0 & 0 \\ 0 & 0 & 0 & 0 & 0 & 0 & 0 & -5.24 & -6.69 & 0 & 28.93 & -6.11 & 0 & 0 & -10.89 & 0 \\ 0 & 0 & 0 & 0 & 0 & 0 & 0 & 0 & 0 & 0 & -6.11 & 22.02 & -9.75 & -6.17 & 0 & 0 \\ 0 & 0 & 0 & 0 & 0 & 0 & 0 & 0 & 0 & 0 & 0 & -9.75 & 9.75 & 0 & 0 & 0 \\ 0 & 0 & 0 & 0 & 0 & 0 & 0 & 0 & 0 & 0 & 0 & -6.17 & 0 & 6.17 & 0 & 0 \\ 0 & 0 & 0 & 0 & 0 & 0 & 0 & 0 & 0 & 0 & -10.89 & 0 & 0 & 0 & 10.89 & 0 \\ 0 & 0 & 0 & 0 & 0 & 0 & 0 & -1.58 & 0 & 0 & 0 & 0 & 0 & 0 & 0 & 1.58 \end{bmatrix} x10^3$$

(A.3)

C has one row (1 grid) and 16 columns (16 nodes). Since grid is in node 1, in column 1 value 1 is added. The rest are zeros. From *C*, matrix *B* is built.

$$C_{1\times16} = \begin{bmatrix} 1 & 0 & 0 & 0 & 0 & 0 & 0 & 0 & 0 & 0 & 0 & 0 & 0 & 0 & 0 & 0 \end{bmatrix} \quad (A.4)$$

$$B_{16\times1} = (-C)^T = \begin{bmatrix} -1 \\ 0 \\ 0 \\ 0 \\ 0 \\ 0 \\ 0 \\ 0 \\ 0 \\ 0 \\ 0 \\ 0 \\ 0 \\ 0 \\ 0 \\ 0 \end{bmatrix} \quad (A.5)$$

D, is a square zero matrix with the size of 1x1 because there is one grid.

$$D_{1\times1} = \begin{bmatrix} 0 \end{bmatrix} \quad (A.6)$$

Matrix J has 16 rows (16 nodes) and 24 columns (24 hours of a day). The transposed matrix is represented for a better representation. In this matrix values of the loads and PVs are added. Column 3 of the transpose of J has the values corresponding to the consumption of load b1.

$$J^{T}_{24\times16} = \begin{bmatrix}
0 & 0 & -0.0004 & 0 & -0.0002 & 0 & 0 & 0 & 0 & 0 & 0 & 0 & -0.0006 & -0.0007 & -0.0012 & -0.0007 \\
0 & 0 & -0.0004 & 0 & -0.0002 & 0 & 0 & 0 & 0 & 0 & 0 & 0 & -0.0006 & -0.0008 & -0.0013 & -0.0008 \\
0 & 0 & -0.0004 & 0 & -0.0003 & 0 & 0 & 0 & 0 & 0 & 0 & 0 & -0.0006 & -0.0008 & -0.0012 & -0.0008 \\
0 & 0 & -0.0004 & 0 & -0.0004 & 0 & 0 & 0 & 0 & 0 & 0 & 0 & -0.0006 & -0.0010 & -0.0012 & -0.0011 \\
0 & 0 & -0.0004 & 0 & -0.0004 & 0 & 0 & 0 & 0 & 0 & 0 & 0 & -0.0006 & -0.0010 & -0.0012 & -0.0011 \\
0 & 0 & -0.0004 & 0 & -0.0005 & 0 & 0 & 0 & 0 & 0 & 0 & 0 & -0.0006 & -0.0011 & -0.0012 & -0.0013 \\
0 & 0 & -0.0005 & 0 & -0.0006 & 0 & 0 & 0 & 0 & 0 & 0 & 0 & -0.0008 & -0.0014 & -0.0015 & -0.0015 \\
0 & 0 & -0.0005 & 0 & -0.0009 & 0 & 0.0038 & 0 & 0 & 0.0014 & 0 & 0 & -0.0009 & -0.0020 & -0.0018 & -0.0022 \\
0 & 0 & -0.0006 & 0 & -0.0011 & 0 & 0.0077 & 0 & 0 & 0.0029 & 0 & 0 & -0.0011 & -0.0024 & -0.0021 & -0.0027 \\
0 & 0 & -0.0005 & 0 & -0.0009 & 0 & 0.0115 & 0 & 0 & 0.0043 & 0 & 0 & -0.0009 & -0.0020 & -0.0018 & -0.0023 \\
0 & 0 & -0.0005 & 0 & -0.0007 & 0 & 0.0154 & 0 & 0 & 0.0058 & 0 & 0 & -0.0008 & -0.0016 & -0.0015 & -0.0018 \\
0 & 0 & -0.0004 & 0 & -0.0007 & 0 & 0.0173 & 0 & 0 & 0.0065 & 0 & 0 & -0.0007 & -0.0016 & -0.0014 & -0.0018 \\
0 & 0 & -0.0004 & 0 & -0.0009 & 0 & 0.0182 & 0 & 0 & 0.0068 & 0 & 0 & -0.0006 & -0.0018 & -0.0013 & -0.0021 \\
0 & 0 & -0.0004 & 0 & -0.0008 & 0 & 0.0192 & 0 & 0 & 0.0072 & 0 & 0 & -0.0006 & -0.0016 & -0.0013 & -0.0019 \\
0 & 0 & -0.0004 & 0 & -0.0005 & 0 & 0.0182 & 0 & 0 & 0.0068 & 0 & 0 & -0.0006 & -0.0012 & -0.0013 & -0.0014 \\
0 & 0 & -0.0004 & 0 & -0.0004 & 0 & 0.0173 & 0 & 0 & 0.0065 & 0 & 0 & -0.0006 & -0.0011 & -0.0013 & -0.0012 \\
0 & 0 & -0.0004 & 0 & -0.0003 & 0 & 0.0154 & 0 & 0 & 0.0058 & 0 & 0 & -0.0006 & -0.0009 & -0.0013 & -0.0009 \\
0 & 0 & -0.0005 & 0 & -0.0004 & 0 & 0.0115 & 0 & 0 & 0.0043 & 0 & 0 & -0.0009 & -0.0012 & -0.0018 & -0.0012 \\
0 & 0 & -0.0007 & 0 & -0.0004 & 0 & 0.0077 & 0 & 0 & 0.0029 & 0 & 0 & -0.0012 & -0.0015 & -0.0025 & -0.0015 \\
0 & 0 & -0.0008 & 0 & -0.0004 & 0 & 0.0038 & 0 & 0 & 0.0014 & 0 & 0 & -0.0014 & -0.0015 & -0.0027 & -0.0014 \\
0 & 0 & -0.0008 & 0 & -0.0004 & 0 & 0 & 0 & 0 & 0 & 0 & 0 & -0.0013 & -0.0015 & -0.0026 & -0.0014 \\
0 & 0 & -0.0007 & 0 & -0.0003 & 0 & 0 & 0 & 0 & 0 & 0 & 0 & -0.0012 & -0.0014 & -0.0025 & -0.0013 \\
0 & 0 & -0.0006 & 0 & -0.0003 & 0 & 0 & 0 & 0 & 0 & 0 & 0 & -0.0011 & -0.0012 & -0.0021 & -0.0012 \\
0 & 0 & -0.0005 & 0 & -0.0003 & 0 & 0 & 0 & 0 & 0 & 0 & 0 & -0.0008 & -0.0010 & -0.0016 & -0.0009
\end{bmatrix} \tag{A.7}$$

Matrix F has 1 row because it is the grid. It has 24 columns because it represents a profile of a whole day.

$$F_{1\times24} = \begin{bmatrix} 1 & 1 & 1 & 1 & 1 & 1 & 1 & 1 & 1 & 1 & 1 & 1 & 1 & 1 & 1 & 1 & 1 & 1 & 1 & 1 & 1 & 1 & 1 & 1 \end{bmatrix} \tag{A.8}$$

A.2 RESULTS

Finally, it is solved the linear system with Eq. (5.4). Table A.1 and Table A.2 show the results.

Table A.1 Voltage in nodes and current in grid for radial configuration in District case from hour 0 am to 11 am.

RADIAL CONFIGURATION												
	Hour											
Voltage (pu)	12 am	1 am	2 am	3 am	4 am	5 am	6 am	7 am	8 am	9 am	10 am	11 am
Node 1	1	1	1	1	1	1	1	1	1	1	1	1
Node 2	0.99996566	0.99996334	0.99996247	0.99995756	0.99995756	0.99995423	0.99994484	0.99997418	1.00000843	1.00007213	1.00013587	1.00016125
Node 3	0.99996565	0.99996333	0.99996246	0.99995754	0.99995754	0.99995422	0.99994483	0.99997416	1.00000841	1.00007211	1.00013586	1.00016124
Node 4	0.99996564	0.99996332	0.99996245	0.99995752	0.99995752	0.99995419	0.99994479	0.99997446	1.00000906	1.00007314	1.00013727	1.00016283
Node 5	0.99995991	0.99995734	0.99995549	0.99994739	0.99994739	0.9999415	0.99993025	1.00005065	1.00017915	1.00034771	1.00051677	1.00059124
Node 6	0.99996002	0.99995746	0.99995564	0.9999476	0.9999476	0.99994175	0.99993054	1.00005112	1.00017974	1.0003482	1.00051715	1.00059163
Node 7	0.99996002	0.99995746	0.99995564	0.9999476	0.9999476	0.99994175	0.99993054	1.00005373	1.00018496	1.00035602	1.00052757	1.00060336
Node 8	0.99996594	0.99996363	0.99996278	0.99995792	0.99995792	0.99995464	0.99994532	0.999973	1.00000553	1.00006723	1.00012897	1.00015341
Node 9	0.99996546	0.99996312	0.99996227	0.99995738	0.99995738	0.99995408	0.99994464	0.9999726	1.00000546	1.00006781	1.00013019	1.0001549
Node 10	0.99996546	0.99996312	0.99996227	0.99995738	0.99995738	0.99995408	0.99994464	1.0000099	1.00008005	1.00017969	1.00027937	1.00032273
Node 11	0.99996546	0.99996312	0.99996227	0.99995738	0.99995738	0.99995408	0.99994464	0.99997239	1.00000503	1.00006716	1.00012933	1.00015393
Node 12	0.99996525	0.99996289	0.99996204	0.99995711	0.99995711	0.99995379	0.99994429	0.99997192	1.00000447	1.00006669	1.00012894	1.00015356
Node 13	0.99996519	0.99996283	0.99996197	0.99995705	0.99995705	0.99995373	0.99994422	0.99997183	1.00000436	1.0000666	1.00012886	1.00015348
Node 14	0.99996513	0.99996276	0.9999619	0.99995695	0.99995695	0.99995361	0.99994408	0.9999716	1.00000409	1.00006637	1.00012869	1.0001533
Node 15	0.99996536	0.99996301	0.99996216	0.99995726	0.99995726	0.99995397	0.9999445	0.99997222	1.00000484	1.000067	1.00012919	1.0001538
Node 16	0.99996548	0.99996315	0.99996225	0.99995724	0.99995724	0.99995384	0.99994439	0.9999716	1.00000383	1.00006581	1.00012785	1.00015227
Current (pu)	0	1	2	3	4	5	6	7	8	9	10	11
Node 1	0.0037845	0.004041	0.0041355	0.0046755	0.0046755	0.00504	0.006075	0.003	-0.000615	-0.00747	-0.0143295	-0.017046

Table A.2 Voltage in nodes and current in grid for radial configuration in District case from hour 12 pm to 11 pm.

	RADIAL CONFIGURATION											
	Hour											
Voltage (pu)	12 pm	1 pm	2 pm	3 pm	4 pm	5 pm	6 pm	7 pm	8 pm	9 pm	10 pm	11 pm
Node 1	1	1	1	1	1	1	1	1	1	1	1	1
Node 2	1.00017092	1.00018736	1.00018563	1.00017738	1.00015765	1.00009349	1.00002782	0.99997473	0.99992845	0.99993155	0.99994085	0.99995403
Node 3	1.0001709	1.00018735	1.00018562	1.00017737	1.00015764	1.00009347	1.0000278	0.99997471	0.99992842	0.99993153	0.99994083	0.99995402
Node 4	1.00017257	1.00018912	1.00018732	1.00017899	1.00015909	1.00009455	1.00002851	0.99997506	0.99992841	0.99993152	0.99994082	0.99995401
Node 5	1.00062201	1.00066607	1.00064583	1.00061528	1.00054927	1.00038332	1.00021616	1.00006466	0.99991887	0.99992229	0.99993255	0.99994708
Node 6	1.00062248	1.00066648	1.00064611	1.0006155	1.00054942	1.00038352	1.00021639	1.00006486	0.99991906	0.99992248	0.99993272	0.99994722
Node 7	1.00063487	1.00067952	1.00065849	1.00062724	1.00055985	1.00039134	1.0002216	1.00006747	0.99991906	0.99992248	0.99993272	0.99994722
Node 8	1.00016266	1.00017859	1.0001772	1.00016937	1.00015051	1.00008833	1.00002465	0.99997345	0.999929	0.99993208	0.99994132	0.9999544
Node 9	1.00016428	1.00018037	1.00017893	1.00017101	1.00015193	1.00008905	1.00002464	0.99997286	0.99992798	0.9999311	0.99994047	0.99995375
Node 10	1.00034144	1.00036685	1.00035609	1.00033884	1.00030112	1.00020094	1.00009923	1.00001016	0.99992798	0.9999311	0.99994047	0.99995375
Node 11	1.00016326	1.00017929	1.00017791	1.00017004	1.00015107	1.0000884	1.00002421	0.99997265	0.99992798	0.9999311	0.99994047	0.99995375
Node 12	1.00016287	1.00017892	1.00017761	1.00016976	1.00015082	1.00008806	1.00002376	0.99997218	0.99992753	0.99993067	0.9999401	0.99995346
Node 13	1.0001628	1.00017886	1.00017754	1.0001697	1.00015076	1.00008797	1.00002364	0.99997204	0.99992739	0.99993054	0.99993999	0.99995338
Node 14	1.00016259	1.00017866	1.00017741	1.00016959	1.00015068	1.00008787	1.00002352	0.99997193	0.99992729	0.99993044	0.9999399	0.9999533
Node 15	1.00016314	1.00017917	1.0001778	1.00016993	1.00015095	1.00008824	1.00002398	0.9999724	0.99992774	0.99993087	0.99994028	0.9999536
Node 16	1.00016136	1.00017742	1.00017634	1.00016863	1.00014994	1.00008758	1.00002372	0.99997254	0.99992814	0.99993125	0.99994058	0.99995381

Current (pu)	12	13	14	15	16	17	18	19	20	21	22	23
Node 1	-0.0180735	-0.0198435	-0.019689	-0.018819	-0.0167235	-0.0098145	-0.002739	0.0029505	0.0078885	0.0075465	0.0065205	0.005067